# TABLE DES MATIÈRES

## LISTE DES TABLEAUX

## LISTE DES FIGURES

# CHAPITRE PREMIER

# INTRODUCTION GÉNÉRALE

La recherche océanographique actuelle favorise une approche des problématiques écologiques fondée sur une meilleure compréhension des interactions entre la variabilité environnementale et la distribution, l'abondance et la productivité des espèces. Les organismes planctoniques qui forment dans toute leur diversité la base des écosystèmes pélagiques sont en effet fondamentalement intégrés à leur environnement physique. L'environnement marin est par nature dynamique et les conditions "normales" d'habitat changent selon des échelles de temps allant de quelques années au siècle (Beaugrand et al., 2002; Lehodey et al., 2006). À la variabilité naturelle s'ajoutent les impacts anthropiques tels que l'altération des débits des cours d'eau en milieu côtier et principalement l'augmentation du $CO_2$ atmosphérique qui engendre, entre autres, une augmentation de la température et de l'acidité des océans (Denman et al., 2007). L'ensemble de cette variabilité influence, directement ou à travers des interactions écologiques, la croissance et la distribution des espèces planctoniques et donc les bilans de masse et d'énergie au sein des écosystèmes (Michel et al., 2006;

Wassmann et al., 2006; Hirche et Kosobokova, 2007; Muraleedharan et al., 2007; Coyle et al., 2008). Une meilleure compréhension des réponses biologiques aux changements de l'environnement physique doit donc permettre l'identification de nouveaux axes d'interprétation des relations et tendances observées au sein des populations et des écosystèmes, afin ultimement de mieux prédire l'évolution des écosystèmes face aux changements climatiques en cours (Eckman, 1994; Bathmann et al., 2001).

Dans ce contexte, les copépodes pélagiques méritent un intérêt particulier en raison de leur rôle clé d'interface entre la production unicellulaire phytoplanctonique et micro-zooplanctonique et les échelons trophiques supérieurs (Verity et Smetacek, 1996). Les copépodes représentent une proportion considérable, croissante avec la latitude, de la biomasse zooplanctonique des océans (entre 60% et 95%; Mauchline, 1998) et exercent un contrôle crucial des flux de masse et d'énergie au sein des écosystèmes (par ex. Roy et al., 2000; Olli et al., 2007). Ces organismes ont un cycle de vie de quelques semaines à quelques années, relativement long par rapport aux cycles cellulaires du phytoplancton et du micro-zooplancton. Les copépodes subissent au cours de leur développement des changements importants de taille (de quelques dizaines de micromètres à quelques millimètres) de fonctions physiologiques et de comportement. Leurs capacités natatoires leur permettent dès les derniers stades nauplii de développer des vitesses

de nages supérieures de plusieurs ordres de grandeurs aux vitesses des courants verticaux (Svetlichnyj, 1993; Yamazaki et Squires, 1996; Incze et al., 2001), ce qui leur permet de diverger significativement du comportement de particule passive dévolu classiquement au plancton (Wiafe et Frid, 1996; Genin et al., 2005). La dynamique des populations de copépodes émerge de ces interactions complexes entre les individus et leur environnement physique (Leising et Franks, 2000, 2002; Woodson et al., 2007; Woodson et McManus, 2007). Le phénomène de résonance spatio-temporelle entre les processus physiques et biologiques détermine la croissance, la distribution et ultimement le succès écologique des populations de copépodes (Frontier, 1991, 2004).

L'étude de la dynamique des populations de copépodes se retrouve donc confrontée à la complexité des nombreux processus physiques et biologiques impliqués et de leurs interactions selon différentes échelles de temps et d'espace (Seuront et Lagadeuc, 2001; Lough et Broughton, 2007; Ludovisi et al., 2008). La modélisation numérique s'avère être ainsi un élément essentiel à tout projet visant une meilleure compréhension de ces systèmes couplés bio-physiques, comme le démontrent les diverses initiatives issues du programme international GLOBEC (Global Ocean Ecosystem Dynamics, http://www.globec.org). La modélisation numérique est un outil multidisciplinaire et intégrateur qui permet de schématiser les conditions complexes observées dans la nature, tout en palliant en partie au

problème chronique du sous-échantillonnage des variables d'intérêt. Elle permet donc des études quantitatives de processus autrement difficiles à mesurer (flux, bilans de masse, etc.), afin d'en dégager de nouvelles pistes d'interprétation et/ou d'exploration. Toutefois, l'identification des échelles spatio-temporelles pertinentes, tant pour l'observation que pour la modélisation, est une étape critique de l'étude numérique de la réponse des organismes marins et des cycles biogéochimiques à la variabilité du forçage physique (Broekhuizen et al., 1995; de Young et al., 2004; Lévy, 2008). L'échelle de la population permet de couvrir les échelles temporelles journalière à inter-annuelle, et donc les échelles spatiales associées, c'est à dire de quelques kilomètres au bassin océanique. Cette gamme d'échelles spatio-temporelles recoupe également la résolution des observations couramment disponibles pour paramétrer, initialiser et valider les modèles de dynamique zooplanctonique, que ce soient des échantillonnages hebdomadaires par filets verticaux, des campagnes acoustiques quasi-synoptiques, ou encore des observations satellitales composites définissant les champs de nourriture disponibles. Les modèles de population permettent de plus de tirer le meilleur profit du couplage éventuel avec un modèle de circulation régionale à haute résolution spatio-temporelle et/ou avec un modèle d'écosystème de type NPZD (par ex. Fennel et Neumann, 2003; Speirs et al., 2006; Slagstad et Tande, 2007). La pertinence des modèles de dynamique des populations de copépodes a conduit au développement récent de types de modèles variés adaptés aux besoins propres aux diverses questions étudiées, et un effort particulier

à été fourni pour solutionner les difficultés techniques inhérentes à cette échelle d'approche, telles que la diffusion numérique, la prise en compte de la variabilité individuelle, le transfert d'échelles, etc. (Gurney et al., 2001; Fennel, 2001; Tittensor et al., 2003; Gentleman et al., 2008; Hu et al., 2008; Record et Pershing, 2008).

Les travaux de doctorat présentés dans cette thèse s'inscrivent dans la problématique générale d'une meilleure compréhension des relations entre la variabilité de l'environnement physique et la dynamique des populations de copépodes. La modélisation numérique est l'outil privilégié pour atteindre l'objectif général de mon doctorat qui est de mieux **comprendre et quantifier le couplage entre la variabilité des processus physiques et la dynamique des populations d'une espèce cible de copépode (*Calanus finmarchicus*) dans le système de l'estuaire et du golfe du St Laurent** (GSL). L'espèce de copépode calanoïde *C. finmarchicus* domine les communautés zooplanctoniques de l'Atlantique Nord et est une importante proie de nombreuses larves d'espèces de poissons d'intérêt commercial (Sameoto et al., 1994; Runge et de Lafontaine, 1996; Lynch et al., 2001; Buckley et Durbin, 2006), d'oiseaux marins (Wojczulanis et al., 2006) et de cétacés (Wishner et al., 1995; Baumgartner et Fratantoni, 2008). Les nombreux travaux menés depuis plus de dix ans dans le cadre du programme international GLOBEC ont mis en évidence le rôle crucial de *C. finmarchicus* dans les flux de

matière et d'énergie des bassins océaniques aux plateaux continentaux d'une part, et des producteurs primaires aux échelons supérieurs du réseau trophique d'autre part. Des exemples de liens étroits entre la variabilité des conditions hydrographiques, la dynamique des populations de *C. finmarchicus* et le recrutement d'espèces exploitées commercialement ont été mis en évidence à l'échelle de l'Atlantique Nord (Cushing, 1984; Anderson, 1994; Alheit et al., 2005; Pershing et al., 2005; Wassmann et al., 2006), et dans le GSL en particulier (Runge et al., 1999; Ringuette et al., 2002, Castonguay et al., 2008). Le GSL est une région particulièrement propice à l'étude de ces liens étroits de par sa situation de mer intérieure située à la limite sud de l'extension du couvert saisonnier de glace de mer, sa forte productivité pélagique mais aussi des bouleversement écologiques subis depuis quelques décennies. Les tendances observées jusqu'à présent et les modèles de circulation générale démontrent que c'est au-dessus de l'océan Arctique et de ses mers ancillaires que les effets des changements climatiques seront les plus intenses (Overpeck et al., 1997; Stempniewicz et al., 2007; Hamilton, 2007; Hirche et Kosobokova, 2007; Wang et al., 2007). Les impacts anticipés se combineront à une situation écologique déjà préoccupante en raison de l'écroulement récent des stocks de poissons de fond (Morue, Sébaste), et de la diminution de la teneur en dioxygène dissout dans les eaux profondes (Gilbert et al., 2005). Ceci justifie d'autant plus les efforts de recherche destinés à mieux comprendre les bases de l'écosystème pélagique du GSL. Trois aspects majeurs de la dynamique des

populations de *C. finmarchicus* ont été abordés au cours de ce doctorat: (1) le comportement de migration verticale, (2) la diapause et (3) la mortalité.

La persistance inter-annuelle de la population de *C. finmarchicus* dans un système fortement advectif tel que le GSL peut résulter de deux phénomènes, soient l'apport advectif d'individus issus de populations extérieures au GSL par ses frontières ouvertes (Détroits de Belle-Isle au nord-est et de Cabot au sud-est) et l'interaction du comportement individuel de migration verticale avec les structures hydrodynamiques verticales et horizontales. Zakardjian et al. (2003) ont élaborés dans le cadre de la composante canadienne du programme GLOBEC un premier modèle 3-D couplé physique-biologie décrivant les variations saisonnières de l'abondance et de la distribution de *C. finmarchicus* sur la plateau continental de l'Atlantique canadien. Ce modèle suggère une importance marquée de la circulation régionale sur la dynamique des populations de *C. finmarchicus* dans cette région. Zakardjian et al. (2003) concluent à un GSL auto-suffisant agissant comme source de *C. finmarchicus* pour les régions avoisinantes, en aval de ce système. Toutefois l'approche climatologique, la résolution horizontale de l'ordre du rayon local de déformation de Rossby (environ 10 km) et l'absence de migrations nycthémérales chez *C. finmarchicus* ne permettent pas à ce modèle de rendre compte pleinement des interactions entre le comportement migratoire des copépodes et la variabilité naturelle à haute fréquence des conditions océanographiques. Les migrations

verticales ontogéniques et nycthémérales du zooplancton sont fondamentales pour le maintient des populations dans les régimes de circulation fortement advectifs tels que les estuaires ou les upwelling côtiers (e.g. Batchelder et al., 2002; Souriseau et al., 2006). Le deuxième chapitre de cette thèse traitera donc de l'**impact du comportement des migrations nycthémérales et ontogéniques sur la variabilité de la distribution et de l'abondance de *C. finmarchicus* dans le GSL**. Un modèle de cycle de vie de *C. finmarchicus* est couplé à un modèle tri-dimensionnel à haute résolution spatio-temporelle de circulation du GSL couplé glace marine - océan (Saucier et al., 2003, 2009) afin de représenter les échelles spatio-temporelles adéquates.

Au delà de la variabilité aux échelles synoptique et saisonnière, la variabilité inter-annuelle de l'abondance et de la distribution d'une espèce de zooplancton faisant face à une variabilité fortement périodique des conditions environnementales repose sur sa capacité à éviter les périodes défavorables en terme de reproduction et/ou de mortalité. Le genre *Calanus* a développé une stratégie de diapause permettant aux stades pré-adultes d'éviter la saison de faible productivité primaire hivernale en résidant en profondeur (de 150 à plus de 2000 m selon la topographie) dans un état de métabolisme réduit (Hirche, 1996). Ce comportement est un élément fondamental de la phénologie de l'espèce, c'est à dire de la succession temporelle des phénomènes périodiques du cycle de vie de *C.*

*finmarchicus* en réponse à la variabilité des facteurs du milieu. La phénologie d'une espèce définit le cadre le plus large et le plus plastique de son adaptabilité à un milieu en changement (Miller et al., 1991). Les mécanismes qui contrôlent l'entrée et la sortie de diapause sont toutefois mal compris, mais il est fréquemment observé que les fenêtres temporelles d'entrée et sortie de diapause peuvent différer entre des régions proches, par exemple entre l'estuaire maritime et le nord-ouest du GSL (Johnson et al., 2008). Ces données ont de plus démontré à l'échelle de l'Atlantique Nord-Ouest l'absence de corrélations entre les patrons spatio-temporels de diapause et les variables environnementales telles que la biomasse phytoplanctonique, la température et la photopériode. Ces observations renforcent la vision de la diapause comme un phénomène intégrateur de l'historique environnemental des individus. De récentes analyses physiologiques, démographiques et génétiques supportent l'hypothèse d'un contrôle de l'entrée et sortie de la diapause par le métabolisme des lipides (Miller et al., 2000; Irigoien, 2004; Saumweber et Durbin, 2006; Tarrant et al., 2008; Johnson et al., 2008). D'importantes quantités de réserves lipidiques sont observées chez les individus en diapause, et une proportion de ces réserves correspondant aux besoins métaboliques associés à la mue vers l'adulte, à la maturation précoce des gonades et à la migration ontogénique vers la surface persiste au sortir de la diapause (Jónasdóttir, 1999; Rey-Rassat et al., 2002; Saumweber et Durbin, 2006). Ainsi un individu entrant en diapause sans une quantité de lipides suffisante pour subvenir aux besoins métaboliques de la longue

période de diapause, de la mue imaginale, de la maturation des gonades et de la migration vers la surface serait perdu pour la population, que ce soit en raison d'une mort par inanition ou d'un retour trop précoce vers les eaux de surface encore inhospitalières de l'hiver. Il apparaît donc nécessaire de développer une formulation mécaniste du phénomène de la diapause au niveau de la population, afin d'obtenir une réponse plastique du modèle de cycle de vie de *C. finmarchicus* face à la variabilité inter-annuelle et à d'éventuels changements du climat océanique (Miller et al., 1991; Speirs et al., 2006). Le troisième chapitre de cette thèse testera donc **l'hypothèse du contrôle de l'entrée et la sortie de diapause par le métabolisme des lipides chez *C. finmarchicus* dans le contexte environnemental du GSL**. Un modèle 1-D de cycle de vie de *C. finmarchicus* tenant compte de la biomasse des stades de développement (adapté de Fennel, 2001) permet de représenter un cycle de vie complet étalé sur deux années consécutives, forcé par des données de température et de nourriture obtenues à deux stations de monitorage dans le nord-ouest du GSL.

Finalement, la mortalité est un processus fondamental pour le contrôle quantitatif de la dynamique des populations de *C. finmarchicus* (par ex. Arnkværn et al., 2005). Bien que s'exerçant au niveau individuel, la mortalité des copépodes transcende les échelles spatio-temporelles à travers les divers processus physiques et biologiques qui la gouvernent, tels que la température (Hirst et al., 2002), le

rayonnement UV (Kouwenberg et al., 1999; mais voir aussi Skreslet et al., 2005), la prédation par les divers invertébrés (Ohman et al., 2008) et vertébrés (Ohman et Hsieh, 2008) marins ou encore par leur congénères (cannibalisme; Ohman et Hirche, 2001; Basedow et Tande, 2006). L'ensemble de ces relations conduit à des réponses non-linéaires des populations aux changements de conditions environnementales (Ohman et al., 2004). Chez les copépodes libérant leurs œufs dans la colonne d'eau lors de la ponte comme *C. finmarchicus*, la mortalité décroît considérablement des œufs et premiers stades nauplii aux stades de développement ultérieurs. Chez *C. finmarchicus* les taux de mortalité des œufs sont considérables avant la floraison phytoplanctonique printanière, et ils semblent exercer une influence déterminante sur les patrons saisonnier et régional de recrutement des stades copépodites dans la Mer de Norvège et la Mer d'Irminger (Ohman et Hirche, 2001; Heath et al., 2008). Ainsi, la description précise et la compréhension des processus à l'origine des patrons spatio-temporels de mortalité demeurent parmi les défis les plus importants de la modélisation de la dynamique des population de zooplancton (Ohman et Wood, 1995; Runge et al., 2004). En effet, la mortalité est un terme de fermeture essentiel aux modèles numériques de dynamique des populations. Une formulation densité-dépendante garantit la stabilité des solutions, et une représentation adéquate des taux de mortalité propre à chaque stade de développement ainsi qu'une formulation pertinente des relations fonctionnelles avec les variables environnementales sont requises pour simuler correctement les timings

et les abondances observées (par ex. Speirs et al., 2006). Toutefois les preuves directes de l'action de processus densité-dépendant, de relations fonctionnelles avec les variables environnementales et de leur impact sur le recrutement et la dynamique des populations de copépodes demeurent rares (Peterson et Kimmerer, 1994; Uye et Liang, 1998; Hirst et al., 2007), en raison de la difficulté d'obtenir des estimés fiables de valeurs de mortalité *in situ*. Ce manque de données limite le développement de fonctions mécanistes de la mortalité des stades de développement de copépodes requises par les modèles bio-physiques de dynamique des populations zooplanctoniques marines (Runge et al., 2005). La méthode des tables de survie verticales (« Vertical Life Table », VLT) est depuis quelques années employée dans le cadre particulier du milieu marin. La méthode VLT est basée sur les ratios des abondances instantanées des stades de développement successifs plutôt que sur l'évolution temporelle de l'abondance de chaque stade de développement. L'approche VLT permet ainsi d'estimer les taux de mortalité et leur variabilité spatiale pour des données synoptiques ou encore leur variabilité temporelle pour des séries temporelles à une station de monitorage. Le quatrième chapitre de cette thèse **testera l'hypothèse selon laquelle les patrons de recrutement des stades nauplii avancés de *C. finmarchicus* dépendent de la variabilité des taux de mortalité (de survie) des tout premiers stades (œufs et nauplii), et non pas seulement de la variabilité du taux de ponte des femelles associé à des taux de mortalité constants**. L'application de l'approche VLT à des

séries temporelles et à des observations synoptiques d'abondance des stades de développement de *C. finmarchicus* et de variables environnementales dans le GSL permet de décrire la climatologie saisonnière et le patron spatial de la mortalité des premiers stades de développement et du recrutement des stades subséquents. Des relations empiriques entre la mortalité, la biomasse phytoplanctonique, la température et l'abondance de femelles adultes permettent quant à elles de contraster l'impact de formulations déterministes et mécanistes de la mortalité sur la dynamique des populations de *C. finmarchicus* dans un modèle simple de cycle de vie.

# CHAPITRE II

# IMPACTS OF THE INTERACTION BETWEEN THE HYDRODYNAMICS AND THE MIGRATION BEHAVIOR ON THE POPULATION DYNAMICS OF *Calanus finmarchicus* IN THE GULF OF ST. LAWRENCE, CANADA: A 3-D MODELING APPROACH

## 1 Résumé

Le golfe du Saint-Laurent (GSL) est un système dynamique qui soutient un écosystème pélagique productif, dominé par le copépode *Calanus finmarchicus*. Cet environnement offre de grands défis pour l'étude des interactions entre la démographie des populations planctoniques et la variabilité des processus océanographiques physiques. Nous avons donc développé un modèle numérique tri-dimensionnel couplé physique-biologique afin d'étudier la dynamique de populations de *C. finmarchicus* dans le GSL, pour l'année 1999. Nous avons couplé un modèle de cycle de vie de *C. finmarchicus* représentant les propriétés moyennes de la population en regard des taux de production d'œufs, de mortalité, de développement et du comportement de nage à un modèle de circulation régionale piloté par des forçages atmosphériques, hydrologiques et océaniques réalistes. La distribution et l'abondance de *C. finmarchicus* se sont révélées très sensibles au comportement de migration en raison des fortes cisailles verticales et horizontales de courant. Le comportement de migration nycthéméral est ainsi essentiel pour reproduire les patrons de distribution observés. Cette étude identifie pour la première fois dans le GSL le « circuit *Calanus* », composé de structures hydrodynamiques distinctes reliées entre elles par la phénologie et le comportement de nage de *C. finmarchicus*.

# 2 Introduction

One fundamental goal of the modern oceanographic research is to gain a better understanding of the complex interactions between the dynamic ocean's physical environment and the distribution, abundance and productivity of the pelagic species (e.g. Eckman, 1994). From this perspective, copepods represent the keystone of pelagic ecosystems, by filtering the environmental variability through trophic transfer from primary production to higher trophic levels (Williams et al., 1994; Smith, 1995; Kobari et al., 2003; Leising et al., 2005; Peters, 2006; Wassman et al., 2006; Olli et al., 2007). Significant links between the variability of physical properties of the ocean, populations dynamics of copepods and fisheries productivity have already been observed (Runge, 1988; Anderson, 1994; Skreslet, 1997; Runge et al., 1999; Sundby, 2000; Lehodey et al., 2006; Loeng and Drinkwater, 2007). However, such relationships remain difficult to explain and quantify by observations alone, owing to the large space and time scales involved (Fromentin and Planque, 1996; Greene et al., 2003), and the complex interactions between the copepod species and their environment (Fiksen et al., 2005; Frost, 2005; Pierson et al., 2005; Pringle, 2007; Basedow et al., 2008; Visser at al., 2009). Copepods undergo important physiological and behavioral changes during their development from the egg stage to the adult (Mauchline, 1998). Their physiologic and demographic responses to the variability of the environment are not linear (e.g.

Campbell et al., 2001). Moreover, the swimming velocities developed by copepodite stages are greater than the typical vertical velocities in the ocean (Yamazaki and Squires 1996; Incze et al., 2001). Several species perform extensive migrations in the water column. Ontogenetic migration associated with the winter-time diapause process has basin-scale implications on the population dynamics of calanoid copepods (Backhaus et al., 1994; Heath et al., 1999, 2008; Falk-Petersen et al., 2008), while the diel vertical migrations (DVM) performed by copepodite stages during the productive season complicates the way they interact at meso- to regional scale with the vertical gradients in the physical and biological environments and the sheared circulation (Hannah et al., 1997; Zakardjian et al., 1999; Batchelder et al., 2002; Genin et al., 2005; Carr et al., 2008).

The GSL is a semi-enclosed marginal sea, characterized by pronounced horizontal and vertical gradients in circulation, temperature and salinity, and the southern-most seasonal sea-ice cover in the North Atlantic area. The physical dynamics of the Gulf of St. Lawrence is, to a large extent, controlled internally rather than remotely by large-scale oceanic processes (e.g., Koutitonsky and Bugden, 1991). The general cyclonic circulation in the GSL is driven by both the seasonal freshwater discharge from the St. Lawrence River and the synoptic meteorological systems (Koutitonsky and Bugden, 1991; Saucier et al., 2003, 2009). This dynamic system sustains a productive pelagic ecosystem, whose zooplankton

community is dominated by the copepod *Calanus finmarchicus* (de Lafontaine et al., 1991). A few studies provide some insight into the interactions between the hydrodynamics and the population dynamics of *C. finmarchicus* in the GSL. Plourde and Runge (1993) developed the concept of the "*Calanus* pump": while in summer females *C. finmarchicus* sustain high egg production rates in the Lower St. Lawrence Estuary (LSLE), the residual surface circulation supply surface-dwelling early development stages to downstream regions of the GSL through the Gaspé Current (GC). Plourde et al. (2001) also argued for the existence of a compensatory upstream advection at depth of overwintering *C. finmarchicus* from the GSL, in order to maintain the population within the estuary. In the shallow southern GSL downstream of the GC, Runge et al. (1999) reported a negative correlation between an index of the St. Lawrence river freshet (RIVSUM index: Koutitonsky and Bugden, 1991) and the *C. finmarchicus* biomass, but no causal relationship however. Using a climatological coupled physical-biological model, Zakardjian et al. (2003) found that advection of *C. finmarchicus* by horizontal currents indeed plays an important role in its population dynamics at the regional scale, between different sub-areas of the GSL / Scotian Shelf system. Only ontogenetic migrations were considered however, and the relatively coarse time and space resolutions of this first modeling study did not allow to explore the interactions between the DVM behavior and the natural variability of the oceanographic conditions. DVM is however a potentially efficient way to retain a zooplankton population into an advective environment

such as the LSLE – GSL system, whenever a vertically (Zakardjian et al., 1999) and/ or horizontally sheared circulation exists (Sourisseau et al., 2006). Hence DVM should be considered with ontogenetic migrations as an element of a life-cycle strategy adapted to this environment, and designed to compensate for the eventual loss by advection (Eiane et al., 1998).



In order to achieve a coherent and comprehensive understanding of the population dynamics of *C. finmarchicus* in the GSL system, we coupled a stage-based biological model of *C. finmarchicus* to a regional circulation model of the GSL, driven by realistic atmospheric, hydrologic and oceanic forcing (Saucier et al., 2003). The model was applied for 1999, the second year of data acquisition of the Atlantic Zonal Monitoring Program (AZMP) of the Department of Fisheries and Ocean Canada which covers the Canadian Atlantic continental shelf with several fixed stations (Therriault et al., 1998). The high spatio-temporal resolution of the model allowed to characterize (1) the predominant features of the spatio-temporal patterns of distribution and abundance of *C. finmarchicus* in the GSL, (2) the sensitivity of these patterns to both the ontogenetic and diel migration behavior of late copepodite stages and (3) to quantify the relative contributions of advection, temperature and food to the environmental forcing.

# 3 Material and Methods

## *3.1 Circulation and ecological models*

The 3-D sea ice-ocean model driving the *C. finmarchicus* life cycle model was detailed in Saucier et al. (2003, 2004) and Smith et al. (2006b). This physical model represents the current sea-ice and ocean components of the Canadian Operational Weather Forecast model GEM (Pellerin et al., 2003), and the Canadian Regional Climate Model (Faucher et al., 2004). The physical model is based on shallow water and hydrostatic approximations. It includes a 3-D flux-corrected transport scheme and a level 2.5 turbulence closure model. The coastal ocean model is coupled to a multi-category dynamic sea ice model and a two-layer plus one snow layer thermodynamics. The model domain covers the estuary and the Gulf of St. Lawrence, from the inland limits of the upper estuary near Québec City (Ile d'Orléans), to the open boundaries delimited by the Strait of Belle-Isle and Cabot Strait (Fig. II-1). The grid resolution is 5 km on the horizontal (approximately half the local Rossby radius of deformation) and 5 m in the vertical, with the free surface and the bottom layers adjusted respectively to the sea level and the local topography. The model was forced by 3-hourly atmospheric fields provided by the Canadian Operational Weather Forecast Model, daily run-off data of 28 major tributaries, a monthly reanalysis of Bourgault and Koutitonsky (1999) for the St.

Lawrence River run-off, and hourly water level (27 co-oscillating tidal constituents) and monthly temperature and salinity profiles prescribed at Cabot Strait and the Strait of Belle-Isle. The forcing fields were interpolated at the time resolution (5 min) of the model. The model computed fully prognostic solutions for water levels, currents, temperature, salinity, turbulent kinetic energy and sea-ice properties. Comparisons of the model outputs to recent and historical observations have shown that the model reproduced the high frequency to inter-annual variability in the circulation, water masses properties and sea-ice conditions of the GSL under the given realistic hydrological and atmospheric forcing (Saucier et al., 2003; Smith et al., 2006b).

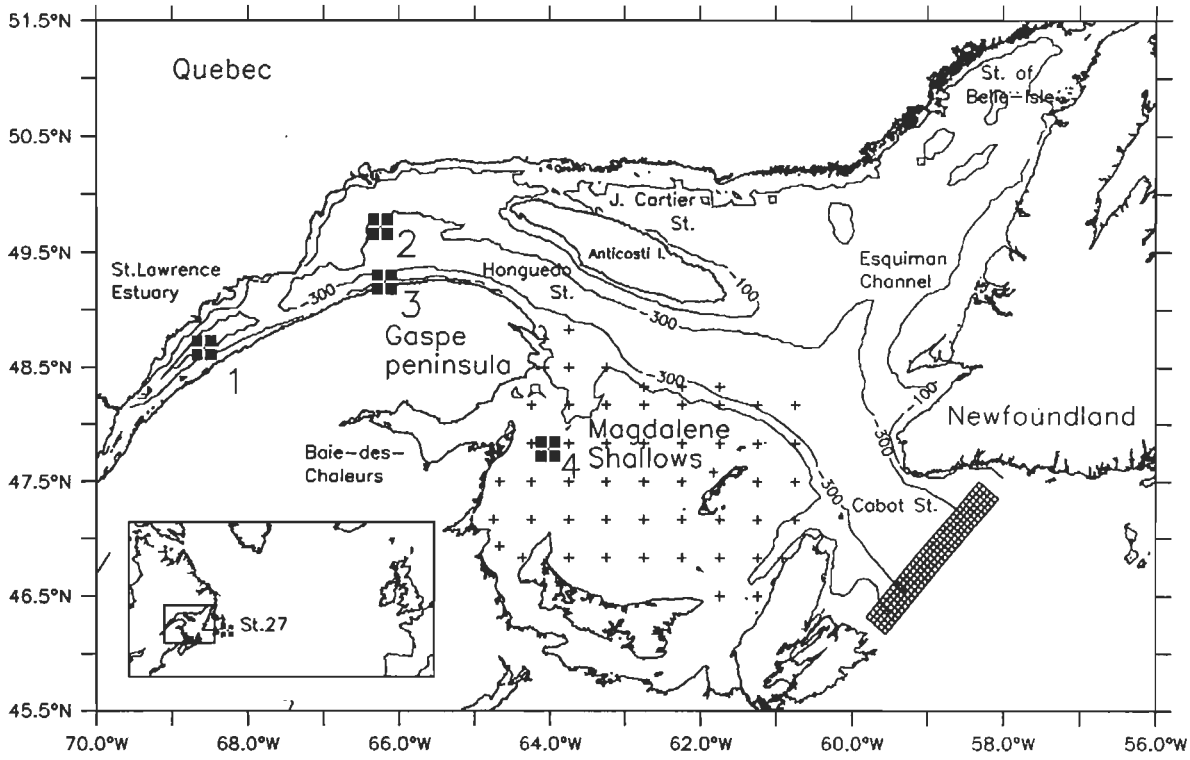


Figure II-1. Model domain with bathymetry and locations of sampling stations. 1 is Rimouski, 2 is Anticosti Gyre (AG), 3 is Gaspé Current (GC) and 4 is Shediac. Small crosses: Sampling grid of the Mackerel stock assessment cruise. Near Cabot Strait is an example of the grid resolution of the model. For this figure and every other map, the Mercator projection is used.

The 3-D Nutrient-Phytoplankton-Zooplankton-Detritus (NPZD) model developed by Le Fouest et al. (2005, 2006) provided food concentrations for the egg production of C6f. It comprised two class of phytoplankton (small and large cells), two classes of zooplankton (micro- and meso-zooplankton), and two classes of detritus (Dissolved and particulate organic matter). The NPZD model was coupled to the 3-D circulation model described above. Profiles of observed Chlorophyll *a* and nitrate concentrations as well as SeaWIFS- and AVHRR-derived data were used to validate the ability of the model to simulate realistic seasonal and spatial patterns at meso- and regional scales in primary production and micro-plankton biomass (Le Fouest et al., 2005, 2006). Food fields were obtained by summing large and small phytoplanktonic cells (Ohman and Runge, 1994). Units of the NPZD model were mmol $N.m^{-3}$, which were converted in mg $C.m^{-3}$ according to a constant conversion factor of 79.5.

## *3.2 C. finmarchicus life history model*

The life-history model of *C. finmarchicus* (Tables II-1, II-2 and II-3) was adapted from Zakardjian et al. (2003). The biological rates of development, reproduction and mortality depended on the local environmental conditions and neglected the individual histories. The model took into account the egg, five

naupliar and six juvenile copepodite stages, along with a diapausing copepodite stage (C5d) and the male and female adult stages (C6m and C6f). The first two non-feeding nauplii stages were grouped together. The model used moulting rates defined from stage-specific, temperature-dependent development times (Campbell et al., 2001). A Monotonic Upstream Scheme for Conservation Laws (MUSCL, van Leer, 1979) was used to compute the transfer from one stage to the next (Record and Pershing, 2008). This numerical scheme significantly reduced the numerical dispersion along the stage axis compared to the forward Euler method routinely employed to resolve the partial differential equations system generated by the biological stage-based model. The final moult into adults was equally partitioned between C6m and C6f. A sexual maturation time of 10 days was assumed for C6f (Plourde and Runge, 1993). The spawning function for C6f varied according to food concentration only (mg C $m^{-3}$), as Runge and Plourde (1996) showed a weak temperature dependence of egg production rates in the GSL area. Spawning occurred only at night.

Table II-1. Differential equations for the time evolution of the state variables in the life-cycle model of *C. finmarchicus*. Functions are given in table II-2 and stage-specific parameters in table II-3.

| | |
|---|---|
| Eggs | $\frac{\partial Egg}{\partial t} = R \times C6f - \left(t_{Egg} + m_{Egg}\right) Egg - \frac{\partial w_{Egg} Egg}{\partial z}$ |
| Generic stage $S_i$ | $\frac{\partial S_i}{\partial t} = t_{i-1} S_{i-1} - \left(t_i + m_i\right) S_i - \frac{\partial w_i S_i}{\partial z}$ |
| Diapausing stage | $\frac{\partial C5d}{\partial t} = D\, t_{C5} C5 - \left((1-D) t_{C5d} + m_{C5d}\right) C5d - \frac{\partial w_{C5d} C5d}{\partial z}$ |
| Adult males | $\frac{\partial C6m}{\partial t} = 0.5(1-D)\left(t_{C5} C5 + t_{C5d} C5d\right) - m_{C6m} C6m - \frac{\partial w_{C6m} C6m}{\partial z}$ |
| Immature females | $\frac{\partial C6j}{\partial t} = 0.5(1-D)\left(t_{C5} C5 + t_{C5d} C5d\right) - m_{C6j} C6j - \frac{\partial w_{C6j} C6j}{\partial z}$ |
| Mature females | $\frac{\partial C6f}{\partial t} = t_{C6j} C6j - m_{C6f} C6f - \frac{\partial w_{C6f} C6f}{\partial z}$ |

Table II-2. Functions of the biological rates for the life-cycle model of *C. finmarchicus*. Stage-specific parameters are given in table II-3.

| | |
|---|---|
| Egg production rate | $R = R^{max}(1-e^{(\alpha\ Food)})$ |
| | with $R_{max}$ = 60 $fem^{-1}.d^{-1}$ and $\alpha$ = -0.02 $m^3.mgC^{-1}$ [(a)] |
| Transfer rate | $t_i = 1/SD_i$ with $SD_i = a_i(Temp+9.11)^{-2.05}$ |
| | for development from Eggs to C5[(b)] and |
| | $SD_i$ = 20 days for C5d exiting from diapause[(c)], |
| | $SD_i$ = 10 days for C6j maturing into C6f[(d)] |
| Diapause | $D_{GSL} = \tanh( (1+\cos( 2\pi(d+35)/365 ) )^2 )$ |
| | $D_{LSLE} = \tanh( 2\times(1+\cos( 2\pi(d+15)/365 ) )^{1.5} )$ |
| Mortality rates: | |
| Temperature | $m^T = ( Temp / 10 )^2$ |
| Egg | $m_{Egg} = m^T ( 0.488 + 0.033 (C6f+C6j+C5) )$[(e)] |
| Nauplii | $m_{Ni} = m^T ( m^0_{Ni} + \Sigma N_i / 8000 )$ |
| Copepodite | $m_{Ci} = m^T ( m^0_{Ci} + \Sigma C_i / 2000 )$ |
| Vertical swimming: | $w_i = w_i^{max} \tanh( 0.03 ( z - z_i^{opt} ) ) \xi$ |
| | with $z_i^{opt} = z_i^{min} + 0.5( z_i^{max} - z_i^{min} )( 1-\tanh( 3$ |
| | $\cos(2\pi t/24) ) )$ |
| | for migrating stages, else see table II-3; |
| | and $\xi = sign( 0.5 - U[0,1] ( 1 - ( z - z_i^{opt} )^2 / 15 ) )$ |

[(a)] Plourde and Runge, 1996; [(b)] Campbell et al., 2001; [(c)] Zakardjian et al., 2003; [(d)] Plourde, unpublished data; [(e)] Ohman and Hirche, 2001

Table II-3. Stage-specific parameters used in the *C. finmarchicus* life-cycle model.

| Stage | Belehradek parameter[a] | Basic mortality rate [b] | Maximum swimming velocity [c] | Ontogenetic convergence depth [d] | Minimum migration depth [d] | Maximum migration depth [d] |
|---|---|---|---|---|---|---|
| | $a_i$ (days) | $m^0_i$ (days$^{-1}$) | $W^{max}$ (m h$^{-1}$) | $Z^{opt}$ (m) | $Z^{min}$ (m) | $Z^{max}$ (m) |
| Eggs | 595 | 0.50 | 1.0 | 5 | - | - |
| N1-2 | 969 | 0.50 | 0.7 | 5 | - | - |
| N3 | 1387 | 0.20 | 1.6 | 5 | - | - |
| N4 | 759 | 0.20 | 1.6 | 5 | - | - |
| N5 | 715 | 0.20 | 1.6 | 5 | - | - |
| N6 | 841 | 0.10 | 2.7 | 5 | - | - |
| C1 | 966 | 0.08 | 3.2 | 5 | - | - |
| C2 | 1137 | 0.06 | 4.7 | 5 | - | - |
| C3 | 1428 | 0.04 | 6.1 | 5 | - | - |
| C4 | 2166 | 0.02 | 7.6 | 5 | 0 | 100 |
| C5 | 4083 | 0.02 | 9.4 | 5 | 0 | 100 |
| C5d | - | 0.002 | 9.4 | 175 | - | - |
| C6m | - | 0.08 | 10.8 | 75 | 50 | 150 |
| C6j | - | 0.02 | 10.8 | 5 | 0 | 100 |
| C6f | - | 0.02 | 10.8 | 5 | 0 | 100 |

[a] Campbell et al., 2001; [b] Fitted; [c] Zakardjian et al., 2003; [d] This study Fig. 3; Plourde and Runge, unpublished

The dynamics of diapause is a key element in the population dynamics of *C. finmarchicus*. A considerable part of the life-cycle is spent in diapause (mainly as C5) deep in the water column (Plourde et al., 2001; Heath et al., 2004; Saumweber and Durbin, 2006). In our model, C5 stage was allowed at the end of its development to either enter diapause (C5d) or to moult into adult in a proportion determined by a seasonally varying function (Fig. II-2). Johnson et al. (2008) showed that the onset of diapause occurs in late summer in both the LSLE and the north-west GSL, while exit from diapause is delayed by at least one month in the LSLE relative to the north-west GSL. The empirical diapause functions were therefore parameterized according to climatology of the abundance of C5 from monitoring stations located in the LSLE and the north-west GSL (Fig. II-2). Owing to the lack of data from central and north-east GSL, the north-west GSL diapause function was uniformly applied to these regions.

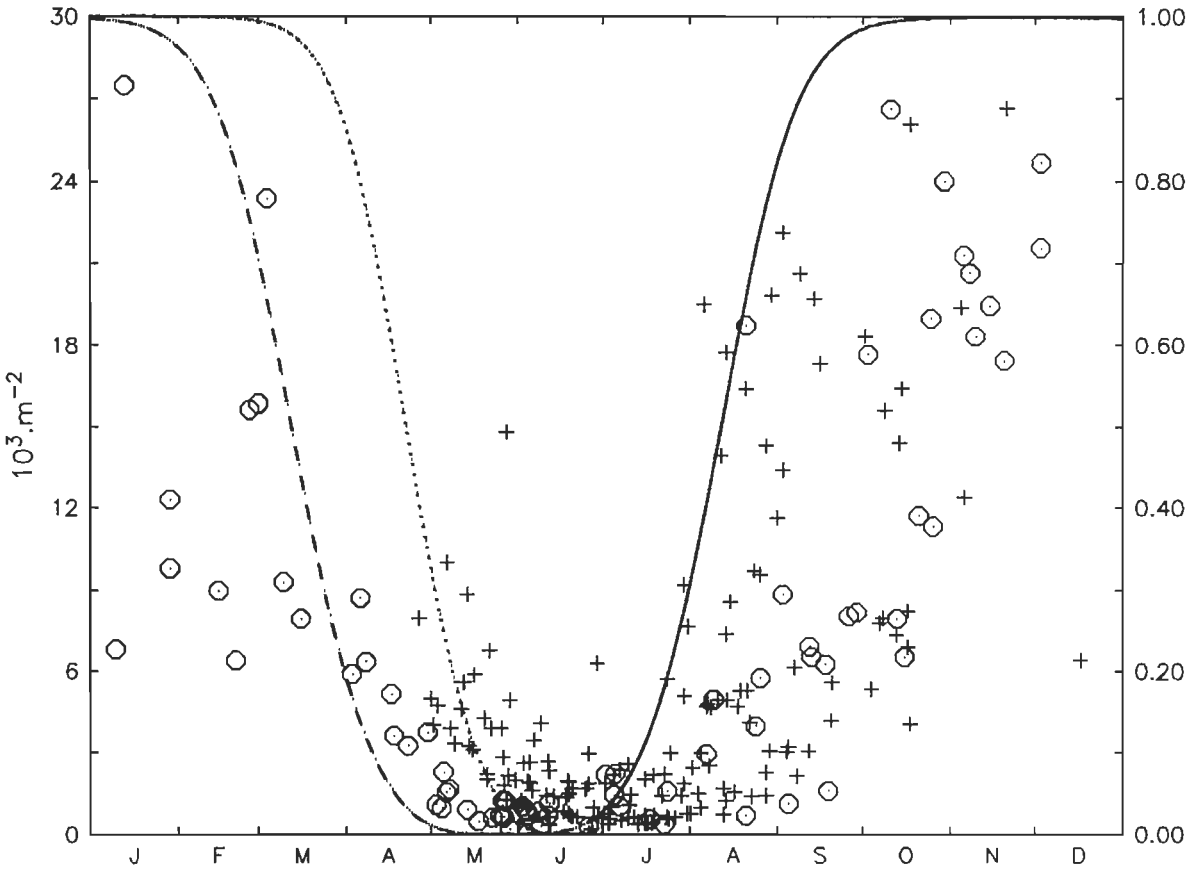


Figure II-2. Vertically integrated abundance ($10^3.m^{-2}$) of C5 observed between 1994 and 2001 at the Rimouski (crosses) and the AG (circles) stations. Lines are the empirical diapause functions derived from the data. Dashed line: proportion of C5d remaining in diapause in the GSL area. Dotted line: proportion of C5d remaining in diapause in the LSLE area. Continuous line: proportion of C5 allowed to enter diapause over the whole domain.

Mortality exerts a major control on population dynamics. In general, stage specific mortality rates in broadcast spawner copepods decay dramatically from eggs to adults (Heath et al., 2000; Hirst and Kiørboe, 2002; Hirst et al., 2007). We used stage-dependent basic mortality rates, decreasing from 0.5 (eggs) to 0.02 $d^{-1}$ (C6f), except for C6m and C5d for which the mortality rate was three times higher than for C6f (Kiørboe, 2006) and 10 times lower than for C5 (Gislason et al., 2007) respectively. Density-dependent formulation of mortality was important for the overall stability of the solution and basic stage-dependent mortality rates were modulated by distinct density-dependent functions for egg, nauplii and copepodites respectively (Table II-2). For eggs, we followed Ohman and Hirche (2001) based on the accumulating evidences of cannibalistic behavior of *Calanus* spp copepodites on con-specific eggs (Bonnet et al., 2004; Basedow and Tande, 2006; Plourde et al., 2009). Finally, mortality increased in all stages for temperature above 10°C (Table II-2), so that it doubles at approximatively 14.1°C (Speirs et al., 2006; Hellaouët and Beaugrand, 2007).

### *3.3 Vertical migrations*

Ontogenetic vertical migrations associated to the diapause process and daily vertical migrations during development in late copepodite stages are generally

observed in *C. finmarchicus* (e.g. Simard et al., 1985). Data collected in spring and early fall 1998 in the north-west GSL showed DVM behavior in some of the copepodite stages (Fig. II-3, Plourde et al., unpublished). In spring, most of C5 were probably still in diapause (Fig. II-3E), while in fall their bimodal distribution at night combined to the depth of the deep component suggest DVM for actively growing C5 within the 0-100m layer, and diapause for the others between 125-150 m (Fig. II-3F). Diapausing individuals were also likely to be responsible of the bimodal night-time vertical distribution of C4 in spring (Fig. II-3C). A weak DVM behavior was present in C1-3 (Fig. II-3A, 3B), whereas C6f showed clear DVM during both periods (Fig. II-3G, 3H).

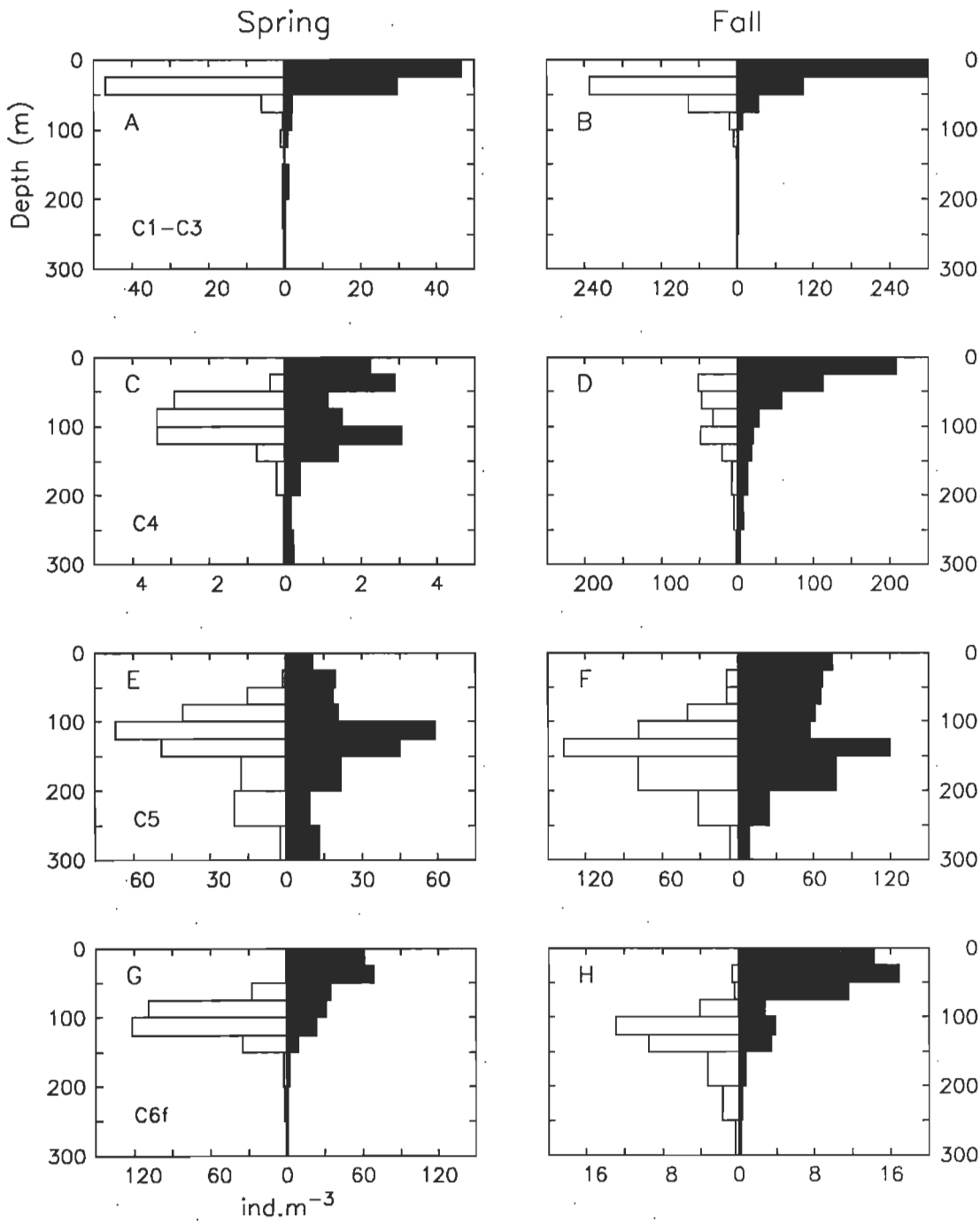


Figure II-3. Diel vertical distribution of C. finmarchicus copepodite stages observed in the north-west GSL and the LSLE during spring (left column) and autumn (right column) 1998. Day-time: white, night-time: black. (A-B) C1-3. (C-D) C4. (E-F) total C5 (active and diapausing). (G-H) C6f.

The GSL environment is characterized by marked heterogeneities, such as the topographic discontinuity formed by the deep channels, the vertically sheared estuarine circulation, the stratification of the water column with the presence of a cold intermediate layer, etc (Koutitonsky and Budgen, 1991). When considering the population dynamics of *C. finmarchicus* in the GSL, vertical migrations are likely to interact strongly with those physical features. Our study considered two scenarios of swimming behavior according to the seasonal observations of the vertical distribution and migration of the *C. finmarchicus* copepodite stages described above. The first scenario (no-DVM) took only into account ontogenetic migration associated with the entry and the exit from diapause with all stages ascribed to a fixed preferential depth (Table II-3). Diapausing C5d were centered at 175 m, while C6f and all other active stages remained near the surface. The second scenario (DVM) allowed DVM between surface and 100 m in copepodite stages C4, active C5 and C6f. Males stayed at 75 m in both scenarios. In both cases, egg sinking was considered (Knutsen et al., 2001), and egg reaching the bottom before hatching were considered lost from the population. The swimming behavior was formulated following Zakardjian et al. (1999). Stage-specific swimming speed was defined as the product of (1) a maximum swimming velocity, (2) a depth dependent hyperbolic tangent function, leading to downward (respectively upward) swimming when copepods are above (respectively below) their stage-specific convergence depth. Ontogenetic migrations corresponded to a constant convergence depth,

while time-varying stage-specific convergence depths allowed to simulate DVM (Table II-3). The maximum velocity was set to three body lengths per second for stages exhibiting DVM in order to get realistic timings of ascend and descend, and to one body length per second for the others. Wherever the converging depth was deeper than local topography it was set to the last layer above the bottom. A random dispersion factor, which could be considered as the statistical expression of individual variability within each stage, was necessary in order to avoid unrealistic concentrations in thin layers (Table II-2). The dispersion factor was a random probability for the swimming velocity to change its sign (i.e., for the modeled stage to change its direction of swimming). At the depth of convergence, the swimming velocity took the sign of a random number following a uniform distribution, and the distribution was gradually shifted toward the original velocity sign (i.e., the original direction of the swimming) as the actual depth was farther from the depth of convergence.

DVM behavior had important implications for several physiological processes considered in the life-cycle model of *C. finmarchicus*. Special consideration was given to the density-dependent mortality formulation of the egg. The original formulation of Ohman and Hirche (2001) depends on the vertically integrated abundance of C6f and C5. The actual feeding mode by which copepodites ingest eggs is not known, whether it is prey switching (Landry, 1981) or independent

feeding (Basedow and Tande, 2006). Moreover, DVM behavior in *C. finmarchicus* copepodites has been related to diel feeding rhythms (e.g. Simard et al., 1985; Durbin et al., 1995; Irigoien et al., 1998), which makes unclear if non-migrating late copepodite stages would eat more than migrating ones on a daily basis. We thus used the original function of vertically integrated abundance ($ind.m^{-2}$) of C6f and C5, and did not try to convert it into a function of the density ($ind.m^{-3}$) of C6f and C5.

### *3.4 Validation*

We used different sources of data to validate our simulations. Time series of *C. finmarchicus* abundance collected as part of the AZMP in 1999 at four monitoring stations located in the western part of the LSLE-GSL system were first used for validation (Fig. II-1). Station 2 (Anticosti Gyre), 3 (Gaspé Curent) and 4 (Shediac) were visited bi-monthly whereas station 1 (Rimouski) was sampled each week from late May to late November. Synoptic distribution of *C. finmarchicus* stages abundance in the Magdalene Shallows was obtained from a grid of 53 stations in late June ($19^{th}$ to $25^{th}$) during the Mackerel stock assessment cruise conducted by DFO (Fig. II-1). Synoptic maps of the data were produced with the Ferret software (NOAA PMEL), using a spline-Laplacian interpolation method. During the AZMP

and Mackerel stock assessment cruise, zooplankton was collected with a 1-m diameter 158 or 202 $\mu$m mesh ring net vertically towed from the bottom to the surface. At the Rimouski station, 73 and 333 $\mu$m mesh size nets were used in combination in order to adequately sample all copepodite stages (Plourde et al., 2001). Samples were preserved in 4% formaldehyde and individuals were sorted by development stage level later in the laboratory. Only copepodite and adult stages were considered for validation because early naupliar stages of *C. finmarchicus* are under sampled with the 158 $\mu$m and 202 $\mu$m nets (Plourde, unpublished data).

### *3.5 Models coupling, initial and boundary conditions*

In order to distinguish local vs. advective effects on the population dynamics, the life-cycle model was first applied within a 1-D framework for both the no-DVM and DVM scenarios. It was forced by temperature and food profiles taken from the 3-D circulation and biogeochemical models at the locations of the four monitoring stations. In order to make straightforward comparison possible, an initial abundance of 30 000 C5d $m^{-2}$ was imposed at each station, based on maximal values observed in autumn and winter in the LSLE and GSL.

In a second approach, the life-cycle model was coupled to the 3-D circulation model and forced by the 3-D temperature and food fields provided respectively by the circulation and ecological models. The partial differential equation describing the evolution in time of a generic concentration *C* is:

$$\frac{\partial C}{\partial t}+\nabla\left(\vec{U}\,C\right)-K_H\nabla_H^2 C-\frac{\partial}{\partial z}\left(K_V\frac{\partial C}{\partial z}\right) = -\frac{\partial W_z C}{\partial z}+sources-sinks \qquad (1)$$

where $\vec{U}$ is the 3-D velocity vector, $K_H$ and $K_V$ are the horizontal and vertical eddy diffusivity coefficients, respectively, $W_z$ is the vertical swimming speed (sinking speed for the eggs) of the modeled stages, and sources and sinks are related to the biological processes described above. At each time step, the transport of each state variable was first computed using a 3-D flux-corrected transport scheme (Saucier et al., 2003), and a Euler forward scheme for the swimming behavior (Andersen and Nival, 1991). Biological source and sink terms were then explicitly computed by the biological routines.

The simulations were carried out for the year 1999, using initial physical fields (temperature and salinity) and boundary conditions based on observations provided by the AZMP in November 1998, which were interpolated on the numerical grid of the model. No data set were available at the appropriate space and time scales over the LSLE-GSL system for the abundance, distribution and stage structure of the *C.*

*finmarchicus* population. The biological initial conditions assumed a late fall – early winter uniform population of C5d within a depth range of 100 to 250 m, with a vertically integrated abundance of 30000 $m^{-2}$. The GSL is thought to be self-sustaining, being a source of *C. finmarchicus* for the downstream areas of the continental shelf (Zakardjian et al., 2003). Thus in order to simplify the interpretation of the results, we did not consider in a first approach inflow of copepods at the open boundaries. However, in a second series of simulations we applied climatological monthly abundances obtained from station 27 (AZMP) off eastern Newfoundland (Fig. II-1) at both the Strait of Belle-Isle and Cabot Strait boundaries, in order to estimate the contribution of external sources to the *C. finmarchicus* population dynamics in the GSL. The integrated abundances of the stages from the climatology where converted in concentrations, according to the DVM scenarios (Table II-3) and the diapause function prescribed in our model. For the fifth copepodite stage, observations did not discriminate diapausing from active individuals. C5 were thus split active and diapausing modeling stages according to the diapause function of the model (Fig. II-2).

### *3.6 Empirical Orthogonal Functions analysis*

Empirical Orthogonal Functions (EOF) were used to quantitatively describe

the dominant spatio-temporal patterns of variability in abundance and distribution of *C. finmarchicus* in relation with relevant environmental variables. EOF analysis is widely used in meteorological, oceanographic and environmental studies (e.g. Fuentes-Yaco et al., 1997; Iida and Saitoh, 2007). EOF analysis extracts a reduced set of descriptors (modes) which represent both the main temporal and spatial variations included in the original data. The temporal variance of the data is successively partitioned into orthogonal spatial patterns (statistically independent) called modes, each one trying to account for the maximum variance possible. The time evolution of each EOF mode is described by the principal component (PC) time series. The observed pattern at a given time is given by the sum of the mean and each EOF mode, weighted by the value of the corresponding PC at that time. In general, only the first few EOF modes, which account for the highest fraction of the variance, are associated with physical processes. Then the causes of variation of those uncorrelated individual orthogonal functions can be examined separately. Thus, EOF analysis provides an effective way to summarize and interpret the few significant spatio-temporal patterns embedded into the data. EOF analyses were performed using the Ferret software (NOAA PMEL) using the algorithm of Chelton et al. (1982) on the daily abundances of Nauplii (1-6), total C5 (active C5 + diapausing C5d) and females.

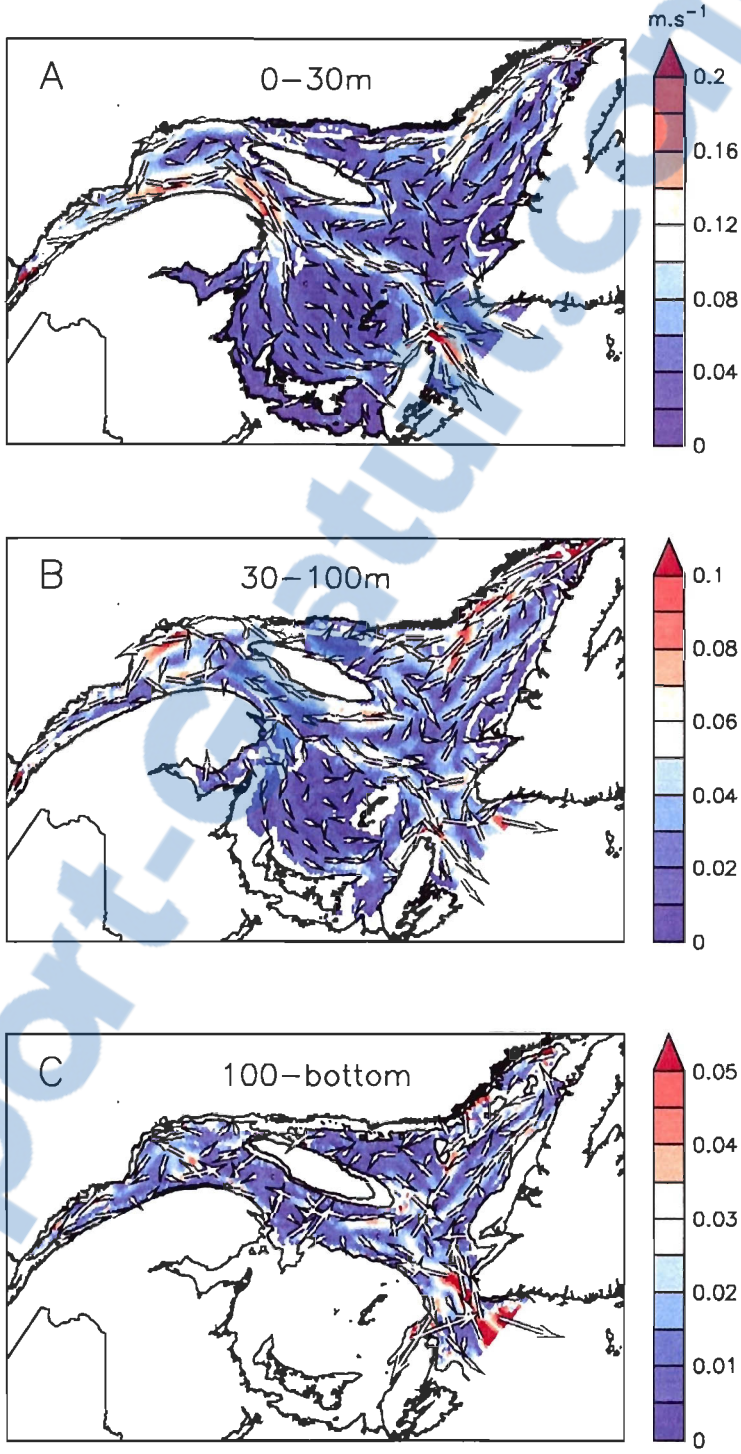


Figure II-4. Annual mean of the simulated currents ($m.s^{-1}$) for 1999 in the GSL between (A) the surface to 30m, (B) 30m to 100m and (C) 100m to the bottom.

# 4 Results

## *4.1 Environmental conditions*

We summarize our current understanding of the circulation in the LSLE-GSL system, illustrated by results from the 1999 simulation of the 3-D physical model (Fig. II-4; Saucier et al. 2003, Smith et al. 2006b). The general surface circulation in the GSL (Fig. II-4A) is cyclonic. The surface currents, mainly driven by the freshwater outflow and wind stress, are the strongest (yearly average of c.a. 0.2 $m.s^{-1}$) along the path of the freshwater outflow through the northwestern GSL, the southern GSL and Cabot Strait. Strong surface currents are also present in the northeastern Gulf owing to the inflow of Labrador Current waters through the Strait of Belle-Isle. The residual eastward component of the general cyclonic circulation is enhanced until early summer, whereas the westward component is strengthened thereafter, in response to the seasonal freshwater and wind forcing (Saucier et al. 2003, 2009). The St. Lawrence river freshwater runoff forms a buoyancy driven unstable baroclinic coastal jet along the south shore of the Gaspé peninsula, the Gaspé Current (GC). Through a buoyancy current, the transport in the first 30 m is increased by a factor of six at the mouth of the Lower Estuary and a factor of 10 through Honguedo Strait, when further adding the contribution from the westward circulation through the Jacques Cartier Strait. The GC is known to form instabilities

which can either join a quasi-permanent barotropic cyclonic gyre west of Anticosti Island, the Anticosti Gyre (AG), or propagate downstream through Honguedo Strait, generating pulses of surface estuarine waters downstream on the Magdalene Shallows (Tang, 1980; Reszka and Swaters, 1999; Sheng, 2001; Saucier et al., 2003). A second branch of the GC follows the deep Laurentian Channel (LC) farther east. Both branches join to exit the GSL through Cabot Strait about 4 to 6 months after freshwater exits the St. Lawrence River.

Another major oceanographic feature of the LSLE-GSL system is the Cold Intermediate Layer (CIL) located between c.a. 30 and 100 m (Banks, 1966; Koutitonsky and Bugden 1991; Gilbert and Pettigrew, 1997; Galbraith, 2006). The CIL is trapped in spring when the onset of stratification caps the near-freezing surface layer ($T < 0°C$ and $S = 32\text{-}33$) between a warm mixed surface layer ($T > 15°C$ and $S = 23\text{-}32$) and denser but warmer deep waters ($T = 4\text{-}6°C$ and $S = 34.6$) of North Atlantic origin (see below, Fig. II-5C). The mean circulation within the CIL shows a general cyclonic motion of about 0.1 $m.s^{-1}$ (Fig. II-4B). It is driven by the tidal "pumping" of intermediate waters at the head of the LC, inflow through the strait of Belle-Isle, and the surface circulation. The vertical shear prevailing between the surface and the intermediate circulation regimes is particularly relevant within the framework of this study and is the strongest at the mouth of the Estuary, and in the Honguedo Strait where it reaches its maximum during the

spring freshet.

The residual upstream circulation of the denser Atlantic layer below the CIL (Fig. II-4C) is mainly driven by fall and winter withdrawal in the Estuary, owing to reduced water column stability and tidal and wind driven mixing and entrainment. The mean velocity is about 0.01 $m.s^{-1}$. The transport of this deep water layer exhibits a strong seasonal pattern which is characterized by a relative isolation of the deeper layer (reduced withdrawal) during spring and summer, and maximum extraction (uplift and entrainment) during fall and winter. The mean residence time is 1.3 yrs between 150 m depth and the bottom. The mean simulated transit time between Cabot Strait and the Estuary is 2.7 yrs, in general agreement with Bugden (1991). While there are still gaps in our understanding of the circulation dynamics of the GSL, the sum of these recent studies give us confidence in the model's ability to produce realistic simulation of the variability of oceanic conditions in the GSL from tidal to seasonal time-scales.

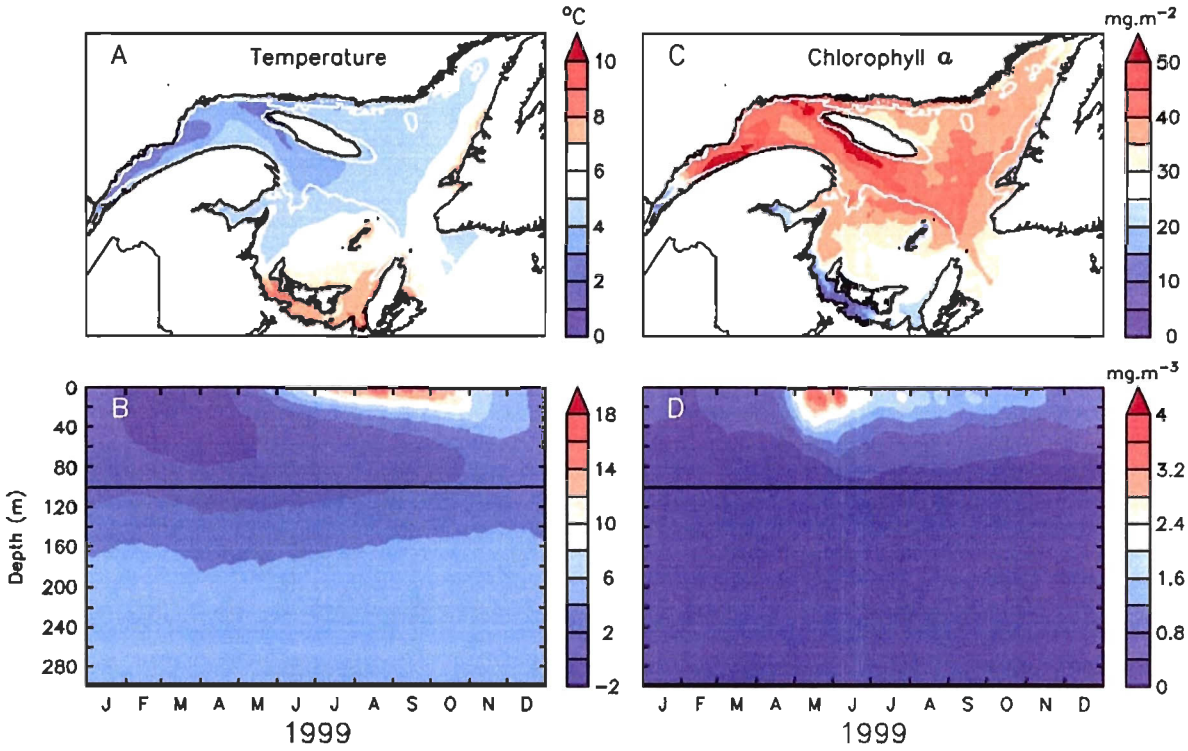


Figure II-5. Environmental conditions simulated for 1999 in the GSL. (A) Annual mean of temperature averaged between 0 and 30 m (°C). (B) Temporal evolutions of temperature (°C) horizontally averaged over the whole area deeper than 100 m. White line: 100 m isobath. (C) Annual mean of chlorophyll *a* integrated between 0 and 30 m ($mg.m^{-2}$). (D) Temporal evolutions of chlorophyll *a* ($mg.m^{-3}$) horizontally averaged over the whole area deeper than 100 m. Thin line : maximum depth (100 m) of migrating active copepodites.

The coupled 3-D physical – NPZD model provided two other important forcing fields (Fig. II-5). There is a clear gradient in the annual spatial pattern of temperature, averaged over the first 30 m of the water column (Fig. II-5A). The lower surface temperatures are found over the deep LSLE and north-west GSL, while warm temperatures are located over the shallow southern and eastern GSL. The circulation has a critical influence over this spatial pattern: the tidal "pumping" of CIL waters at the head of the LC is the main source of cold waters in the surface layer in the LSLE, while synoptic upwelling events along the north shore could act as local sources of cold waters along the north coast. Water masses from estuarine origin slowly warm up during their transit over the Magdalene Shallows (<70 m) in summer and fall. On the eastern margin of the GSL, the inflow of Atlantic Waters at Cabot Strait bring warmer waters along the shore of Newfoundland. The time evolution of the temperature averaged over the area of the GSL deeper than 100m clearly shows the seasonal trend and the formation of the CIL (Fig. II-5B). The coldest surface temperature occurred in February-March, whereas the warmest occurred between August and September. Warm temperatures (> 10°C) however remained constrained to the first 20 m of the water column by the CIL (< 2°C), which forms at the surface during winter and remains until late fall.

Chlorophyll *a* biomass integrated over the first 30 m of the water column shows an annual spatial gradient in complete opposition with the temperature

spatial pattern (Fig. II-5C). Chlorophyll biomass is highest in the LSLE, the north-west GSL and the Honguedo Strait area, and the lowest in the north-east and south-east GSL. The cold waters pumped at the head of the LC bring nutrients to the surface, which add to the nutrient load of the St Lawrence river run-off. Nutrients are then consumed by the primary production as the surface water masses follow the residual circulation. Over the deep LC, episodic events of strong wind mixing and upwelling maintain the nutrients level around their limiting concentrations, while on the shallower areas (Magdalene Shallows), the absence of this kind of nutrient inputs allows only regenerated primary production during most of the productive season. The phytoplanktonic bloom develops in cold waters in May and June, prior to the onset of thermal stratification of the water column (Fig. II-5D).

### *4.2 Comparison of observed and simulated patterns: the influence of circulation*

Data from the four monitoring stations located along the main west-to-east surface circulation axis in the GSL system (See Fig. II-1 and Fig. II-4A) provided information on the temporal trends, and the abundance patterns of the copepodite stages of *C. finmarchicus* within this advective area. We present the results for the C5 stage, which complete the life-cycle of the population through the diapause process in the deep layer, and C6f which produce the second generation of the

population within the productive surface layer. Both the 1-D and 3-D simulations of each scenario are presented.

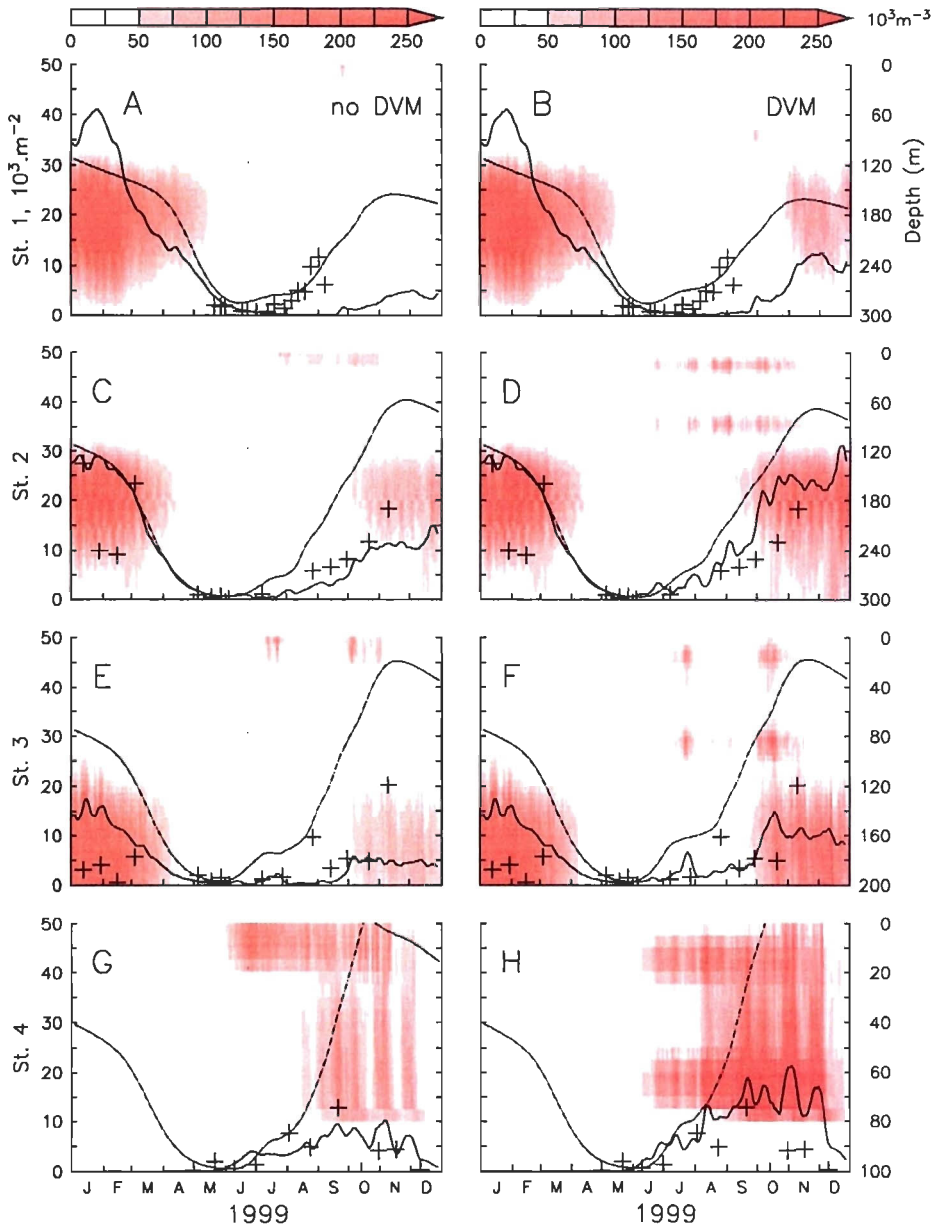


Figure II-6. Observed (crosses) and simulated (Dashed line: 1-D; continuous line: 3-D simulations) vertically integrated abundances ($10^3.m^{-2}$) of *C. finmarchicus* total C5 (active and diapausing). Background shading: simulated vertical densities ($10^3.m^{-2}$) of active and diapausing C5 at the stations locations. Left column: simulations for the no-DVM migration scenario. Right column: simulations for the DVM migration scenario. Observations are the same in both cases. (A-B) Station 1. (C-D) Station 2. (E-F) Station 3. (G-H) Station 4.

The abundance of the total C5 (active and diapausing components) simulated within the 1-D framework were similar between both the no-DVM (Fig. II-6, left column) and DVM (Fig. II-6, right column) scenarios. Simulated abundances generally increased from station 1 to station 4, because of a lower cumulative mortality of *C. finmarchicus* stages driven by shorter development in response to positive gradient in temperature. 1-D simulations overestimated observations in each station except at station 1, which is characterized by a short period of sampling and a sharp increase in abundance of C5 in late summer (Fig. II-6A, 6B). Observed abundances of C5 at each station showed a typical seasonal pattern with high abundances in winter in the deep LC (St. 2), a minimum in the abundance of C5 in May-June and the build-up of the diapausing C5 stock in late summer-early autumn (Runge and de Lafontaine, 1996; Plourde et al., 2001; Zakardjian et al., 2003). The observed differences between the stations are well reproduced by the 3-D simulations, which took into account the impacts of the circulation. It shows a lower abundance of C5 at the coastal station 3 in late winter and late autumn (in diapause in the model), and the late appearance of C5 in early summer at the shallow station 4. Simulated abundances of C5 were lower in the 3-D than in the 1-D simulations, and they were generally underestimated relative to observation in the no-DVM scenario. The 3-D DVM scenario produced a better match with the observations. Comparing 1-D and 3-D results, station 2 appeared to be the least affected by the hydrodynamics in the DVM scenario. On the contrary, the strong

vertical shear in the estuarine circulation affected the abundance pattern of C5 at station 1, where deep dwelling diapausing C5 were advected upstream in winter, and surface-dwelling early stages were flushed downstream in summer.

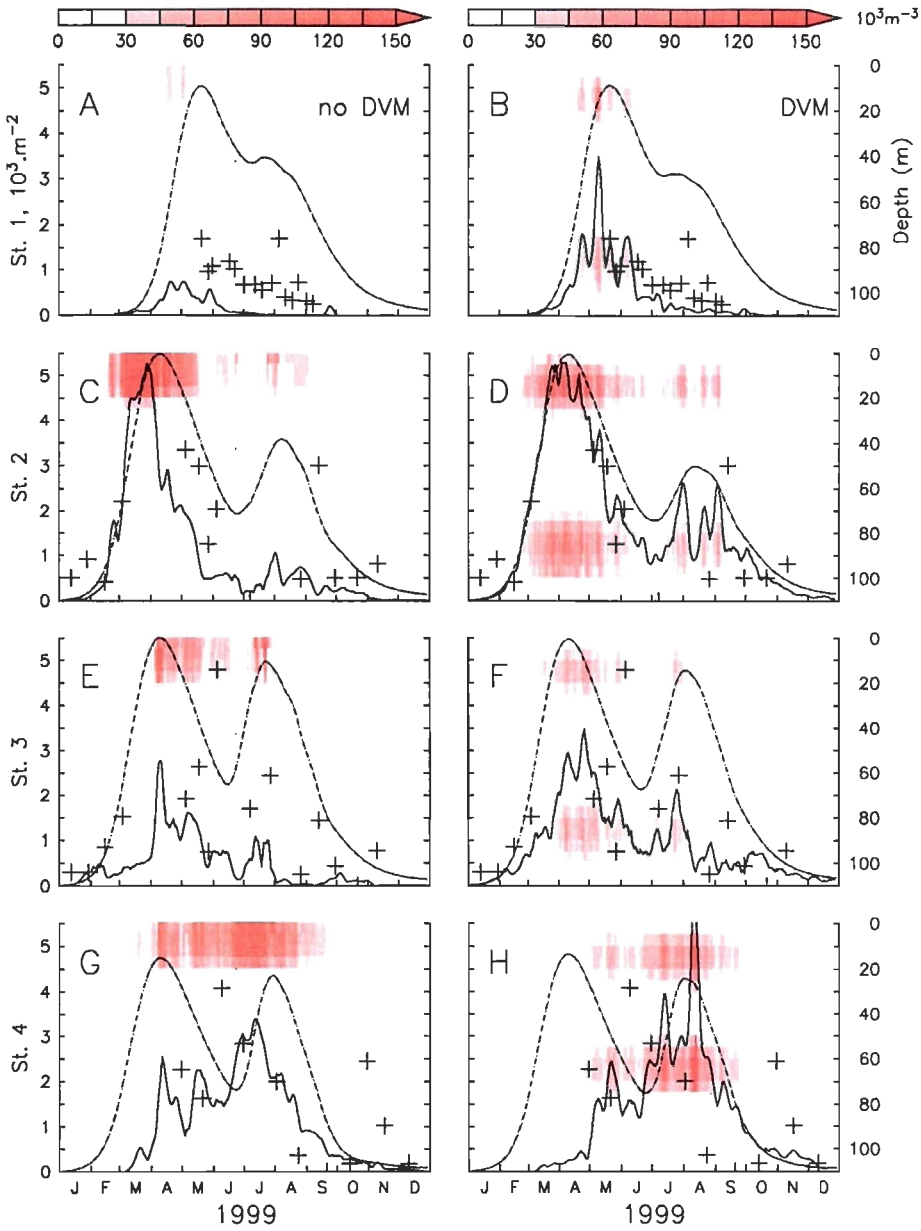


Figure II-7. Observed (crosses) and simulated (Dashed line: 1-D; continuous line: 3-D simulations) integrated abundances ($10^3.m^{-2}$) of C. finmarchicus C6f. Background shading: simulated vertical densities ($10^3.m^{-2}$) of C6f at the stations locations. Left column: simulations for the no-DVM migration scenario. Right column: simulations for the DVM migration scenario. Observations are the same in both cases. (A-B) Station 1. (C-D) Station 2. (E-F) Station 3. (G-H) Station 4.

No major differences in the simulated abundances of C6f appeared either within the 1-D framework between the no-DVM (Fig. II-7, left column) and DVM (Fig. II-7, right column) scenarios. The 1-D simulations results overestimated observations in every station, and simulated abundances of the second generation of C6f increased from station 1 to station 4 in both scenarios, following, again, the spatial gradient in temperature. The major issue revealed by the analysis of the C5 remained valid for the C6f; the observed local differences between the stations are better reproduced by the 3-D simulations for the DVM scenario, for at least three of the four stations. Moreover, station 2 appeared to be the least affected by the hydrodynamics when DVM behavior occurred (Fig. II-7C, D). However, circulation dramatically affected the abundance of C6f at station 1, where surface-dwelling C6f were largely flushed downstream in the no-DVM scenario. Results from both scenarios did not convincingly matched the observations at the shallow station 4. For this location, the no-DVM scenario seemed however to better reproduce observations.

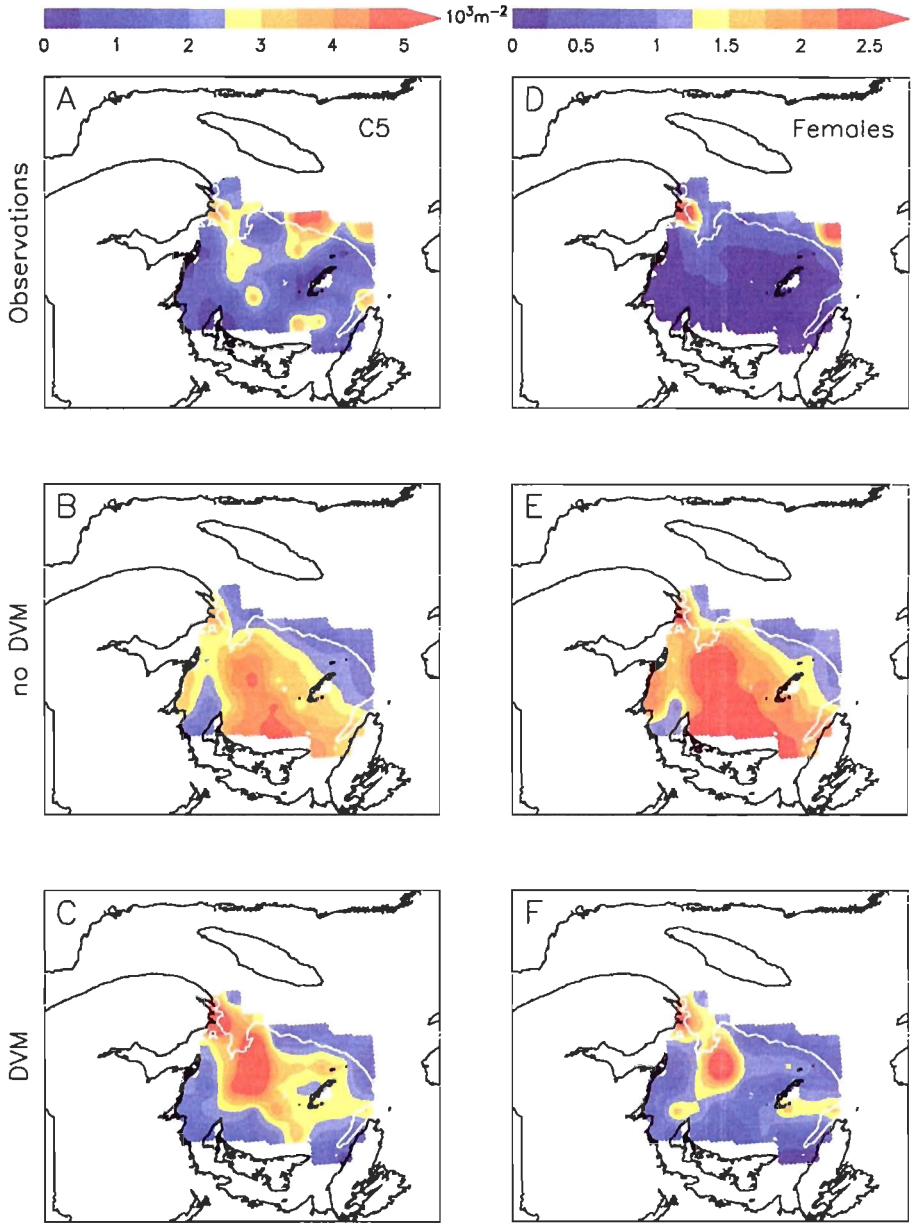


Figure II-8. Integrated abundances ($10^3.m^{-2}$) of *C. finmarchicus* total C5 (left column) and C6f (right column). (A, D) Observations from the 19th to the 25th of June 1999 over the Magdalene Shallows. Results from the (B, E) no-DVM and the (C, F) DVM scenario were sampled in space and time following the cruise track, and then interpolated in the same way as the observed abundances. The white line indicates the 100m isobath.

The distributions of C5 and C6f of *C. finmarchicus* observed on the Magdalene Shallows in late June 1999 allow the assessment of the realism of the spatial patterns simulated for these stages in both the no-DVM and DVM scenarios (Fig. II-8). Observations showed that a major proportion of C5 (Fig. II-8A), and almost all of the C6f (Fig. II-8D) were constrained by the steep slope at the southern limit of the LC, around the 100 m isobath. The deeper Shediac Valley off the Gaspé peninsula seemed to be the route taken by some C5 and C6f to spread over the Magdalene Shallows (Fig. II-8A, D). However , our scenarios leaded to marked differences. In the no-DVM scenario, C5 and C6f distributions were similar, with maximum abundances in the central and southern Magdalene Shallows (Fig. II-8B, E). In the DVM scenario however, maximum abundances were located close to the tip of the Gaspé peninsula, and immediately downstream of the Shediac Valley (Fig. II-8C, 8F). The overall distributions of both stages were patchy, forming spatial patterns closer to the observations than what resulted from the no-DVM scenario.

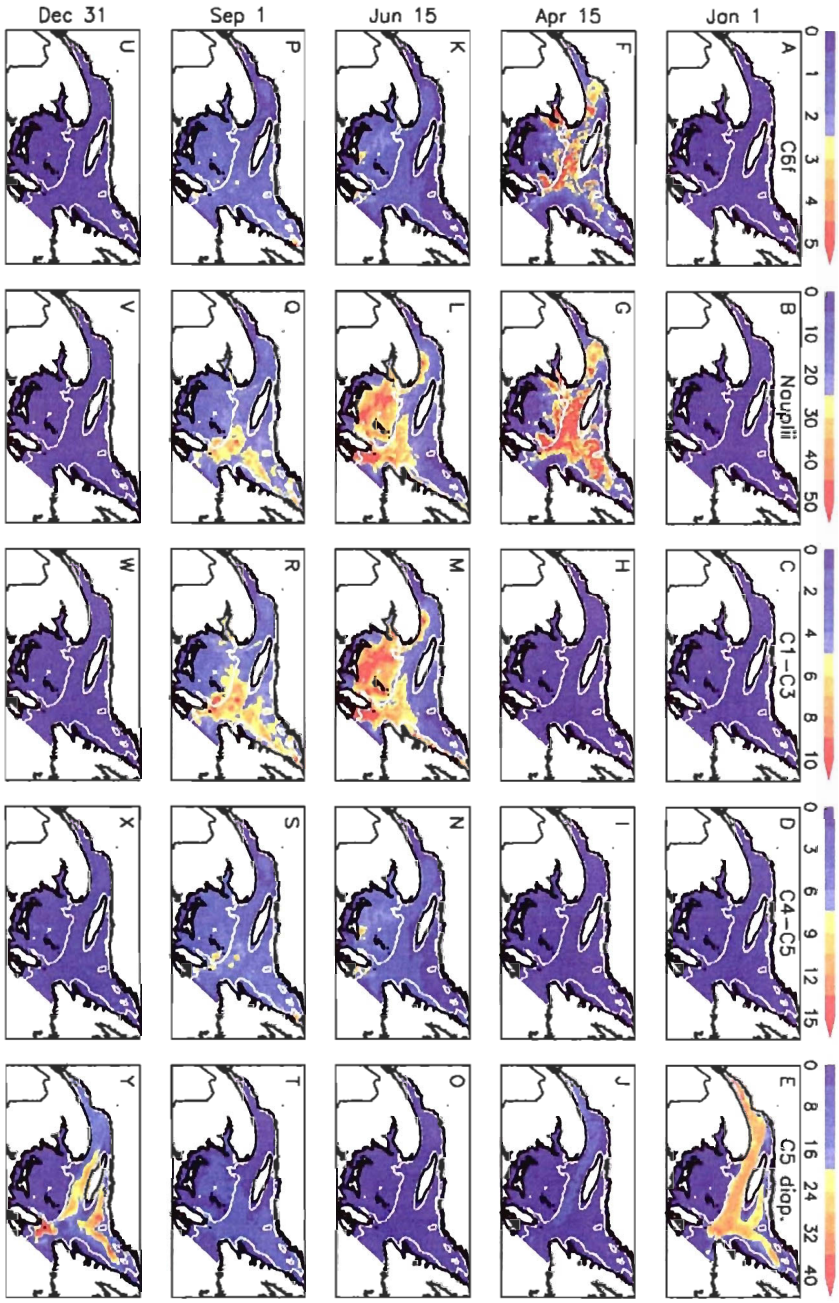


Figure II-9. Simulated vertically integrated abundances ($10^3.m^{-2}$) of development stages of *C. finmarchicus* for the no-DVM scenario. First column: C6f. Second column: nauplii. Third column: copepodites 1 to 3. Fourth column: copepodites 4 and 5. Fifth column: C5d. First row: 1st of January 1999. Second row: 15th of April. Third row: 15th of June. Fourth row: 1st of September. Fifth row: 31st of December.

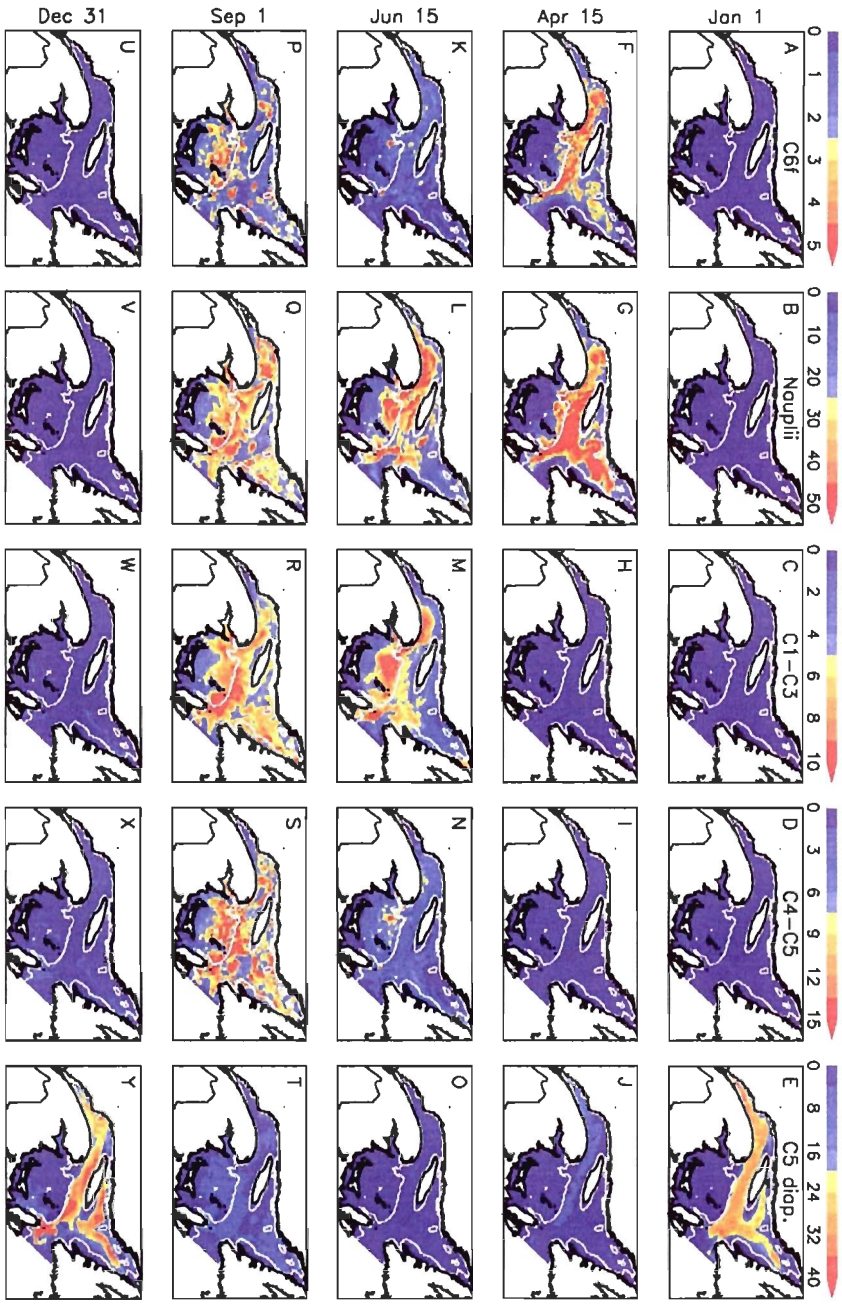


Figure II-10. Simulated vertically integrated abundances ($10^3.m^{-2}$) of development stages of *C. finmarchicus* for the DVM scenario. First column: C6f. Second column: nauplii. Third column: copepodites 1 to 3. Fourth column: copepodites 4 and 5. Fifth column: C5d. First row: 1st of January 1999. Second row: 15th of April. Third row: 15th of June. Fourth row: 1st of September. Fifth row: 31st of December.

### *4.3 DVM vs. no-DVM impacts on the simulated C. finmarchicus dynamics*

For both migration scenarios the population was composed exclusively of diapausing C5d, located in the deepest parts of the GSL at the beginning of 1999 (Fig. II-9E, Fig. II-10E). Differences among scenarios appeared in April with females and nauplii of the first generation. In the no-DVM scenario, C6f recently molted in April (Fig. II-9F) and the first generation of nauplii (Fig. II-9G). Both C6f and nauplii were mainly located over the west and central LC, but also deep within the Baie-des-Chaleurs and the Shediac Valley. They were less abundant in the LSLE and the eastern GSL, owing to the St Lawrence freshwater runoff and the inflow of Atlantic waters through Cabot Strait, respectively. The patchy distribution of these stages formed complex mesoscale structures. In June, the abundance of females was low (Fig. II-9K) and the population structure was dominated by nauplii (Fig. II-9L) and early copepodite stages (Fig. II-9M). The production area was displaced south and east, and the resulting distributions over the Magdalene Shallows were more homogeneous in summer than in spring. High abundances of nauplii and early copepodites were found south of Cabot Strait. In the western GSL, high abundances remained within the Gaspé Current instabilities. In September, the production area of the second generation moved further eastward (Fig. II-9Q, 9R). The highest abundances were found for all the stages within the Cabot Strait area, south-east off

Anticosti Island and within the north-east GSL, while the lowest were in the LSLE and west GSL. The abundances of active C5 and diapausing C5d increased (Fig. II-9S, 9T) while the abundances of the larval stages decreased. Finally, the last day of 1999 the C5d stock was formed within the deepest parts of the GSL (Fig. II-9Y). An eastward spatial gradient appeared, with abundance of C5d comparable to the initial conditions only east of Honguedo Strait.



For the DVM scenario, the distribution of C6f (Fig. II-10F) and nauplii (Fig. II-10G) in April corresponded well to the previous distribution of the C5d stock, which was constrained by the topography of the GSL (Fig. II-10E). The abundance of C6f, and thus the abundance of the newly produced nauplii, were high in the north-west, and north-east GSL and in the central LC. However few females were found over the Magdalene Shallows (Fig. II-4B). The low abundances along the eastern margin of the GSL resulted from the inflow of Atlantic waters through Cabot Strait, as in the no-DVM case. In June, C6f from the first generation (Fig 10K), nauplii (Fig 10L) and copepodites stages (Fig. II-10M, 10N) remained present within the whole GSL system. The stage structure of the population was dominated by nauplii and early copepodite stages, and the major production areas were located in the western GSL, the northern half of the Magdalene Shallows, and the central LC until west of Cabot Strait. The lowest abundances were found on the southern half of the Magdalen Shallows and in the north-east GSL. In early September, the second generation of

C6f (Fig. II-10P) was well established in the GSL, with highest abundance on the Magdalen Shallows, while the second generation of nauplii (Fig. II-10Q) and copepodites (Fig. II-10R, 10S) was still abundant in the whole GSL system. Finally, in December the diapausing C5d stock was mostly observed in the deeper areas of the region (Fig. II-10Y). The abundance of C5d were slightly higher than the initial conditions, but the distribution similar, except for the upstream LSLE.

### *4.4 Spatio-temporal scale of variability revealed by EOF analysis*

The EOF analysis was focused on three stages or groups of stages: (1) total C5 which could present DVM behavior as active C5 and which closed the life cycle of the population with the diapause process within the deep layer of the GSL, (2) C6f which could perform DVM between the surface layer and the CIL and whose dynamics governed the production of the new generations and (3) Nauplii which remained associated to the surface layer in both migration scenarios and initiated the new generations. The annually averaged abundances of each of the three development groups are presented in fig. II-11. The first three EOF modes together accounted for approximately 70% to 90% of the variance in the abundance of each stage analyzed in both migration scenarios (Table II-4).

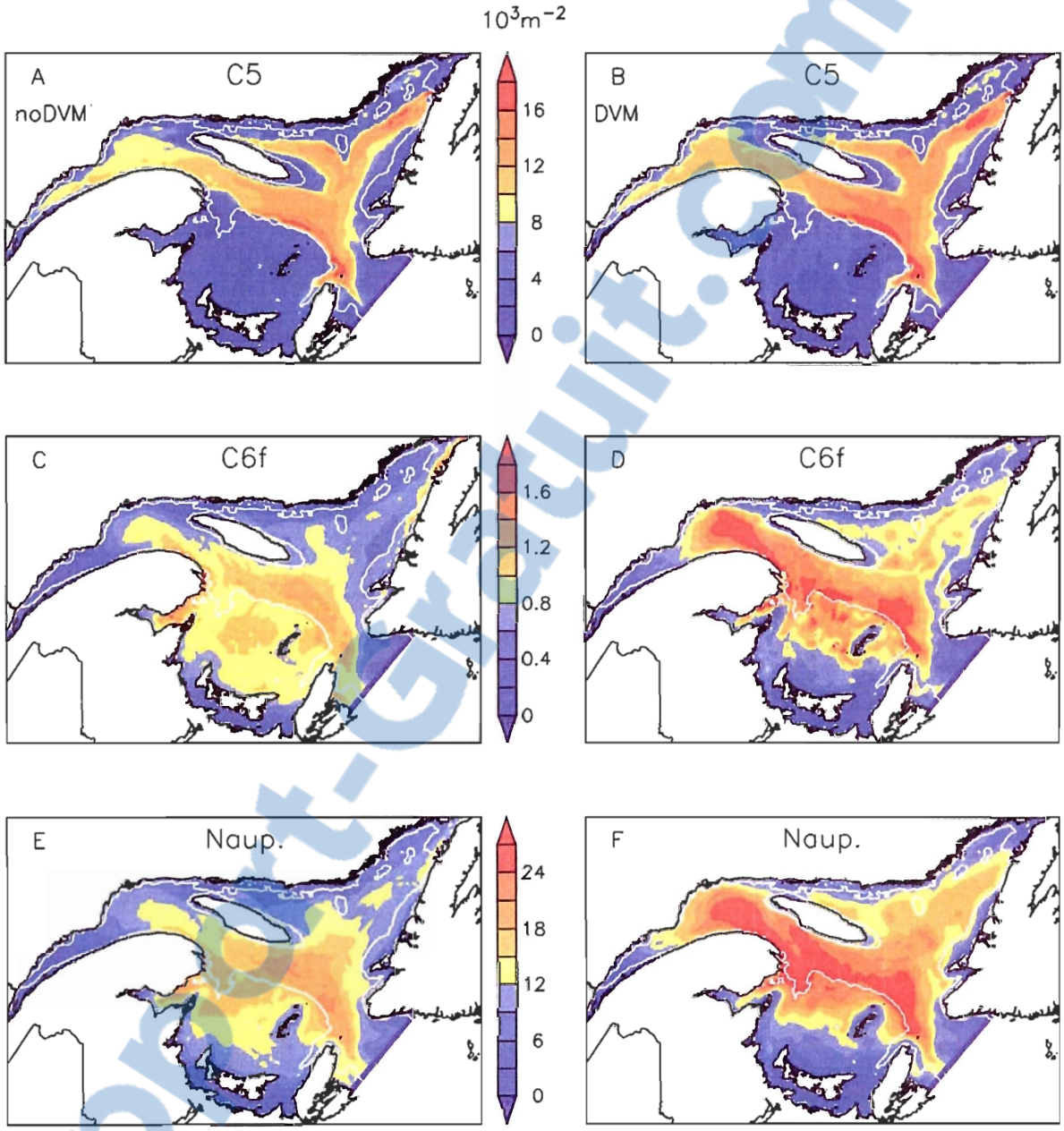


Figure II-11. Annual average abundances of total C5 (Upper row), C6f (Middle row) and nauplii (Lower row) from the no-DVM (Left column) and DVM (Right column) scenarios. White line: 100 m isobath.

Table II-4. Proportion of the variance of the abundance of total C5 (active and diapausing), C6f and nauplii from both migration scenarios accounted for by the first three modes of the Empirical Orthogonal Functions (EOF) analysis.

| no-DVM / DVM | EOF 1 (%) | EOF 2 (%) | EOF 3 (%) |
|---|---|---|---|
| C5-C5d | 64.4 / 68.1 | 22.1 / 15.6 | 4.3 / 4.5 |
| C6f | 45.2 / 45.2 | 26.1 / 19.6 | 5.7 / 3.7 |
| Nauplii | 60.3 / 60.8 | 14.9 / 11.3 | 6.7 / 4.9 |

The first EOF mode accounted between 45 and 70 % of the variability in abundance (Fig. II-12). This mode was characterized by coherent variations (positive eigenvalues only) over the whole GSL, according to a bimodal principal component (PC) corresponding to the production of the two generations. In general, the second generation of *C. finmarchicus* appears earlier in the no-DVM scenario, but it has a stronger contribution to the spatio-temporal patterns in the DVM scenario. This reflects the influence of colder temperature on the development times of the stages performing DVM within the CIL, and it also enlightens the sustained productivity in the western and northern GSL, owing to the greater retention of the developing population in the DVM scenario (Fig. II-12F, 12I). Thus the first EOF mode quantified that about half to two-third of the spatio-temporal variability in the abundance of the stage analyzed was explained by the response of *C. finmarchicus* to its environment in terms of demographic processes (timing of diapause, development times, egg production, etc.).

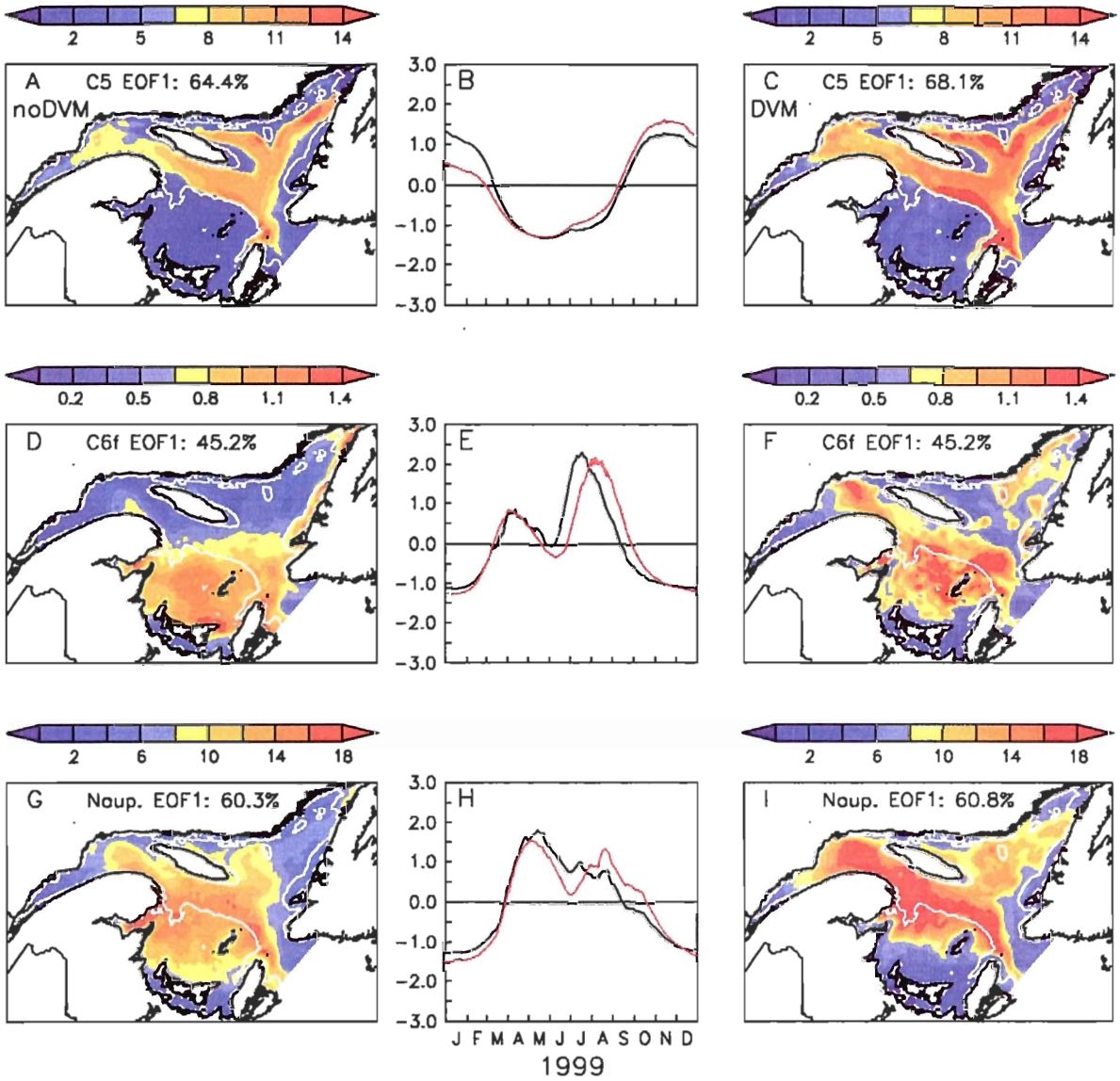


Figure II-12. Eigenvalues and associated principal components of the first modes of the Empirical Orthogonal Functions (EOF) analysis of the vertically integrated abundance of total C5 (Upper row), C6f (Middle row) and nauplii (Lower row) from the no-DVM (Left column) and DVM (Right column) scenarios. Middle column: principal components; black line: no-DVM scenario; Red line: DVM scenario.

Specific response to the environmental forcing appeared in the successive second and third EOF modes. The second EOF mode accounted for about 11 to 26% of the variance in the abundance of the stages (Fig. II-13). This mode showed for each scenario a clear dichotomy between the first generation of females and nauplii, occurring in spring over the deepest part of the GSL, and the second generation developing over the shallow southern GSL and along the east and north shores. The contrasted pattern revealed by the second EOF mode probably reflected the imprint of the surface residual circulation at the regional and seasonal scale on the two successive generations of *C. finmarchicus* in the LSLE-GSL system, during the period delimited by the exit from and the entry into diapause.

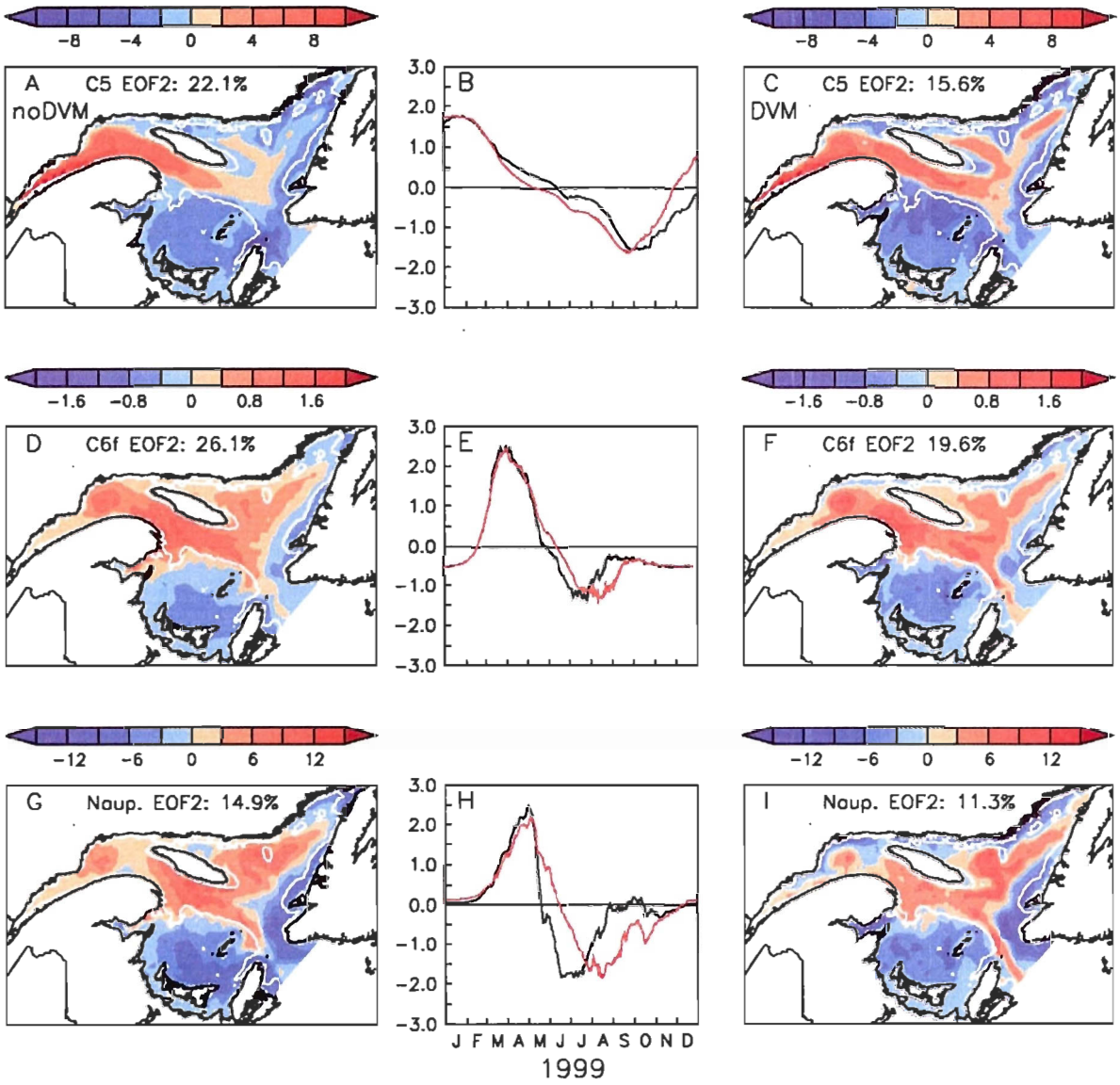


Figure II-13. Eigenvalues and associated principal components of the second modes of the Empirical Orthogonal Functions (EOF) analysis of the vertically integrated abundance of total C5 (Upper row), C6f (Middle row) and nauplii (Lower row) from the no-DVM (Left column) and DVM (Right column) scenarios. Middle column: principal components; black line: no-DVM scenario; Red line: DVM scenario.

Finally, the third EOF mode accounted for approximately 4 to 6% of the variance in the abundance of the stages (Fig. II-14 and Fig. II-15). It brought however some relevant information for the C6f and nauplii stages. There were important differences between both migration scenarios for C6f (Fig. II-14). In the no-DVM scenario, the third EOF showed an important contribution to the spatial pattern of abundance of C6f from the deepest part of the GSL in February and March, excluding the LSLE (Fig. II-14A). An abrupt shift occurred later between April and May (Fig. II-14B) when the influence of C6f increased in the LSLE, within the GC and over the Magdalene Shallows. This corresponds to the distinct timing of arousal from diapause for females from the GSL and the LSLE (see Fig. II-2). In the DVM scenario, the third EOF mode described a patchy spatial pattern of variability (Fig. II-14C) characterized also by an abrupt shift, but occurring in summer in this case (Fig. II-14D). According to this mode, in early summer C6f in the downstream estuarine flow, within the instabilities of the GC, over the northern half of the Magdalene Shallows and off south-west Newfoundland contributed more to the distribution pattern. From August onward, the more important distribution areas are found in the Baie-des-Chaleurs and southern Magdalene Shallows, in the south-east LC, the north-east GSL and along the north coast of the GSL and LSLE. This spatio-temporal pattern presented striking similarities with the second dominant mode of variability of surface temperature (Fig. II-14E). Beyond the overwhelming contribution of the seasonal trend in surface temperature (94.8% of the variance

explained by the first EOF mode of temperature), the second EOF mode of surface temperature reflects the seasonality of the surface circulation. In the DVM scenario, the third EOF mode mainly represented the impacts of the mesoscale surface circulation on the second generation of C6f. For nauplii however, the third EOF mode revealed spatio-temporal patterns similar for both migration scenarios (Fig. II-15). The first generation of nauplii appeared in the north-east GSL in early spring, but it rapidly spread in the west and south GSL, where the production remained until late summer when north-east GSL once again contributed more to the distribution pattern of the second generation. This pattern mimics in spring the second dominant mode of variability in chlorophyll *a* (Fig. II-15E, 15F). The clear distinction between the importance of the central and north-east GSL before the end of April, and the west and south GSL thereafter reflects the detrimental effect of both the flushing by the spring freshet (Zakardjian et al., 2000) and the turbidity of estuarine water masses on the phytoplankton productivity in the western GSL in spring (Le Fouest et al., 2005). Hence the third EOF mode of the abundance of nauplii reflect the impact of the spatio-temporal patterns of the spring phytoplankton bloom on the production of offspring by the females.

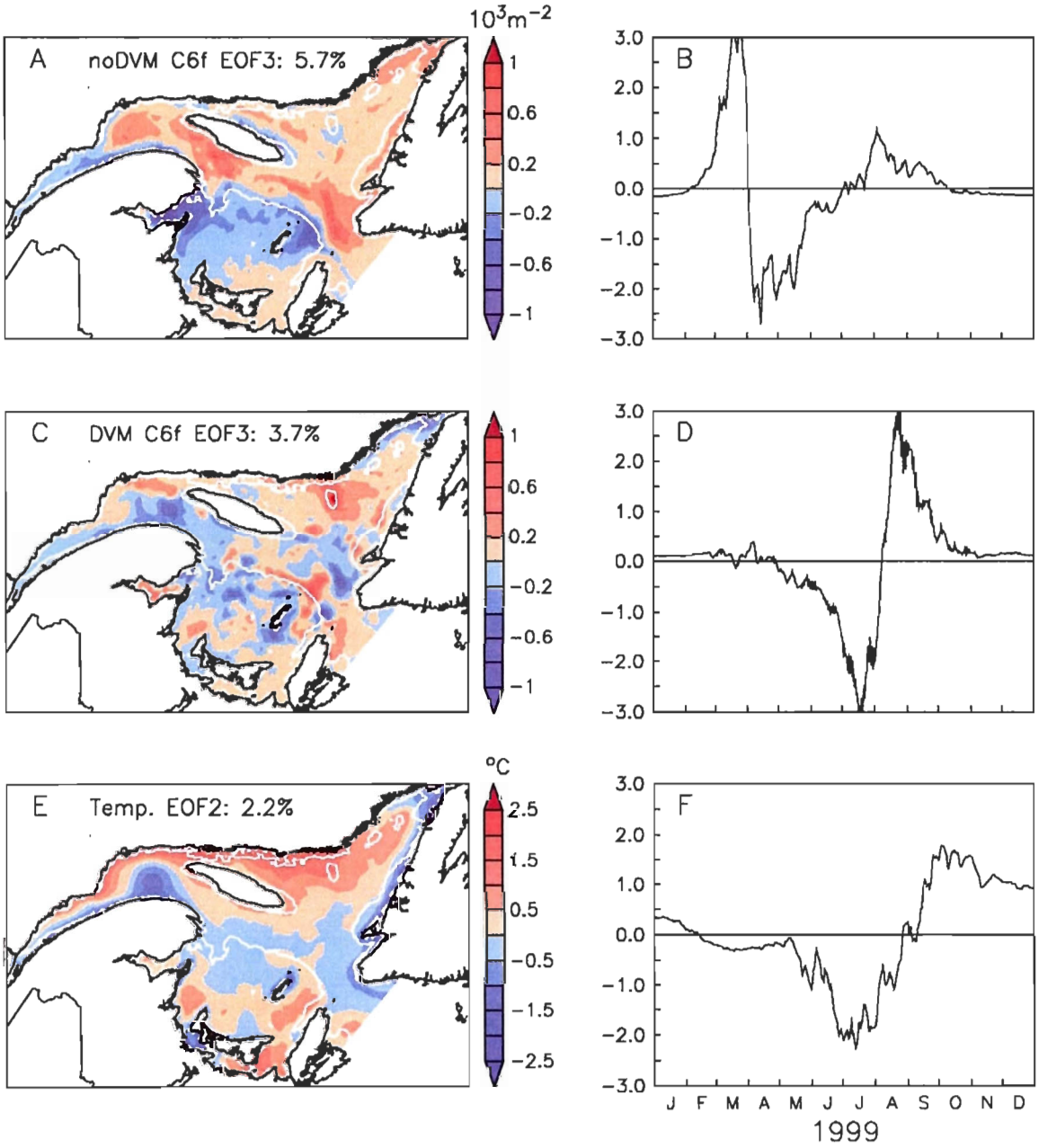


Figure II-14. Third modes of the Empirical Orthogonal Functions (EOF) analysis of the vertically integrated abundance of (A-B) C6f from the no-DVM scenario and (C-D) C6f from the DVM scenario. (E-F) Third mode of the EOF analysis of temperature vertically averaged between 0 and 30 m.

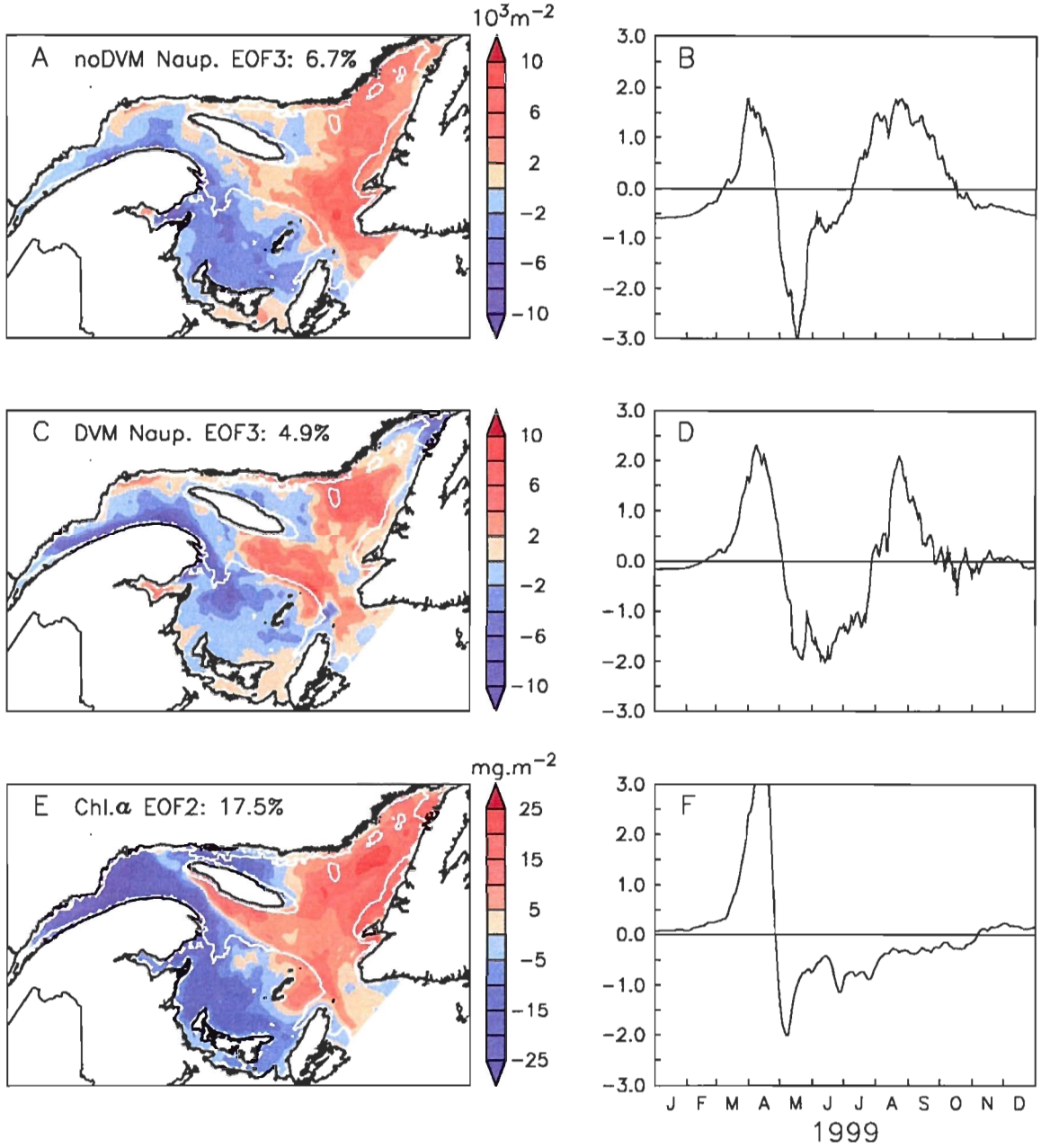


Figure II-15. Third modes of the Empirical Orthogonal Functions (EOF) analysis of the vertically integrated abundance of (A-B) nauplii from the no-DVM scenario and (C-D) nauplii from the DVM scenario. (E-F) Third mode of the EOF analysis of chlorophyll *a* vertically integrated between 0 and 50 m.

### 4.5 *Influence of the open boundaries*

When the monthly climatology of *C. finmarchicus* abundance of St. 27 (Fig. II-16A) was imposed at the open boundaries, the amount of diapausing C5 at the end of the simulated year is increased by 13.6% and 11% in the no-DVM and DVM scenario, respectively (Fig. II-16B, 16C). The lower productivity of the no-DVM scenario explained this difference. In both scenario, the anomaly of abundance of C5d extended from the Cabot Strait area toward the north-east GSL, along the Newfoundland coast. The influence of inflows of Labrador Current waters through the Strait of Belle-Isle appeared limited compared to inflows of surface and deep Atlantic waters through Cabot Strait. A dense aggregation formed south-west off Newfoundland, owing to the deep circulation patterns. The high abundance of C5d found in this area ($> 10^4.m^{-2}$) corresponds to the concentration imposed at the Cabot Strait boundary in December (Fig. II-16A). Hence the contribution of the surface dwelling productive stages seems of little importance to the overall population dynamics of *C. finmarchicus* in the GSL.

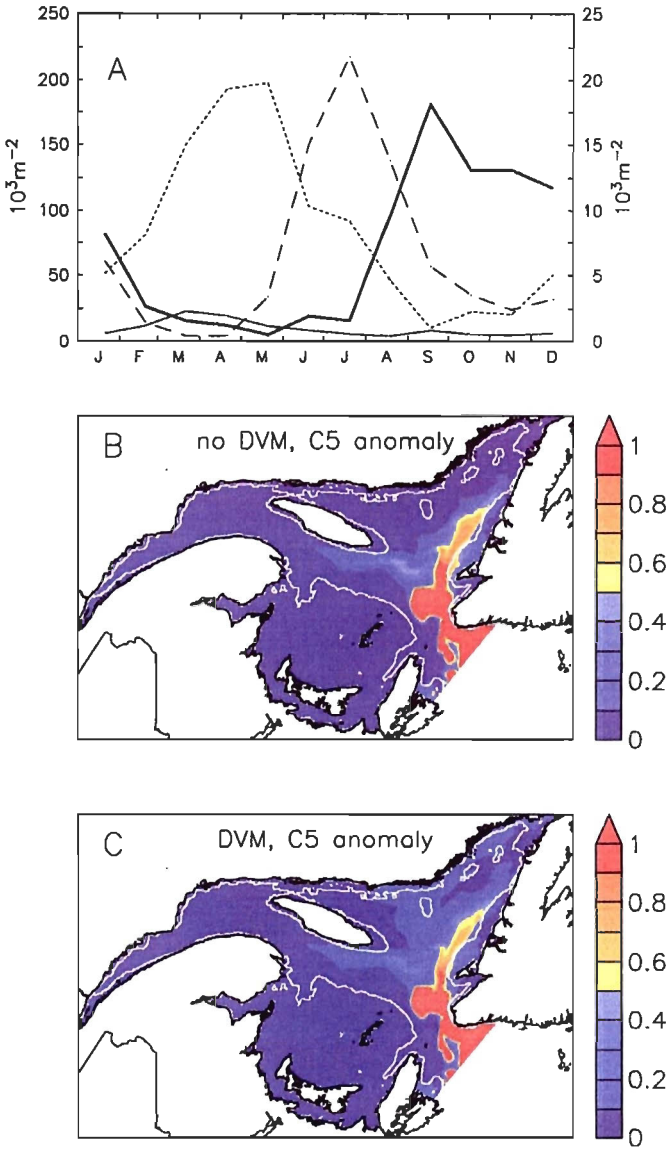


Figure II-16. (A) Time series of the climatological abundances of *C. finmarchicus* obtained at St. 27. Dotted line: integrated abundance of nauplii, left-hand scale. Dashed line: copepodites 1 to 3, right-hand scale, as each following stages. Bold line: copepodite 4 and 5 (active and diapausing). Continuous line: adult females. Anomaly (in proportion) of the vertically integrated abundance of C5d the 31$^{st}$ of December 1999 for the (B) no-DVM and (C) DVM scenario, between a simulation with the climatology of *C. finmarchicus* stage structure imposed at the open oceanic boundaries, and a simulation without import of *C. finmarchicus*.

# 5 Discussion

## *5.1 Response to environmental variability*

A major consequence of the increase in the surface temperature experienced in different sub-regions in the GSL was an increase in net productivity in the 1-D simulations, which was clearly observed in the greater abundance of C5d at the end of the growing season along the general positive temperature gradient from station 1 to 4 (Fig. II-5A; Fig. II-6). This greater net recruitment at higher temperature resulted from a shorter development time of the surface-dwelling early stages leading to a reduced cumulative mortality during development, despite an increase in mortality prescribed in the model when temperature exceeds 10°C. The presence of the CIL induced a delay in the maturation of the second generation in the DVM scenario because of the longer development times of the copepodite stages (C4-C5) migrating within the CIL. The overall productivity between both scenarios remained similar because the low mortality rates of the migrating stages (Table II-3) had little influence on the cumulated mortality of the population, as egg and naupliar stages experienced much greater mortality rates in our model.

In the 3-D simulations, the no-DVM scenario showed a lower overall

productivity (lesser overwintering stage abundance) relative to the DVM scenario (Fig. II-9-12). This partly reflected the influence of chlorophyll *a* concentration on the egg production rate of females. The concurrent but opposite eastward motion of *C. finmarchicus* population (Fig. II-9) and westward increase in primary production during summer (Fig. II-5B) resulted in a spatial mis-match hindering the population egg production. Taking into account the impacts of hydrodynamics by coupling the model with the 3-D circulation model was actually critical to get a realistic representation of the patterns of abundance of *C. finmarchicus* stages in the GSL system (Fig. II-6-7). The observed and simulated time series at the monitoring stations in the western GSL showed three distinct regimes: the upstream LSLE (St. 1), the north-west AG-GC area (St. 2 and 3), and the downstream western Magdalene Shallows (St. 4). Advection plays an essential role in the connectivity between these locations. The model simulations allowed to "fill the gaps" between the stations and to characterize the spatio-temporal scale of variability across the whole system. According to the results, the DVM in late copepodite stages positively impacted abundances and generally lead to a better simulation of observed temporal patterns in a system characterized by important vertical shears between the surface (downstream residual currents, Fig. II-5A) and the CIL (upstream residual currents, Fig. II-5B), as well as important meso-scale horizontal circulation features. The spatial pattern remained however conditioned by the topography and the pattern of ontogenetic migrations associated to the diapause (Fig. II-13).

## 5.2 *Diel vertical migrations*

The DVM behavior emerged as a critical feature of the population dynamics of *C. finmarchicus* in the LSLE-GSL system. However DVM has been mostly overlooked in region-scale 3-D modeling studies of the dynamics of *C. finmarchicus* (Bryant et al., 1997; 1998; Lynch et al., 1998; Miller et al., 1998; Speirs et al., 2005, 2006). The differences in the distribution patterns between both migration scenarios resulted essentially from direct interactions between the migration behavior of late copepodites and both hydrodynamic features and the steep topography of the GSL. Relative to the no-DVM scenario, DVM promoted the maintenance of the first generation in the north-west and central GSL. Later in summer, it hindered the transport of late copepodite stages in the surface outflow near Cabot Strait. These findings agree with the patterns revealed in a previous study of the interactions between the hydrodynamics and the migration behavior of zooplankton within the Irish Sea, in the north-east Atlantic continental shelf (Emsley et al., 2005). Without the DVM behavior, the second generation of C6f was concentrated in the south-east GSL in late June – early July, within strong surface outflow on the south side of Cabot Strait (Fig. II-4A). This scenario resulted in a massive export of the second generation of *C. finmarchicus*. Losses by advection at the open boundaries of the system in the no-DVM scenario was 5 to 10 times greater than losses estimated in the DVM simulation. In the no-DVM scenario, egg mortality was increased relative

to the DVM scenario mainly because of a greater egg loss to the bottom owing to the displacement of the C6f over the shallow southern GSL. Thus, in the absence of DVM, interactions between hydrodynamic and demographic processes lead to a poor representation of abundance patterns in the western GSL (Fig. II-6-7), unrealistic spatial structures (Fig. II-8) and a marked west to east spatial gradient, even in the winter diapausing stock (Fig. II-9Y). The contribution of the populations from the surrounding continental shelf are limited to the central and eastern GSL (Fig. II-16B-C), and hence is not likely to counter this tendency.

The year-round maintenance of the *C. finmarchicus* population in the GSL system requires a mechanism for the population to avoid the losses due to the eastward residual surface circulation. *C. finmarchicus* late copepodite stages should migrate between the surface layer and its underneath counter current within the CIL to remain in the western LSLE-GSL system. According to the 2-D modeling study of Zakardjian et al. (1999), individuals should stay four times longer within the CIL to compensate for the flushing at the surface. However, the 3-D spatio-temporal pattern in circulation considerably alters this theoretical 2-D dynamics. Sourisseau et al. (2006) explored with a model of swimming krill coupled to the same 3-D circulation model as ours, the potential for krill populations to form dense aggregations at the head of the LC. They did not manage to reproduce the dense aggregations observed with their diel migration scenario, but they stressed that the

upstream advection along the northern shore of the estuary and north-west GSL should play a key role. Analysis of the fluxes at the LSLE mouth in our simulations (not shown) revealed that upstream inflow of *C. finmarchicus* can be as high at the surface along the north shore as within the CIL in late summer – early autumn, when the overwintering deep-dwelling stock is formed. Upstream surface advection resulted from the interactions between the instabilities of the GC and the quasi-permanent AG, which could generate synoptic, high-frequency recirculation features along the the north shore of the north-west GSL (See Fig. II-10Q, R, S). However the presence of the diapausing population during fall and winter within the residual upstream currents of the deep layer remained essential for the persistence of the population in the GSL. Our formulation of the diapause process could even have underestimated the contribution of the C5d stage, if more of the first generation of C5 were to enter diapause in summer. A fixed proportion of each generation of C5 entering diapause is indeed an alternative formulation, which is yet only supported by its simplicity and apparent efficiency in different situations (e.g. Miller et al. 1998, Tittensor et al. 2003, Speirs et al. 2006, Slagstad and Tande 2007).

In our DVM scenario, the diel and ontogenetic vertical migrations of *C. finmarchicus* ensures the presence of the population within the most dynamic upstream flow regimes, according to the season: migrating stages within the CIL in spring and summer and diapausing stage in the deep layer in autumn and winter.

The inclusion of DVM also promotes accumulation, compression and retention, or dispersion processes at the relevant spatio-temporal scales (Mackas et al., 1985; Malchow et al., 2001). Interactions between the swimming abilities of migrating stages and the horizontally or vertically sheared currents shape the spatial scale of the plankton patchiness in the system (Franks,1992; Genin et al., 2005). In this regional study, the importance of the interactions between the migration behavior and advection contrasts with the oceanic basin scale situation, where those interactions are of limited relevance with respect to the perennial spatio-temporal patterns of the *C. finmarchicus* population (Speirs et al., 2006). DVM does not seem to confer any adaptive advantage to the open ocean hydrodynamic environment. However, in the deep oceanic basins stage-specific ontogenetic position in the water column is a useful adaptation to escape during diapause the bad environmental conditions of the mixed surface layer, deepened by the strong winter-time mixing processes.

The migration behavior remains a schematic deterministic function of our model, which is in part responsible for the remarkable match between the spatio-temporal scales in vertical migrations and the vertical shear of the currents. Spatio-temporal variability is likely to occur in reality (Heywood, 1996), and results of our simulations did not rule out the possibility of a more flexible behavior for some of the stages. Copepods face the constant need to balance immediate constraints like

the requirement for food, the visual predation risk in surface waters and the reduced growth in cold waters. The environmental conditions prevailing during the spring phytoplankton bloom are characterized by a relatively homogeneous temperature profile, high food concentration and low predators biomass. Hence, limited migrations could benefit the females in spring (Lampert et al., 2003; Liu et al., 2003). Then, the onset of the DVM should coincide with the following increase in zooplankton biomass, as late copepodite stages can reduce predation risk by migrating within (or beneath) the CIL. Thus the complex DVM behavior could be, in a further step, mechanistically formulated in terms of weighted influences on the swimming behavior of the light penetration profile, the depth of the CIL and the depth of the maximum phytoplankton concentration (Batchelder et al., 2002; Liu et al., 2006; Neumann and Fennel, 2006). However, more field observations are needed to support such developments, and population level models such as ours still lack the ability to take into account the physiological conditions of the individual, for example.

### *5.3 Influence of circulation regimes*

The analysis of the coupling between the life-cycle of *C. finmarchicus* and the 3-D circulation in the western GSL allows to complement the "*Calanus* pump"

hypothesis (Plourde and Runge, 1993). This hypothesis stressed the role of the LSLE/GC system as an important source of *C. finmarchicus* for the rest of the GSL during summer. All year long, the GC forms baroclinic instabilities (meanders), probably triggered by the interaction between the freshwater runoff and eastward wind events (Mertz et al., 1988, 1991). According to our results, during summer these instabilities increase the residence time of surface waters west of Honguedo Strait, while sporadic wind forcing leads to pulsed transport of these surface water masses over the western Magdalene Shallows and the central GSL. This mechanism fits with the "*Calanus* pump" hypothesis, but it extends to the north-west GSL as well the source region for the southern and eastern GSL. The tight coupling between the LSLE and the north-west GSL is characterized by important recirculation events taking place from mid-summer (August) until winter, during the whole period of production of the second generation of *C. finmarchicus*. Recirculation features are visible in the abundances from the DVM scenario (Fig. II-10P-S). Variability due to mesoscale surface circulation features represents less than 5% of the variability in females on the scale of the whole GSL, but it actually has major consequences for local dynamics. This circulation regime tightens the connection between the LSLE and the north-west GSL during a period of low abundance of the second generation in the LSLE. This mechanism provides surface-dwelling copepodite stages from the north-west GSL for the build-up of the overwintering stock in the LSLE, a few months before the deep circulation carries

upstream diapausing C5 originating from the north-west GSL. The existence of two contrasting circulation regimes in the north-west GSL challenges the generally accepted view of a permanent frontal zone between the GC and the AG (Sevigny et al., 1979; Tang, 1980; Fortier et al., 1992). The simulation results showed that high frequency circulation events, such as summer GC instabilities, act to couple both circulation features. These circulation modes also extend their influence further downstream, especially in spring and summer.

These findings allow to answer to one of the most significant linkage found between physical and ecological processes in the GSL. The abundance of *C. finmarchicus* females and the index of Mackerel recruitment are significantly and positively correlated with each other, but inversely correlated to the St Lawrence river freshwater run-off index (RIVSUM index). In order to explain the negative correlation between the freshwater run-off and the zooplankton biomass in the southwest GSL, Runge et al. (1999) hypothesized that when relaxed, the buoyancy driven surface circulation allowed more of the *C. finmarchicus* rich waters from the central Laurentian Channel (LC) to spread over the Magdalene Shallows. 1999 was a year of below average run-off and high abundance of *C. finmarchicus* in the southern GSL (Castonguay et al., 2008). According to our results, variability in the seasonal colonization of the southwest GSL is more likely to result from variations in the efficiency of the "*Calanus* pump" previously described. Advection of

individuals between the central LC and the Magdalene Shallows did not contribute to the variability of the system, and no unusual circulation feature occurred across the southern limit of the LC. Ouellet et al. (2003) showed that the spatial scale of variability of the SST was larger and more isotropic in the central GSL (between 100 and 175 km) than in the western part of the GSL (less than 100 km), including the western Magdalene Shallows which is the major route for zooplankton patches to penetrate within the area. The seasonal colonization of the southern GSL is similar in several aspects to the mechanism first hypothesized by Backhaus et al. (1994) for the North Sea (see also Gallego et al., 1999; Harms et al., 2000). The major difference is the smaller spatial scales involved in the GSL, which greatly increases the importance of the DVM (Hannah et al., 1997). Contrary to the southern GSL, the north-east GSL is able to maintain high abundances of both diapausing and active stages of *C. finmarchicus* throughout the year, especially in the DVM scenario. According to our results, it would nonetheless benefit from external imports through the open boundaries. The surrounding areas of the continental shelf essentially contribute through Cabot Strait (Fig. II-16), and the influence of inflowing waters is strongly limited west of Esquiman Channel. Thus the inter-annual maintenance of the *C. finmarchicus* population within the GSL system did not rely on external sources, and the GSL can actually act as a source of *C. finmarchicus* for the downstream continental shelf area, as suggested by Zakardjian et al. (2003). More data are however needed to explore further the

dynamics of the north-east GSL.

Our model results showed that the few monitoring stations and the frequency of sampling cannot allow a comprehensive understanding of the *C. finmarchicus* population dynamics in the LSLE-GSL system. However the data available constitute a good starting point to build models in order to gain a more thorough understanding of the mechanisms driving the pelagic ecosystem of the GSL. Data sets are needed to initialize such models, and ideally others are needed to confront the results of the model to the observations. The AZMP program could advantageously benefit from additional stations in the eastern part of the GSL, as already proposed by Ouellet et al. (2003).

## 6 Conclusion

Our study is the first to quantify, on a regional scale and for a specific year, the key patterns in the distribution, abundance and stage composition of the *C. finmarchicus* population in a dynamic continental shelf area, the LSLE-GSL system. It is moreover the first study to explicitly link the variable migration behavior exhibited by *C. finmarchicus* with the various circulation patterns occurring in its habitat along the year, as an essential element of a successful life-cycle strategy. It is

the first study to demonstrate the existence of a resident *C. finmarchicus* population in a coastal area, with limited contribution of external oceanic populations. Some studies improved our understanding of the impacts of the interactions between the hydrodynamics and ontogenetic migrations (e.g. Johnson et al., 2006), or the swimming behavior of active stages (e.g. Hannah et al., 1997; Emsley et al., 2005; Carr et al., 2008) on the population dynamics of *C. finmarchicus* in the complex coastal domain. Our study is however the first to integrate in a comprehensive way both DVM and ontogenetic migrations into a complete life-cycle model of *C. finmarchicus* during a whole year. This is an important step in our ability to draw robust explanations for the "*Calanus* circuit" formed by circulation features separated in time and space, but linked together by the life-cycle of *C. finmarchicus*. Saucier et al. (2009) showed through sensitivity studies of the same 3-D circulation model that realistic alterations of either the wind forcing or the fresh water run-off affect considerably the hydrodynamics of the GSL, as well as the exchanges with the Labrador Current and the North Atlantic waters. The apprehended climatic changes will affect in a yet unpredictable way both hydrological and wind forcing. Hence, the hydrodynamics inside the complex and heterogeneous GSL will probably be affected in a near future, and consequently impact the planktonic species whose perennial presence rely on well established recurrent patterns.

# CHAPITRE III

# THE CONTROL OF DIAPAUSE BY THE LIPID METABOLISM IN *Calanus finmarchicus* : A POPULATION MODEL PUT TO THE TEST

## 7 Résumé

Afin de survivre dans un environnement boréal fortement saisonnier, *Calanus finmarchicus* dépend d'une phase de diapause pendant laquelle l'espèce échappe aux conditions environnementales hivernales défavorables. De récentes données démographiques, physiologiques et génétiques suggèrent un rôle crucial du métabolisme des lipides dans le contrôle de la diapause. Nous présentons dans cette optique un modèle de cycle de vie de *C. finmarchicus* implémentant une approche mécaniste du contrôle de la diapause, basée sur le métabolisme des lipides. Le mécanisme du modèle de diapause obéit à deux règles: (1) les stades copépodites 5 (C5) actifs entrent en diapause lorsque le ratio lipides sur carbone total excède une valeur seuil, et (2) les C5 en diapause en sortent lorsque leurs réserves lipidiques approche d'une valeur seuil. Nous avons appliqué le modèle en 1-D à une colonne d'eau, et nous avons comparé nos résultats à deux années consécutives de données d'abondance des copépodites et de contenu lipidique des C5, provenant du nord-ouest du golfe du Saint-Laurent. Le modèle reproduit une phénologie et des patrons d'abondance et de contenu lipidique de *C. finmarchicus* réalistes en réponse aux forçages environnementaux, ainsi que des variations inter-annuelles du timing d'entrée en diapause et de la contribution relative des différentes générations au stock en diapause. Nos résultats supportent l'hypothèse d'un contrôle par le métabolisme des lipides de l'entrée et de la sortie de diapause chez *C. finmarchicus*.

# 8 Introduction

The pelagic copepod *Calanus finmarchicus* is a dominant component of the zooplankton community across the North Atlantic boreal domain. Its life-cycle shows two distinct phases, a period of active growth and reproduction during the spring-summer within the productive surface layer, and an extended overwintering period (diapause) at depth, essentially as copepodite 5 (C5) stage (Hirche, 1996a, 1996b). The phenology of *C. finmarchicus* shows regional plasticity at the scale of the North Atlantic, probably related to regional variations in environmental conditions (Planque et al., 1997). The timing of initiation and termination of diapause could vary by several months at smaller spatial scale across the continental shelf in the Northwest Atlantic (Johnson et al., 2008).

The relationships between the key environmental parameters (temperature and food) and the physiological processes (growth, development and egg production) of *C. finmarchicus* are relatively well characterized owing to numerous laboratory, mesocosm and *in situ* studies (e.g. Harris et al., 2000; Campbell et al., 2001). However, no equivalent knowledge is yet available regarding the control of the diapause phase of the life cycle. Johnson et al. (2008) concluded that in the Northwest Atlantic "no consistent pattern in the gradients of environmental cues

[...] could explain the observed dormancy entrance and exit patterns". Meanwhile, modeling studies showed the inability of simple trigger mechanisms such as the level of chlorophyll *a* biomass or photoperiod to explain the timing of entrance in diapause at the scale of the North Atlantic (Speirs et al., 2006). Those conclusions enlighten the integrative nature of the diapause process, which translates the variability of multiple environmental factors into one particular life-cycle strategy.

What could be the role of the diapause process for *C. finmarchicus* facing a changing environment (Denman et al., 2007) ? The phenology is more susceptible to follow rapid changes in environmental conditions than is the metabolism of a species, either by acclimation or adaptation (Miller et al., 1991). If environmental changes remain within an acceptable range, diapause dynamics may buffer possible detrimental effects by allowing *C. finmarchicus* to avoid periods of unfavorable conditions leading to low reproductive output or high mortality, hence maximizing the reproductive value of the species.

Recent physiologic (Jónasdóttir, 1999; Miller et al., 2000; Rey-Rassat et al., 2002; Hassett, 2006; Saumweber et al., 2006), genetic (Tarrant et al., 2008) and demographic (Johnson et al., 2008) evidences support the hypothesis of a crucial role for the lipid metabolism in the control of diapause (Irigoien, 2004; Saumweber

and Durbin, 2006; Johnson et al., 2008). High amounts of wax esters are generally observed in animals in diapause, confined within their oil sac (Miller et al., 1998b; Ingvarsdottir et al., 1999; Jónasdóttir, 1999; Saumweber and Durbin, 2006). A variable but significant proportion of lipid storage remains at the end of the diapause period (Plourde and Runge, 1993; Saumweber and Durbin, 2006), which apparently matches the metabolic needs of both the gonad maturation associated to the final molt (Rey-Rassat et al., 2002) and of the ontogenetic vertical migration of newly molted adult females (Jónasdóttir, 1999). Therefore, the difference between the initial and the final amount of lipid storage would cover the energetic costs associated with several months in diapause. One could reasonably argue for some threshold level of lipid storage above which diapause can be initiated, which would support the metabolic requirement during the diapause period, and the maturation process at the time of molting (Fiksen, 2000). The rationale is that individuals entering diapause without a sufficient amount of lipid would eventually be lost from the population, as they will be starving at depth or migrating to the surface in unfavorable environmental conditions. However, along this hypothesized lipid-driven diapause mechanism (Saumweber and Durbin, 2006), it is possible for other cues to influence the time of exit from diapause. These signals could be either internal, like a reduced development rate, or external like the stimulating effect of the advection bringing individuals into the surface layer, as suggested by some observations and incubation experiments (e.g. Durbin et al., 1997).

For the last ten years, numerous modeling studies brought quantitative insights on the population dynamics of *C. finmarchicus*. However the lack of a clear understanding of the controls of the diapause lead previous investigators to (1) impose alternatively the date of its initiation or the fraction of each generation entering diapause and (2) to impose the date of its termination, in order to reproduce the targetted phenology (Carlotti and Wolf, 1998; Lynch et al., 1998; Miller et al., 1998a; Tittensor et al., 2003; Zakardjian et al., 2003; Speirs et al., 2006; Slagstad and Tande, 2007). Such a deterministic approach precludes sensitivity studies of *C. finmarchicus* population dynamics to inter-annual or long term variations in environmental forcing. Thus a few authors developed mechanistic approaches of the diapause. Fiksen (2000) added three model "genes" to *C. finmarchicus* individuals, which lead to a rule for entry into diapause involving the lipid over somatic tissue ratio, while the exit from diapause remained forced by the length of the day. Hind et al. (2000) assumed that diapause duration was controlled by the normal development processes operating at a reduced rate, after it was initiated by a low food availability threshold. Speirs et al. (2006) however showed that this model failed to reproduce the large variations in phenology across the whole geographic area of *C. finmarchicus*. Our study represents to our knowledge the first attempt to test a mechanistic approach based entirely on the lipid metabolism for the control of the diapause in a population model of *C. finmarchicus*. We adapted the stage-resolved biomass population model of copepods developed by

Fennel (2001) and modified by Stegert et al. (2007) to *C. finmarchicus*.

In our study the diapause process obeyed to two rules: (1) active C5 enter diapause when their ratio of lipid to total body carbon exceeds a fitted threshold value and (2) diapausing C5 exit diapause when their lipid storage approaches a given proportion of their structural mass (minimal threshold). We implemented the model in a 1-D water column framework, and compared our results to observations of abundance of copepodite stages, body carbon and lipid contents of C5 from three monitoring stations located in the north-west Gulf of St. Lawrence, eastern Canada.

## 9 Materials and Methods

### *9.1 0-D base model design*

We developed a stage-resolving biomass model for *C. finmarchicus* following Fennel (2001) and Stegert et al. (2007). The model computed stage-specific biomass ($B_i$) and abundance ($N_i$), and the resulting mean individual mass ($m_i = B_i / N_i$). According to the critical moulting mass (CMM) concept developed by Carlotti and Sciandra (1989), the stage-specific CMM was the mass threshold above which

moulting to the net stage occurred. Thus the development of the stages resulted from the interplay of the stage-specific growth ($g_i$) and CMM, both driven by environmental conditions of food and temperature, which gives for a generic model stage:

$$\frac{dB_i}{dt} = t_{i-1,i} B_{i-1} + \left(g_i - t_{i,i+1}\right) B_i$$

$$\frac{dN_i}{dt} = t_{i-1,i} N_{i-1} - t_{i,i+1} N_i$$

with $t_{i,i+1} = f(m_i)$ the transfer rate between the state variables, controlled by the mean individual mass of the stage. Detailed descriptions of the formulations of CMM, growth and transfer rates are given in the following sections, and all equations and parameters are presented in Tables III-1 and III-2. The number of stages described by the model resulted from the trade-off between the needs for an accurate representation of growth and development processes and computational efficiency. We considered the egg stage, a non-growing category grouping nauplii 1 and 2 (N1-N2), stage nauplii 3 divided in three size classes ($N3_1$, $N3_2$, and $N3_3$) in order to cope with the continuous recruitment from non-growing stages (see discussion), and each other nauplii (N4-N6) and copepodite stage(C1-C6) individually. New adults were shared equally between males (C6m) and females (C6f). We also defined a diapausing stage (C5d). The model allows a better determination of the variation of the stage duration, the individual mean mass

threshold condition for moulting preventing numerically induced "premature maturation" inherent to simple stage-based model. Moreover, it allows the inclusion of structural and lipid compartments in the formulation of the diapause process during stage C5, as described hereafter.

Table III-1. State variables and equations used to simulate the temporal and spatial evolution of the state variables.

| State variables | Description |
|---|---|
| $B_i$ | Biomass of stage $i$ |
| $B_{iS}$ | Biomass of structural compartment of stage $i$ |
| $B_{iL}$ | Biomass of lipid compartment of stage $i$ |
| $B_{C5} = B_{C5S} + B_{C5L}$ | Biomass of stage C5 |
| $B_{C5d} = B_{C5dS} + B_{C5dL}$ | Biomass of stage C5d |
| $N_i$ | Abundance of stage $i$ |

Table III-1. Continued.

Differential equations

Biomass

$$\frac{\partial B_E}{\partial t} = R B_{C6f} - \left(t_{E,N12} + k_E\right) B_E + \frac{\partial w_E B_E}{\partial z} \qquad \text{Egg} \qquad (1)$$

$$\frac{\partial B_{N12}}{\partial t} = t_{E,N12} B_E - \left(t_{N12,N3} + k_{N12}\right) B_{N12} + \frac{\partial w_{N12} B_{N12}}{\partial z} \qquad \text{Non-growing nauplii} \qquad (2)$$

$$\frac{\partial B_i}{\partial t} = t_{i-1,i} B_{i-1} + \left(g_i - t_{i,i+1} - k_i\right) B_i + \frac{\partial w_i B_i}{\partial z} \qquad \text{Generic stage} \qquad (3)$$

$$\frac{\partial B_{C5S}}{\partial t} = t_{C4,C5} B_{C4} + (1-p_2) g_{C5} B_{C5} - \left(t_{C5,C6} + k_{C5}\right) B_{C5S} + \frac{\partial w_{C5} B_{C5S}}{\partial z} \qquad \text{C5 structural} \qquad (4)$$

$$\frac{\partial B_{C5L}}{\partial t} = p_2 g_{C5} B_{C5} - \left(t_{C5,C6} + k_{C5}\right) B_{C5L} + \frac{\partial w_{C5} B_{C5L}}{\partial z} \qquad \text{C5 lipid} \qquad (5)$$

$$\frac{\partial B_{C5dS}}{\partial t} = d \cdot t_{C5,C6} B_{C5S} - \left(t_{C5d,C6} + k_{C5d}\right) B_{C5dS} + \frac{\partial w_{C5d} B_{C5dS}}{\partial z} \qquad \text{Diapause structural} \qquad (6)$$

$$\frac{\partial B_{C5dL}}{\partial t} = d \cdot t_{C5,C6} B_{C5L} - g_{C5d} B_{C5dS} - \left(t_{C5d,C6} + k_{C5d}\right) B_{C5dL} + \frac{\partial w_{C5d} B_{C5dL}}{\partial z} \qquad \text{Diap. lipid} \qquad (7)$$

$$\frac{\partial B_{C6f}}{\partial t} = \frac{1}{2}\left( (1\text{-}d) t_{C5,C6} B_{C5} + t_{C5d,C6} B_{C5d} \right) - k_{C6f} B_{C6f} + \frac{\partial w_{C6f} B_{C6f}}{\partial z} \qquad \text{Adult female} \qquad (8)$$

Abundance

$$\frac{\partial N_E}{\partial t} = \frac{R B_{C6f}}{M_E} - \left(t_{E,N12} + k_E\right) N_E + \frac{\partial w_E N_E}{\partial z} \qquad \text{Egg} \qquad (9)$$

$$\frac{\partial N_i}{\partial t} = t_{i-1,i} N_{i-1} - \left(t_{i,i+1} + k_i\right) N_i + \frac{\partial w_i N_i}{\partial z} \qquad \text{Generic stage} \qquad (10)$$

$$\frac{\partial N_{C6f}}{\partial t} = \frac{1}{2}\left( (1\text{-}d) t_{C5,C6} N_{C5} + t_{C5d,C6} N_{C5d} \right) - k_{C6f} N_{C6f} + \frac{\partial w_{C6f} N_{C6f}}{\partial z} \qquad \text{Adult female} \qquad (11)$$

Table III-1. Continued.

Parameters equations:

Critical moulting mass

$$M_i^T = a_{1,i} + a_{2,i} T \qquad \text{Temp. dependence} \quad (12.1)$$

$$M_i^F = 1 - a_{3,i}\, e^{\left(-a_4 (F-5)\right)} \text{ for C4-C6, else } M_i^F = 1 \qquad \text{Food dependence} \quad (12.2)$$

$$M_i = M_i^T \cdot M_i^F \qquad \text{Stage-specific CMM} \quad (12)$$

Growth

$$g_i^T = a_{5,i} + a_{6,i} T \qquad \text{Temp. dependence} \quad (13.1)$$

$$g_i^F = 1 - e^{\left(-a_{7,i} (F-5)\right)} \qquad \text{Food dependence} \quad (13.2)$$

$$g_i^m = 1 - \left(\frac{m_i - M_i}{M_i^X - M_i}\right)^2 \text{ if } m_i \geqslant M_i \text{, else } g_i^m = 1 \qquad \text{Mass dependence} \quad (13.3)$$

$$g_i = g_i^T \cdot g_i^F \cdot g_i^m \qquad \text{Stage-specific growth} \quad (13)$$

Egg production

$$R^T = a_8\, e^{\left(a_9 \cdot T\right)} \qquad f(\text{Temperature}) \quad (14.1)$$

$$R^F = 1 - e^{\left(-a_4 (F-5)\right)} \qquad f(\text{Food}) \quad (14.2)$$

$$R = R^T \cdot R^F \cdot (1 - g_{C6f}^m) \qquad \text{Egg production} \quad (14)$$

$$g_{C6f} = R^T \cdot R^F \cdot g_{C6f}^m \qquad \text{Female's growth} \quad (15)$$

Transfer from stage to stage

$$t_{i,i+1} = \frac{1}{a_{10,i}\,(T+9.11)^{-2.05}} \quad \text{if } T > 0, \text{ else } t_{i,i+1} = 0 \qquad \text{Non-growing st.} \qquad (16.1)$$

$$t_{i,i+1} = \frac{(m_i - M_i^t)^3}{(m_i - M_i^t)^3 + (M_i^X - M_i^t)^3} \quad \text{if } m_i \geq M_i^t, \text{ else } t_{i,i+1} = 0 \qquad \text{Growing st.} \qquad (16.2)$$

$$t_{C5d,C6} = \frac{(M_{C5d}^t - m_{C5d})^3}{(M_{C5d}^t - m_{C5d})^3 + (M_{C5d}^t - M_{C5d}^X)^3} \quad \text{if } m_i \leq M_i^t, \text{ else } t_{i,i+1} = 0 \qquad \text{Diapause} \qquad (16.3)$$

Diapause

$$d = \frac{(r_L - 0.9p_1)^2}{(r_L - 0.9p_1)^2 + (0.1p_1)^2} \quad \text{if } r_L = \frac{m_{C5L}}{m_{C5}} \geq 0.9p_1, \text{ else } d = 0 \qquad f(\text{Lipid}) \qquad (17)$$

Mortality of non-feeding stages

$$k_{\{E,N12\}} = a_{11} + a_{12}\int_{bott.}^{surf.} N_{C6f} \quad \text{if} \quad \int_{bott.}^{surf.} N_{C6f} \geq 2000 \text{ ind.m}^{-2} \qquad f(\text{Density}) \qquad (18.1)$$

else $k_{\{E,N12\}} = 0.51$ (18.2)

Swimming behaviour

$$z_i^{mig} = z_i^{sup} + \Delta z_i^{inf-sup}\left(1 - \tanh\left(3\cdot\cos\left(2\pi\frac{t+4}{24}\right)\right)\right) \qquad \text{Optimal depth} \qquad (19.1)$$

$z_i = z_i^{mig}$ for migrating stages, else see Table III-2

$$\varepsilon = \text{sign}\left(\frac{1}{2} - U[0,1]\left(1 - \left(\frac{z - z_i}{15}\right)^2\right)\right) \qquad \text{Stochastic param.} \qquad (20.2)$$

$$w_i = w_i^X \cdot \tanh\left(a_{13}(z - z_i)\right)\cdot\varepsilon \qquad \text{Swimming speed} \qquad (20)$$

Table III-2. Parameters descriptions, units and values. ← means "same as left", – means "not defined" and Var. means "variable" (see text).

| Description & Units | | | Egg | N12 | N3 | N4 | N5 | N6 | C1 | C2 | C3 | C4 | C5 | C5d | C6f | C6m |
|---|---|---|---|---|---|---|---|---|---|---|---|---|---|---|---|---|
| Differential equations | | | | | | | | | | | | | | | | |
| $p_2$ | Allocation of growth to lipid | Nd | Fitted (see text) | | | | | | | | | | | | | |
| Critical moulting mass | | | | | | | | | | | | | | | | |
| $a_{1,i}$ | Temp. coef. | $\mu$g C | 0.23 | 0.23 | 0.5 | 0.76 | 1.14 | 1.8 | 3.4 | 9.4 | 28.9 | 94 | 332 | - | 262 | - |
| $a_{2,i}$ | Temp. coef. | $\mu g.°C^{-1}$ | 0 | ← | ← | ← | ← | ← | -0.06 | -0.28 | -1.09 | -4.71 | -18.8 | - | -6.26 | - |
| $a_{3,i}$ | Food effect | Nd | 0 | ← | ← | ← | ← | ← | ← | ← | ← | 0.25 | 0.5 | - | 0.5 | - |
| $a_4$ | Shape coef. | $m^3.mg^{-1}$ | 0.02 | | | | | | | | | | | | | |
| Growth | | | | | | | | | | | | | | | | |
| $a_{5,i}$ | Temp coef. | $d^{-1}$ | - | - | 0.015 | ← | ← | ← | 0.07 | 0.065 | 0.05 | 0.055 | 0.025 | 0.005 | 0.025 | - |
| $a_{6,i}$ | Temp coef. | $d^{-1}.°C^{-1}$ | - | - | 0.025 | ← | ← | ← | 0.14 | 0.028 | 0.027 | 0.015 | 0.01 | 0 | 0.01 | - |
| $a_{7,i}$ | Shape coef. | $m^3.mg^{-1}$ | - | - | 0.04 | ← | ← | ← | 0.03 | ← | ← | 0.02 | ← | - | ← | - |
| $m_i$ | mean mass | $\mu$g C | $B_i/N_i$ | ← | ← | ← | ← | ← | ← | ← | ← | ← | ← | ← | ← | ← |
| $M_i^X$ | Max. mass | $\mu$g C | $1.1M_i$ | ← | ← | ← | ← | ← | ← | ← | ← | ← | $0.9M_i$ | $1.1M_i$ | - | |
| Egg production | | | | | | | | | | | | | | | | |
| $a_8$ | Temp coef. | $d^{-1}$ | 0.02198 | | | | | | | | | | | | | |
| $a_9$ | Temp coef. | $°C^{-1}$ | 0.116 | | | | | | | | | | | | | |

Table III-2. Continued.

| | | | | | | | | | | | | | | | | | | | |
|---|---|---|---|---|---|---|---|---|---|---|---|---|---|---|---|---|---|---|---|
| **Transfer** | | | | | | | | | | | | | | | | | | | |
| $a_{10,i}$ | Belehrádek coef. | d | 595 | 969 | - | - | - | - | - | - | - | - | - | - | - | - | - | - | - |
| $M_i^t$ | Transfer mass | $\mu$g C | $0.9M_i$ | ← | ← | ← | ← | ← | ← | ← | ← | ← | ← | $1.1M_i$ | $0.9M_i$ | - | | | |
| **Diapause** | | | | | | | | | | | | | | | | | | | |
| $p_1$ | Lipid ratio threshold | Nd | Fitted (see text) | | | | | | | | | | | | | | | | |
| **Mortality** | | | | | | | | | | | | | | | | | | | |
| $a_{10}$ | coef. | $d^{-1}$ | 0.35 | | | | | | | | | | | | | | | | |
| $a_{11}$ | coef. | $m^2.ind^{-1}$ | 8.E-5 | | | | | | | | | | | | | | | | |
| $k_i$ | constant | $d^{-1}$ | - | - | 0.25 | 0.15 | 0.1 | 0.08 | 0.05 | 0.4 | 0.03 | 0.03 | 0.02 | 0.002 | 0.02 | 0.04 | | | |
| **Swimming behaviour** | | | | | | | | | | | | | | | | | | | |
| $z_i^{sup}$ | Min. depth | m | Var. | ← | ← | ← | ← | ← | ← | ← | ← | ← | ← | 150 | Var. | 50 | | | |
| $z_i^{inf}$ | Max. depth | m | - | - | - | - | - | - | - | - | - | 100 | 100 | 300 | 100 | 150 | | | |
| $w_i^X$ | Max. speed | $cm.h^{-1}$ | 0.3 | 1 | 1.1 | 1.6 | 2.2 | 2.7 | 3.2 | 4.7 | 6.1 | 7.6 | 9.4 | 9.4 | 10.8 | 10.8 | | | |
| $a_{13}$ | Shape coef. | Nd | 0.03 | | | | | | | | | | | | | | | | |

Table III-2. Continued.

| | | | | | | | | | | | | | | | | | |
|---|---|---|---|---|---|---|---|---|---|---|---|---|---|---|---|---|---|
| **Transfer** | | | | | | | | | | | | | | | | | |
| $a_{10,i}$ | Belehrádek coef. | d | 595 | 969 | - | - | - | - | - | - | - | - | - | - | - | - | - |
| $M_i^t$ | Transfer mass | $\mu$g C | $0.9M_i$ | ← | ← | ← | ← | ← | ← | ← | ← | ← | ← | $1.1M_i$ | $0.9M_i$ | - | |
| **Diapause** | | | | | | | | | | | | | | | | | |
| $p_1$ | Lipid ratio threshold | Nd | Fitted (see text) | | | | | | | | | | | | | | |
| **Mortality** | | | | | | | | | | | | | | | | | |
| $a_{10}$ | coef. | $d^{-1}$ | 0.35 | | | | | | | | | | | | | | |
| $a_{11}$ | coef. | $m^2.ind^{-1}$ | 8.E-5 | | | | | | | | | | | | | | |
| $k_i$ | constant | $d^{-1}$ | - | - | 0.25 | 0.15 | 0.1 | 0.08 | 0.05 | 0.4 | 0.03 | 0.03 | 0.02 | 0.002 | 0.02 | 0.04 | |
| **Swimming behaviour** | | | | | | | | | | | | | | | | | |
| $z_i^{sup}$ | Min. depth | m | Var. | ← | ← | ← | ← | ← | ← | ← | ← | ← | ← | 150 | Var. | 50 | |
| $z_i^{inf}$ | Max. depth | m | - | - | - | - | - | - | - | - | - | 100 | 100 | 300 | 100 | 150 | |
| $w_i^X$ | Max. speed | $cm.h^{-1}$ | 0.3 | 1 | 1.1 | 1.6 | 2.2 | 2.7 | 3.2 | 4.7 | 6.1 | 7.6 | 9.4 | 9.4 | 10.8 | 10.8 | |
| $a_{13}$ | Shape coef. | Nd | 0.03 | | | | | | | | | | | | | | |

*Critical Moulting Mass (CMM).* Constant masses for the egg and nauplii stages were taken from the literature (Runge and Plourde, 1996; Harris et al., 2000; Hygum et al., 2000a), whereas copepodites' critical molting mass (CCM) were a function of temperature (Campbell et al., 2001). The size (body length and mass) of *C. finmarchicus* copepodite stages is positively correlated to food concentration. The prosome length of copepodite stages decreases with decreasing food concentration, and severely limiting food concentrations further induce a significant reduction of the carbon content of C4, C5 and adults compared to individuals of the same body length at high food concentration (Hygum et al., 2000b; Campbell et al., 2001). Variability in food concentration induced a maximum of 25% of variation in carbon body mass for C4, and 50% for C5 and C6f. The maximum body mass of the stage was defined as 110% of the CMM.

*Growth.* Physiological processes such as respiration and ingestion were implicitly taken into account by linking temperature and carbon concentration, as a proxy of potential ingestion rate, to the net growth rate. A carbon /chlorophyll *a* ratio of 50 was used to convert chlorophyll *a* data into carbon concentration (Rivkin et al., 1996). stage-specific growth rate was formulated as a function of temperature and carbon concentration. The growth vs. temperature and growth vs. food concentration relationships were adapted from Campbell et al. (2001). Growth was

further modulated by a parabolic function of the mean individual mass ($g^m_i$, table III-1), ensuring that no growth occurred when the mean body mass exceeds the maximum body mass of the stage (Stegert et al., 2007).

*Egg production.* Mass specific egg production rate (EPR) was a function of temperature and carbon concentration, assuming an egg carbon mass of 0.23 $\mu$g (Runge and Plourde, 1996). The parabolic function of the mean individual mass of C6f ($g^m_i$) implied that egg production increased as the female became heavier. Egg production was maximum when the mean mass of C6f reached its CMM, hereby corresponding to the mass at maturity. The growth of C6f was directly linked to EPR: as long as the mean mass of C6f remains below its CMM, the proportion of growth not allocated to EPR was invested into the somatic growth of C6f. Egg laying was assumed to occur at night between 20h00 and 4h00 (Runge and Plourde, 1996).

*Transfer.* The transfer rate of biomass from one stage to the next was a function of the mean individual mass of the stage. A sigmoid function was used to ensure that the transfer rate was zero before the stage reached 90% of its CMM, and maximum when it reached its maximum body mass (Stegert et al., 2007). For non-feeding development stages, the transfer rate of biomass from one stage to the next

was simply the inverse of the development duration of the stage, formulated as a Belehrádek temperature function (Campbell et al., 2001).

*Diapause.* Stage C5 was divided into an active (C5) and a diapausing (C5d) category. For each of these categories, biomass was divided into structural and lipid compartments. We assumed that the biomass of C4 contributes only to the structural compartment of the C5. The growth of C5 was split between lipid and structural compartments according to a constant allocation coefficient, $p_2$ (Tables III-1 and III-2). A parabolic function of the ratio of lipid carbon to total body carbon drove the transfer of C5 toward either C5d or adults so that 50% of the C5 transferred to C5d when the ratio reached a constant threshold, $p_1$. Owing to the absence of published and reliable data for the parameterization of both $p_1$ and $p_2$, they were defined as free parameters, selected within the uniform distributions $p_1 \sim U[0.2,0.8]$ and $p_2 \sim U[0.5,1]$. In order to determine the optimal set of free parameters $\{p_1,p_2\}$ under a realistic annual forcing of food and temperature, we ran simulations within the parameters' space, cycling ten times through the same climatological environmental conditions. The simulation approaching the most to a quasi-stationary state of population dynamics provided the optimal solution. Lipid accumulated by the actively growing C5 fueled the metabolic demand of the non-feeding C5d stage. "Growth rate" in C5d was negative and corresponded to the

demand of the structural tissues upon the lipid storage, according to a constant basal metabolic rate derived from respiration rate of diapausing *C. finmarchicus* at 5°C (Saumweber and Durbin, 2006). This temperature corresponds to the mean temperature observed in the deep waters of Atlantic origin filling the Laurentian Chanel where the C5d overwinter in the Gulf of St. Lawrence (Saucier et al., 2003). As a result, transfer of biomass and individuals from C5d to C6m and C6f was driven by the reciprocal of the mass-dependent transfer function, increasing as the mean body mass decreased toward a lower body mass threshold. This threshold was defined as the structural mass at the time of entrance into diapause, in addition to a residual amount of lipid corresponding to half the structural mass. This residual amount of lipid matched the range of minimum lipid mass found in the individuals exiting diapause in the Gulf of Maine (Saumweber and Durbin, 2006), a value within the range of those estimated to be necessary to support moulting to adult female and gonad maturation (70 $\mu$gC in Ingvarsdottir et al., 1999; 40 $\mu$gC in Rey-Rassat et al., 2002).



*Mortality.* We used stage-specific daily mortality rates decreasing exponentially from N3 to adults within the range of mortalities observed for *C. finmarchicus* in different regions (Ohman et al., 2004), except for eggs and N1-N2 stages for which the potential effect of cannibalism by adult female was taken into account. We used the function of adult female abundance given by Ohman et al.

(2002). The mortality rate in C5d was 10% of daily mortality in non-diapausing C5 (e.g. McLaren et al., 2001; Gislason et al., 2007). The mortality rate in C6m was twice the mortality rate of C6f (Kiørboe, 2006).

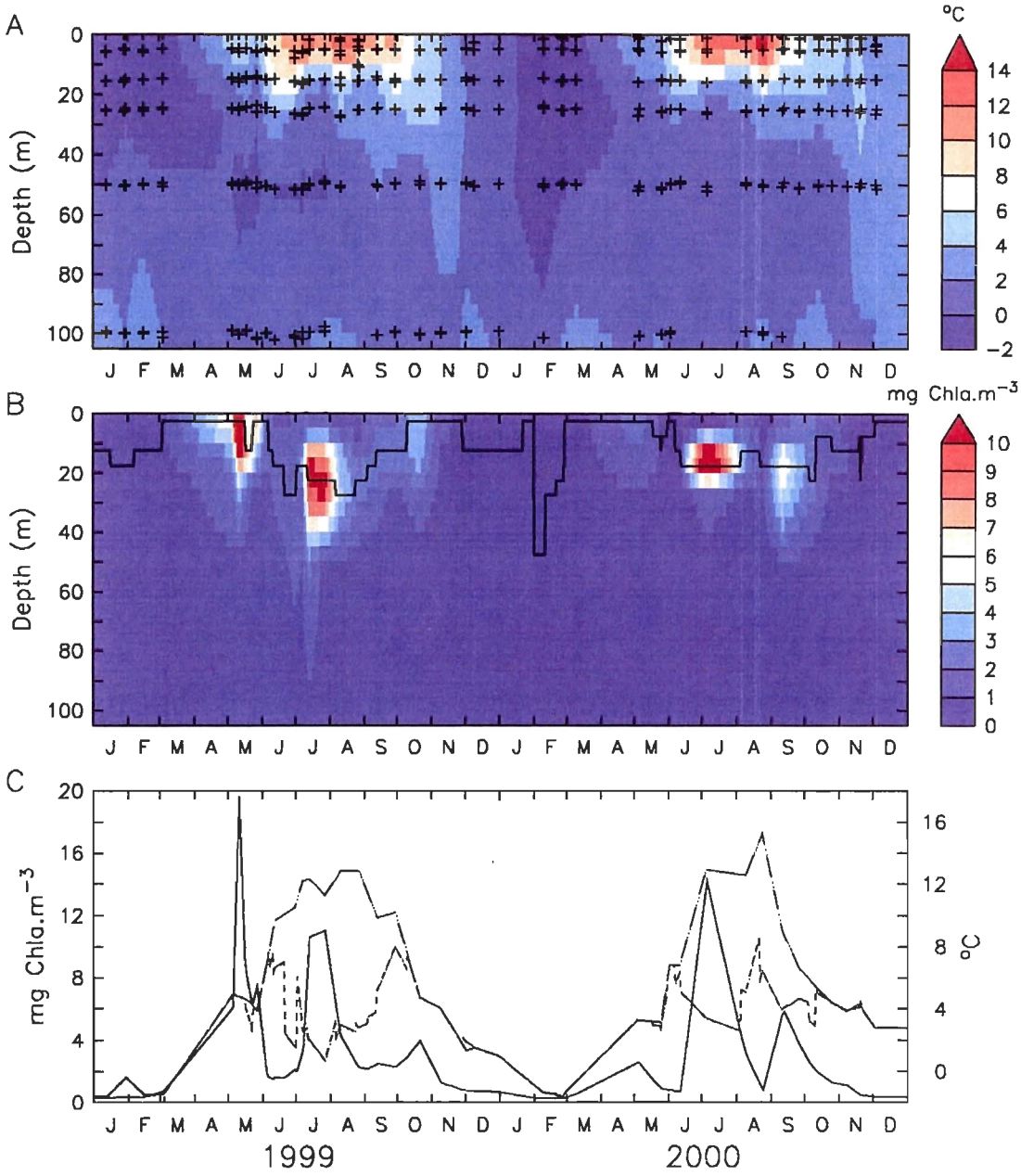


Figure III-1. (A) Temperature and (B) chlorophyll *a* forcing used in the 1-D simulations. Measurements (crosses) taken at the AG and GC monitoring stations (St. 1 and 2, Fig. II-1) were linearly interpolated in space and time. The depth of maximum chlorophyll *a* concentration is indicated by the line. (C) Maximum chlorophyll *a* concentration (continuous line), surface temperature (dashed line) and temperature at the depth of maximum chlorophyll *a* (short-dashed line).

## *9.2 1-D water column model*

Deep-dwelling diapausing individuals are generally found well below the actively growing stages, present mainly in the first tens of meters of the water column (Head and Pepin, 2007). Simard et al. (1985) showed that diel vertical migrations (DVM) of active copepodite stages of *C. finmarchicus* was associated with a diel feeding rhythm in the St Lawrence estuary during summer. Observations collected in spring and late summer 1998 in the north-west GSL also showed evidence of DVM in some components of the C4, C5 and C6f stages between the near surface at night and c.a. 100 m during the day (Fig. II-3). C5 showed no evidence of DVM in spring as they were probably still in diapause, while in late summer the bimodal distribution at night combined to the depth of the deep component suggest DVM for actively growing C5, and diapause for the others. No DVM was obvious in C1-3 whereas C6f showed clear DVM in both seasons. Seasonal stratification in the GSL and unique features like the cold intermediate layer (CIL, Fig. III-1A) are likely to influence any temperature dependent physiological rate of migrating copepods. We thus implemented the 0-D model into a 1-D framework in order to explore the response of the model to the vertical structure typical of the GSL. We tested two scenarios of migration behavior. The first (no-DVM scenario) followed Basedow et al. (2008), with vertical segregation of different development

stages according to chlorophyll *a* concentration preference, without DVM. Nauplii and young copepodite stages were assigned to the depth of the 1 mg chlorophyll *a* $m^{-3}$, C4 to the depth of the 1.5 mg chlorophyll *a* $m^{-3}$, and both C5 and C6f seek the depth of maximum in chlorophyll *a* biomass. In the second scenario C4, C5 and C6f performed DVM between the depth of maximum chlorophyll *a* biomass at midnight and 100 m at noon, with a duration of ascent/descent of 4 h. We made assumptions regarding (1) the CMM computation (see below) and (2) the daily growth rate of the migrating stages. In analogy with a diel feeding rhythm, the daily growth rate was completed during the surface period, between 20 h and 4 h (e.g. Simard et al., 1985; Durbin et al., 1995; Irigoien et al., 1998). The modeled domain was 300 m deep, with a vertical resolution of 5m, and a time step of 5 min.

*Swimming.* Stage-specific swimming speed was defined as the product of: (1) a maximum swimming velocity (three body lengths per second for migrating stages, one for the others), (2) a depth dependent function leading to downward (upward) swimming when copepods were above (below) a target depth (Zakardjian et al., 1999) and (3) a random dispersion term in order to avoid unrealistic concentrations in thin layers. The targeted depth was stage-specific and it could be a constant, a depth of specific food level, or a periodic function of time to mimic DVM. Egg sinking was considered (Knutsen et al., 2001), and it contributed to the egg mortality if eggs reached the bottom before hatching. A basic first order Eulerian

forward scheme was used to compute the evolution of the state variables (biomass and abundance) with time. This scheme is conservative, stable, fast, monotonicity preserving and compatible (Lipscomb and Hunke, 2004). Hence the computation of the ratio of biomass over abundance, i.e. the mean body mass, did not produce spurious values (Christian, 2007). The upstream Eulerian scheme was however diffusive, but preserving strong spatial feature was not desired as an additional stochastic biological diffusivity term was used.

*Adaptation of the CMM to the 1-D framework.* The stage-specific relationship between temperature, food and the CMM is essential for the coupling between growth and development. Observed empirical *in situ* relationships between body size, temperature and food revealed seasonal and inter-annual trends (e.g. Mauchline, 1998). Inter-molt body size represents an integration of the environmental conditions experienced by the individuals during their growth. In the north-west GSL, strong gradients in temperature are observed in the first tens of meters of the water column, owing to the CIL located between 30m to 110m (Fig. III-1A). Chlorophyll *a* biomass also showed a marked vertical distribution varying with time (Fig. III-1B). It appeared thus inappropriate to compute stage-specific CMM from the local conditions of temperature and food as late development stages would migrate across these strong gradients in the DVM scenario (see below). Spurious transfer from one stage to the next would occur as soon as the locally

computed CMM would fall below the actual mean body mass of the stage. Hence we considered two situations : (1) early stages aggregating around a target depth, and (2) late copepodite stages migrating between a surface (night) and a deep (day) optimal depth. For surface dwelling stages, the CMM was a function of temperature and food concentration at the target depth. For migrating stages, the CMM was a function of the median temperature and the maximum food concentration found between the upper and lower depths.

*In Situ data for forcing and validation.* We used environmental and *C. finmarchicus* stages abundance data collected as part of the Atlantic Zonal Monitoring Program (AZMP) conducted by the Department of fisheries and Ocean, Canada (Therriault et al., 1998; see Harvey et al., 2005 for zooplankton sampling details). We forced the 1-D model with profiles of temperature and chlorophyll *a* collected during two consecutive years (1999-2000) at two adjacent monitoring stations located in the Anticosti Gyre (AG) and Gaspé Current (GC) in the Northwest GSL (Fig. II-1). Data were generally collected on a fortnightly basis. They were linearly interpolated in space and time and averaged to construct profiles representative of the north-west GSL environment (Fig. III-1). Only detailed abundance data for copepodite stages were available for comparison with model results because early nauplii stages of *C. finmarchicus* are heavily under-sampled with the sampling gear used in the AZMP.

Indirect quantification of total and lipid carbon content in C5 were obtained following Miller et al. (2000) and Saumweber and Durbin (2006), using measurements of prosome length and estimates of lipid sac volume with an image analysis system on preserved C5. Comparative analysis between preserved and fresh individuals showed that values from preserved individuals were on average underestimated by 10% (Plourde et al., unpublished). Data of total and lipid carbon content in C5 were available for the AG station, and for a station located in the St. Lawrence Estuary (Station 1, Rimouski, Fig. II-1), sampled from spring to late autumn. Whereas abundance patterns of *C. finmarchicus* could be markedly different between the Rimouski and the AG-GC stations in the Northwest GSL owing to the regional hydrodynamic regime (Plourde and Runge, 1993; Plourde et al., 2001), the carbon and lipid conditions of the individuals proved to be more homogeneous at this regional scale (Plourde et al., unpublished). The biological initial conditions assumed an early winter population of C5d spread within a depth range of 200 to 300 m, with a realistic integrated abundance of 15 000 ind.$m^{-2}$ (Plourde et al., 2001; Harvey et al., 2005), a mean body mass of 200 $\mu$g of carbon, and a ratio of lipid to body mass of 50% the first of January 1999.

*Optimization of the free parameters and sensitivity analysis.* The optimal set of free parameters $\{p_1,p_2\}$ was chosen by running simulations within the parameters' space in order to minimize the product of the root mean squared deviations

(RMSD) computed for the abundance of each copepodite stage, representing the mean deviation of the simulated values compared to the observations (Piñeiro et al., 2008). We estimated sensitivity of the DVM scenario to selected demographic variables and to the parameters influencing the timing and duration of diapause. Those parameters were mortality in Egg – N1-2 (non-feeding stages) and in females, the proportion of the growth in C5 allocated to lipids ($p_2$), the ratio of lipid carbon to total carbon threshold driving entry into C5d ($p_1$), and the rate of consumption of lipids during diapause. We computed the RMSD of the abundance of C5d from the simulations ran with parameters altered by ±10% with respect to the reference simulation.

## 10 Results

### *10.1 0-D simulations*

*Development.* Within the frame of our formulation, stage durations resulted from the interaction of the stage-specific growth rates and critical moulting masses (CMM). The stages duration from N3 to adults simulated by the model at 4°C, 8°C and 12°C under non-limiting food conditions were slightly overestimated at 12°C relative to Campbell et al. (2001), but equiproportionality was preserved (Fig. III-

2A). The 0-D model reproduced within a few days of difference the development times from egg to C5 observed by Campbell et al. (2001) under three temperatures and three food conditions (Table III-3). The absence of numerical diffusion in the model was demonstrated by the cumulative percentage of the different stages of *C. finmarchicus* at 8°C, showing realistic synchrony in the transfer from one stage to the other (Fig. III-2B). The mass structure of the stages from the egg to adult female was compared with the CMM, and showed an exponential increase in body mass occurring during the development (Fig. III-2C). The slope of the curve defined by the successive mass trajectories corresponded to the growth rate of the cohort.

Table III-3. Development times from egg to C5 observed by Campbell et al. (2001) and simulated by the 0-D base model. H is for high (~350 $\mu$gC.L$^{-1}$), M for medium (~40 $\mu$gC.L$^{-1}$) and L for low (~25 $\mu$gC.L$^{-1}$) food concentrations.

| Treatment | Campbell et al. 2001 | Model |
|---|---|---|
| 12°C / H | 22/23 | 21 |
| 8°C / H | 32 | 31 |
| 8°C / M | 46 | 43 |
| 8°C / L | 59 | 63 |
| 4°C / H | 56 | 54 |

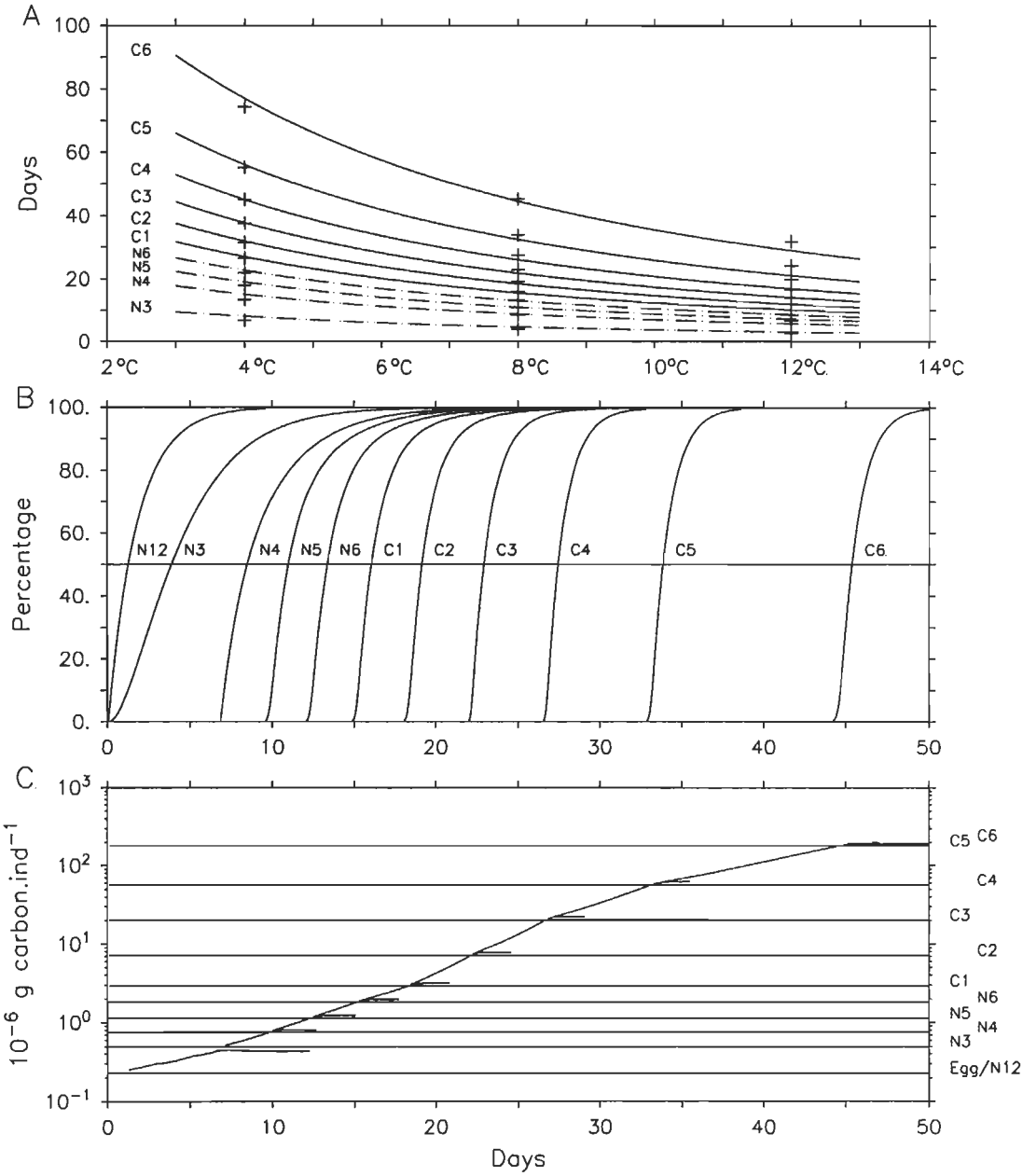


Figure III-2. (A) Development time as a Belehrádek function of temperature for N3 to C6 stages (curves, Campbell et al. 2001) and simulated under non-limiting food concentration at 4°C, 8°C and 12°C by the 0-D base model (crosses). (B) Cumulative proportions and (C) mass trajectories of the stages simulated at 8°C and non-limiting food concentration (short-dashed lines: critical moulting mass; continuous lines: mean body mass).

*Diapause.* In order to test the ability of our formulation to generate a diapausing population, we imposed in a first 0-D scenario a ratio of lipid carbon to body carbon threshold for the initiation of diapause of 50% ($p_1$), and allocated 80% of the C5's growth toward lipid storage ($p_2$). The model was forced by temperature and food conditions typical of the mixed layer in the north-western Gulf of St Lawrence mixed layer (Fig. III-1). Simulation was initiated with one hundred eggs normally distributed around day 90, when temperature exceeds 0°C and the phytoplankton biomass increases. Both stage C5d (58.2 %) and adults (41.8%) appeared on day 174 (Fig. III-3B). Stage C5d moulted into adults roughly 120 days later, when their decreasing body mass triggers the molt toward adults (Fig. III-3C). The values of the parameters $p_1$ and $p_2$ imposed in this scenario did not allow the diapausing stage to last until the following spring, generating an unrealistic second generation issued form C5d at the end of the season.

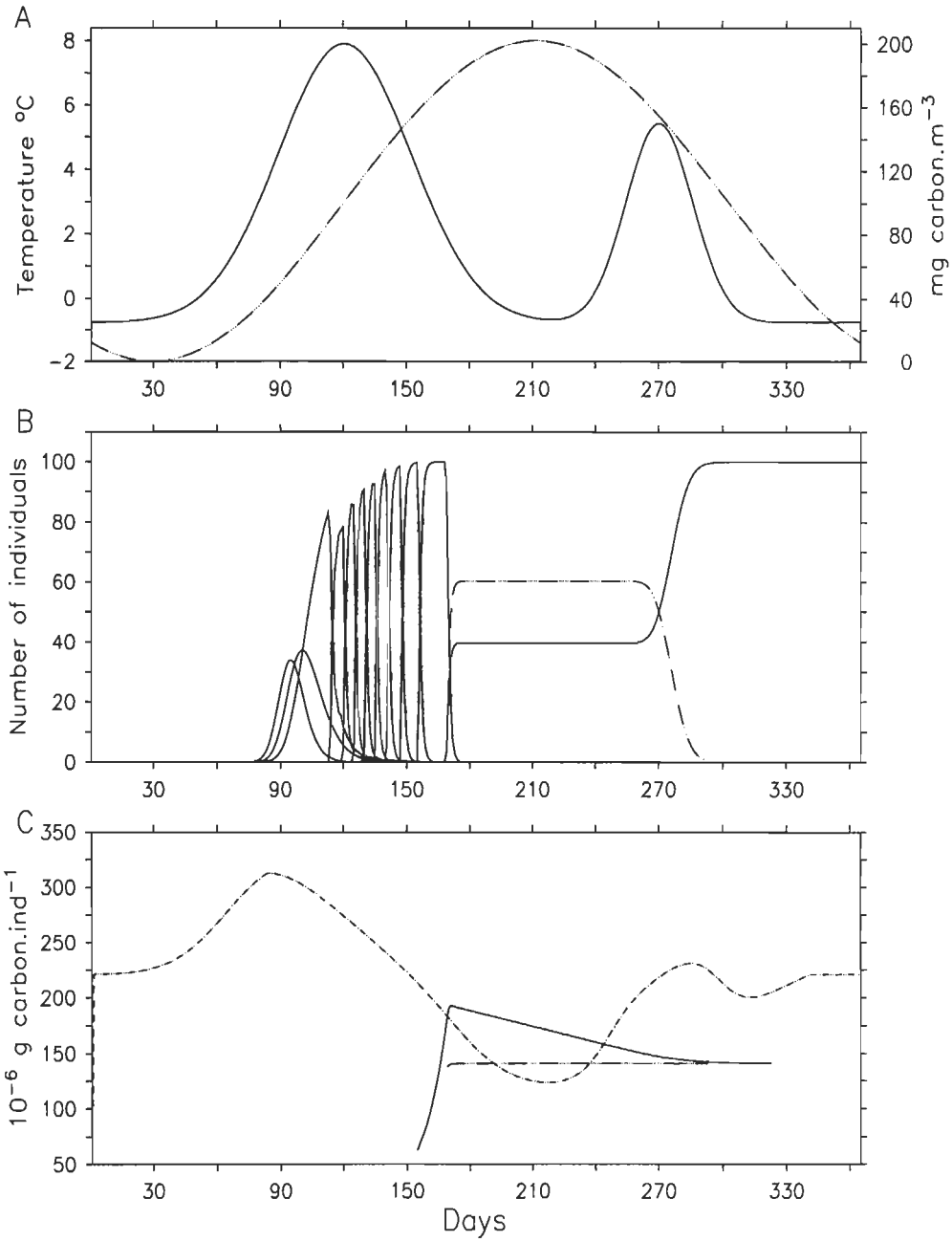


Figure III-3. (A) Chlorophyll *a* (continuous line) and temperature (dashed line) forcing used in the 0-D simulations. (B) Abundances of a simulated cohort initiated with a normally distributed total of 100 eggs (dashed line: C5d). (C) Mean mass of total C5 (active and diapausing; continuous line), critical moulting mass (CMM) of C5 (short-dashed line), and CMM of diapausing C5d (dashed line).

*Population dynamics.* In a second 0-D scenario, we took into account population dynamics processes as sources (egg production) and sinks (mortality). A quasi-stationary population structure was reached for an optimal combination of the free parameters $p_1$ = 53% and $p_2$ = 83%. Our simulated population produced two generations of C6f, the first ($G_0$) during winter-time emergence from diapause and the second ($G_1$) at the beginning of summer (Fig. III-4B). Then cohorts develop throughout summer and autumn. The maximum abundance of C6f occurred at the beginning of March, about 2 months prior to the maximum egg abundance. The negative temperatures at emergence from diapause prevented growth and egg production, until positive temperature occurred around day 90. Another 20 days were required for C6f to attain the minimum body mass allowing the initiation of egg production, which is equivalent to the maturation time observed (e.g. Runge and Plourde, 1996). C6f from $G_0$ persisted during the 120 days needed for the $G_1$ to appear, owing to their low mortality rates. The mean body mass of C6f decreased each time new females were recruited, and it was maximum in spring, minimum in summer and intermediate in autumn (Fig. III-4C).

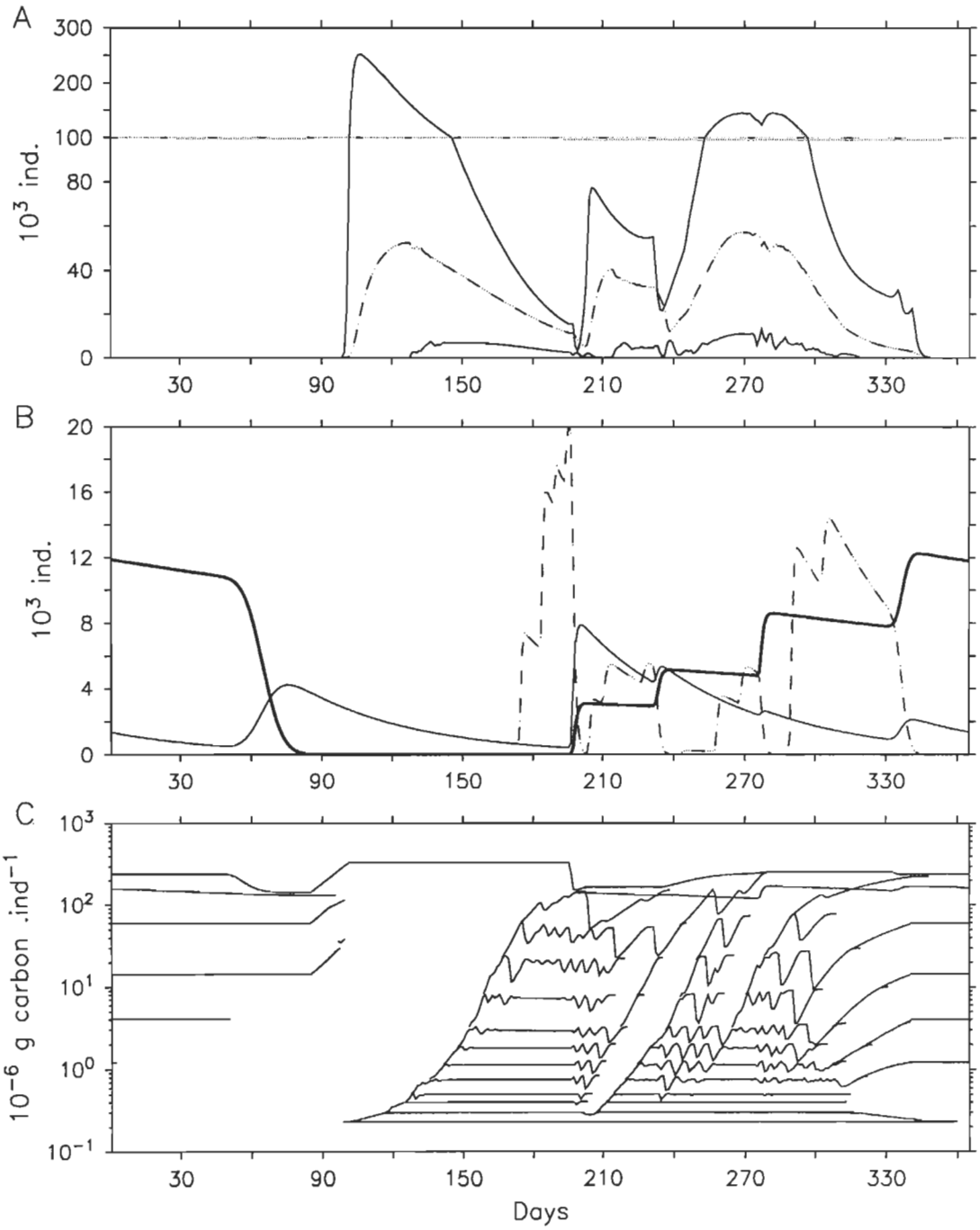


Figure III-4. Abundance of (A) eggs, N3 (dashed line), N6 and (B) C5 (dashed line), C5d (bold line) and C6f (thin line). (C) Mass trajectory of each successive stage. Results are stable time series obtained after ten cycles of the same environmental forcing as Fig. III-3.

There were three events of egg recruitment (Fig. III-4A). The first one resulted from the emergence of mature C6f from the overwintering stock, the increase in temperature and the high food concentration. The second event resulted from the appearance of the second generation of C6f during a period of lower food availability but higher temperature and higher females' body mass. The third event of high egg production closely followed the autumnal bloom while temperature and females abundance were decreasing. Seasonal changes in C6f body mass also influenced the abundance of eggs, as the egg production rate was formulated as a proportion of the body carbon content of the females. These three periods of high egg abundance were tracked in the abundance of N3, but they were dampened in the following stages, which generated several successive abundance pulses. N3 was the first growing stage of *C. finmarchicus*, and its stage duration was longer than any other larval stage (Campbell et al., 2001). Those characteristics lead to the important difference in abundance between N3 and N4, as the high mortality rate of N3 (0.25 $d^{-1}$) applied for an extended period. Successive events of recruitment into C5 and C5d contributed to the progressive build-up of the diapausing stock during late summer and autumn, while abundance of C6f gradually declined from mid-summer onward. The trajectories of the mean body mass of stages clearly showed the appearance of the first generation around day 120 (Fig 6C), which takes about 80 days to achieve adulthood. It was followed by several pulses of early stages tractable along the body mass trajectories. The growth rate showed seasonal

variability: the slope of the curve obtained for the several cohorts developing throughout the year was maximal in summer between days 210 and 270, and decreased thereafter, being null when the temperature reached zero degrees.

### *10.2 1-D simulations*

*Environmental setting.* Temperature and food profiles constructed from field data showed features typical of the northwest GSL. The temperature field was characterized by the cold intermediate layer (CIL, defined here by the 2°C isotherms in Fig. III-1A). The CIL is formed in spring and persists until late autumn, creating a strong temperature gradient over the first 50m of the water column. Differences in temperature profiles between 1999 and 2000 were weak (Fig. III-1A). The seasonal pattern in chlorophyll *a* biomass was characterized by a spring bloom during the onset of the surface thermal stratification, a sub-surface summer bloom below the thermocline and a more variable autumnal bloom (Fig. III-1B). Temperatures associated wih the depth of maximum chlorophyll *a* biomass were typical of the upper CIL and remained cold throughout summer (4°C on average, Fig. III-1C). Interannual variability was however high; the surface spring bloom was stronger, and the sub-surface summer bloom was deeper in 1999 than in 2000. The autumn bloom occurred later and was weaker and shallower in 1999. The temperature and

food conditions were thus similar in July of both years (high chlorophyll *a*, low temperature) but markedly different in August, with high chlorophyll *a* (4 $mg.m^{-3}$) and low temperature (3°C) in 1999, and low chlorophyll *a* (< 1 $mg.m^{-3}$) combined with warmer temperature (c.a. 8°C) in 2000.

*no-DVM scenario*. Optimization of the free parameters gave $p_1$= 46% and $p_2$ = 76%. The abundance of diapausing C5d was close to the observations in late autumn and winter 1999-2000, and sufficient to initiate an adequate $G_0$ of females in spring of 2000 (Fig. III-5A,B). Despite the difference in the environmental conditions between 1999 and 2000, the overwintering stock in autumn 2000 was also close to the observations. The diapause window was similar between the two years studied. The time of exit of diapause was in early April in both years, and the principal annual event of recruitment of C5d occurred in both years in August when the first generation ($G_1$) of C5 achieved its CMM. Thereafter C5d composed more than 50% of the total C5 population (active C5 + diapausing C5d; Table III-4).

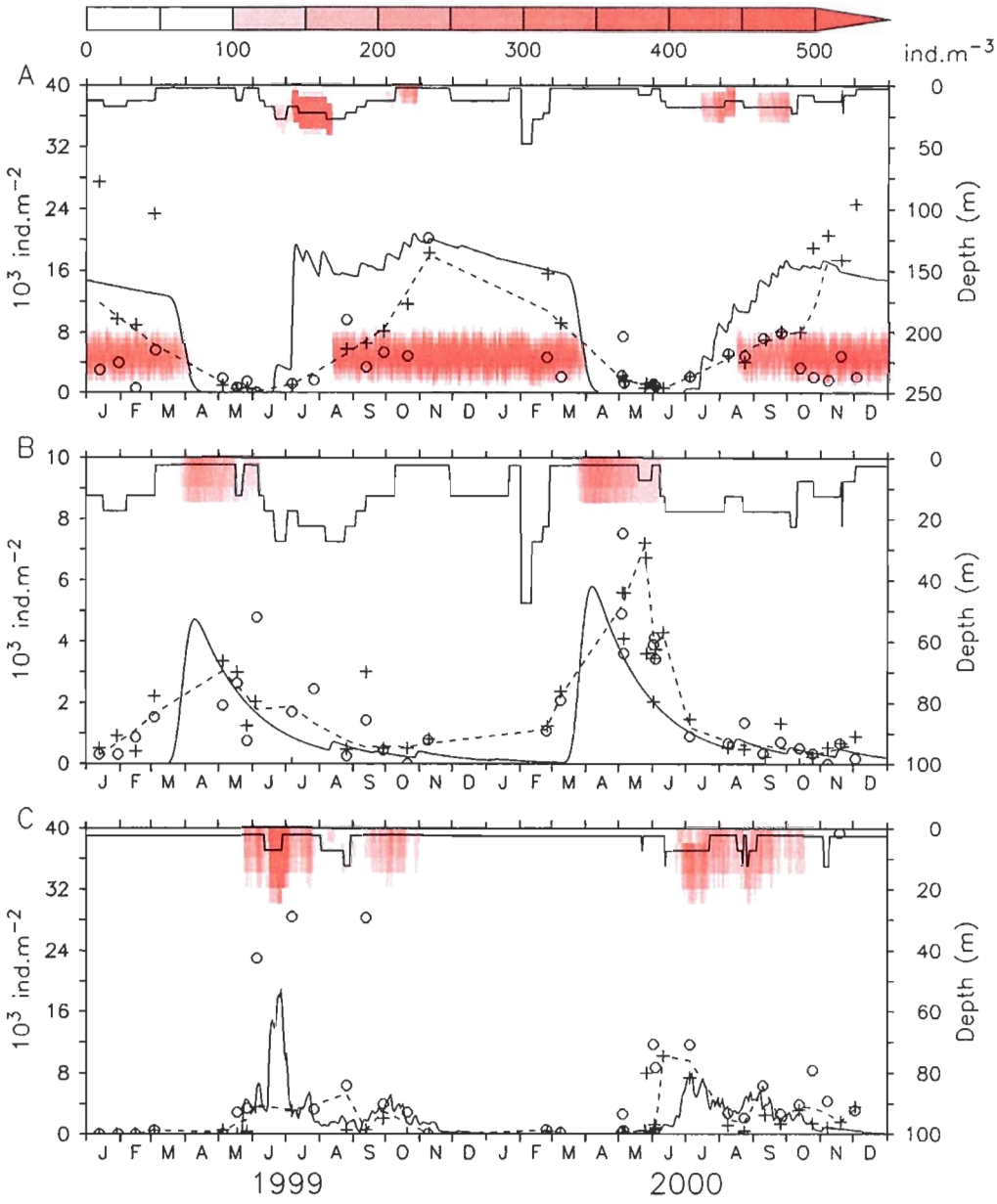


Figure III-5. 1-D simulation, no-DVM scenario: swimming stages seek stage-specific levels of chlorophyll *a*. Observed and simulated abundance of (A) total C5 (active and diapausing), (B) C6f and (C) C1-C3. Observed (crosses: AG, circles: GC, short-dashed line: LOWESS curve) and simulated (lines) abundance refer to the left-hand scale. The corresponding simulated density in background refer to the color scale above. The upper line represents the target depth of the stages and it refers to the right-hand scale.

Inter-annual variability in environmental conditions impinged on the smaller successive events of recruitment of C5d in summer and autumn of each year, which were more variable in time and in relative contribution to the diapausing stock (Table III-4). The abundance of C5 was overestimated in summer 1999. Massive recruitment of C5 in 1999 followed an earlier peak in the simulated abundance of C1-3 in late June – early July which did not occur in 2000, neither in the simulation nor in the observations (Fig. III-5C). The high abundance of C1-3 in early summer 1999 was close to the highest observed abundance (between 20,000 and 30,000 ind.$m^{-2}$) reported for the same period of 1999. However the abundance of C1-3 was underestimated in spring 2000 and its maximum was delayed by one month until early July. The simulated abundance of C6f was to the contrary one month early both years compared to the observations. Maximum abundance of C6f followed the exit from diapause in April, whereas the observed maximum occurred in May. The comparison should however be considered with some caution owing to the lack of data in April of both years. The abundance of females slowly decreased until August when a weak second generation appeared, followed by several cohorts during autumn.

Table III-4. Timing of the major events of recruitment of C5d in the DVM scenario, and associated relative contribution to the total diapausing stock of each year.

| | | | |
|---|---|---|---|
| 1999 | 13 August | 30 September | 1 November |
| Proportion (%) | 69 | 8 | 23 |
| 2000 | 19 August | 6 October | 19 November |
| Proportion (%) | 57 | 38 | 5 |

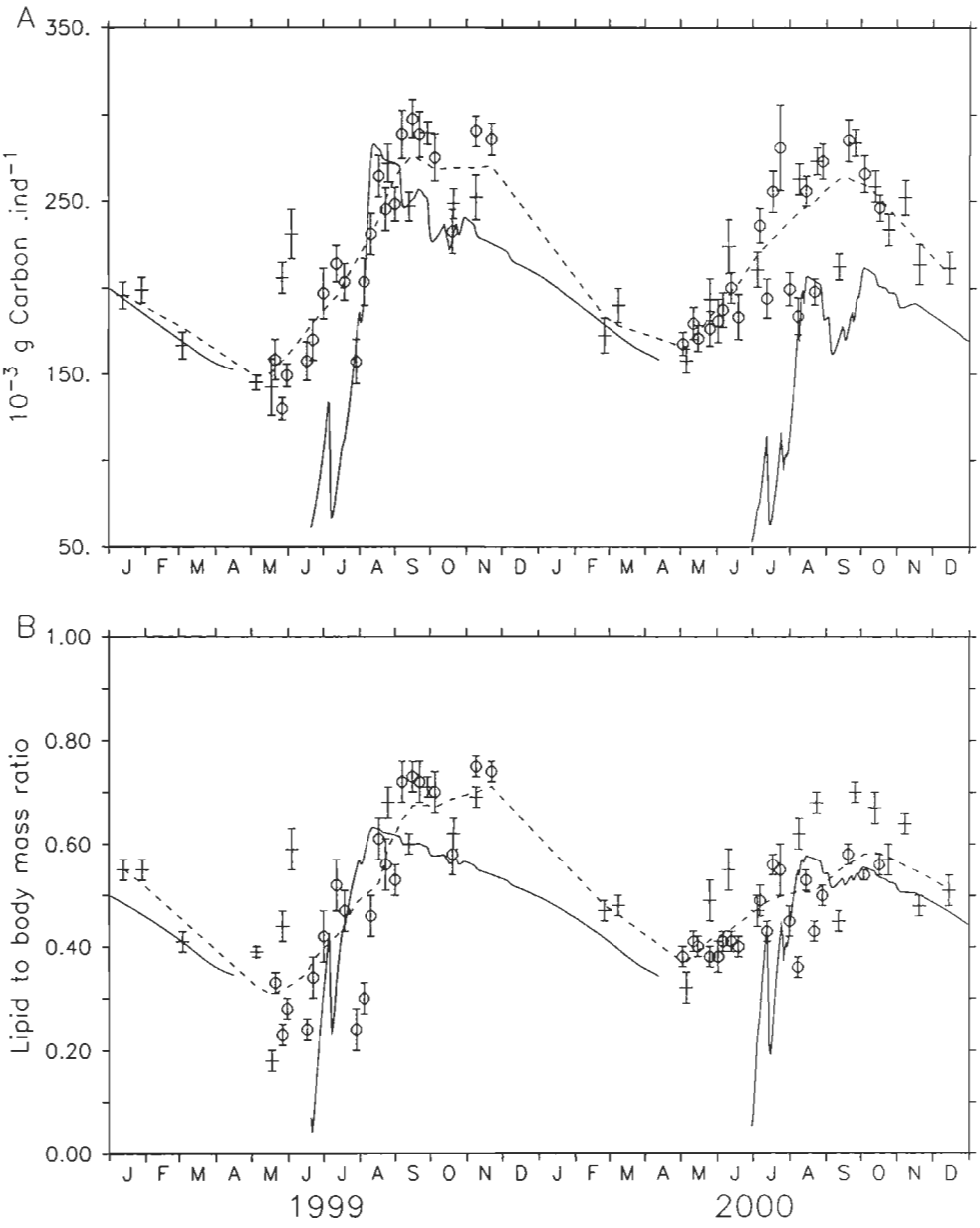


Figure III-6. 1-D simulation, no-DVM scenario: swimming stages seek stage-specific levels of chlorophyll *a*. Observed (crosses: AG, circles: LE, short-dashed line: LOWESS curve) and simulated (continuous line) (A) mean body carbon content and (B) lipid proportion of total C5 (active and diapausing).

Simulated averaged body mass of C5 lied within the lower range of observed values in summer and autumn 1999, but was underestimated relative to observations in summer and autumn of 2000 and during early recruitment of C5 in June both years (Fig. III-6A). The ratio of lipid to body mass was also underestimated both years, and while recruiting C5 had no lipid content in the model, the minimum proportion of lipid observed in C5 ranged from 20% in 1999 to almost 40% in 2000 (Fig. III-6B). During the overwintering period between August 1999 and March 2000, C5d lost almost 40% of their body mass (Fig. III-6A), which means a ratio of lipid to body carbon decreasing from 60% to 35% (Fig. III-6B).

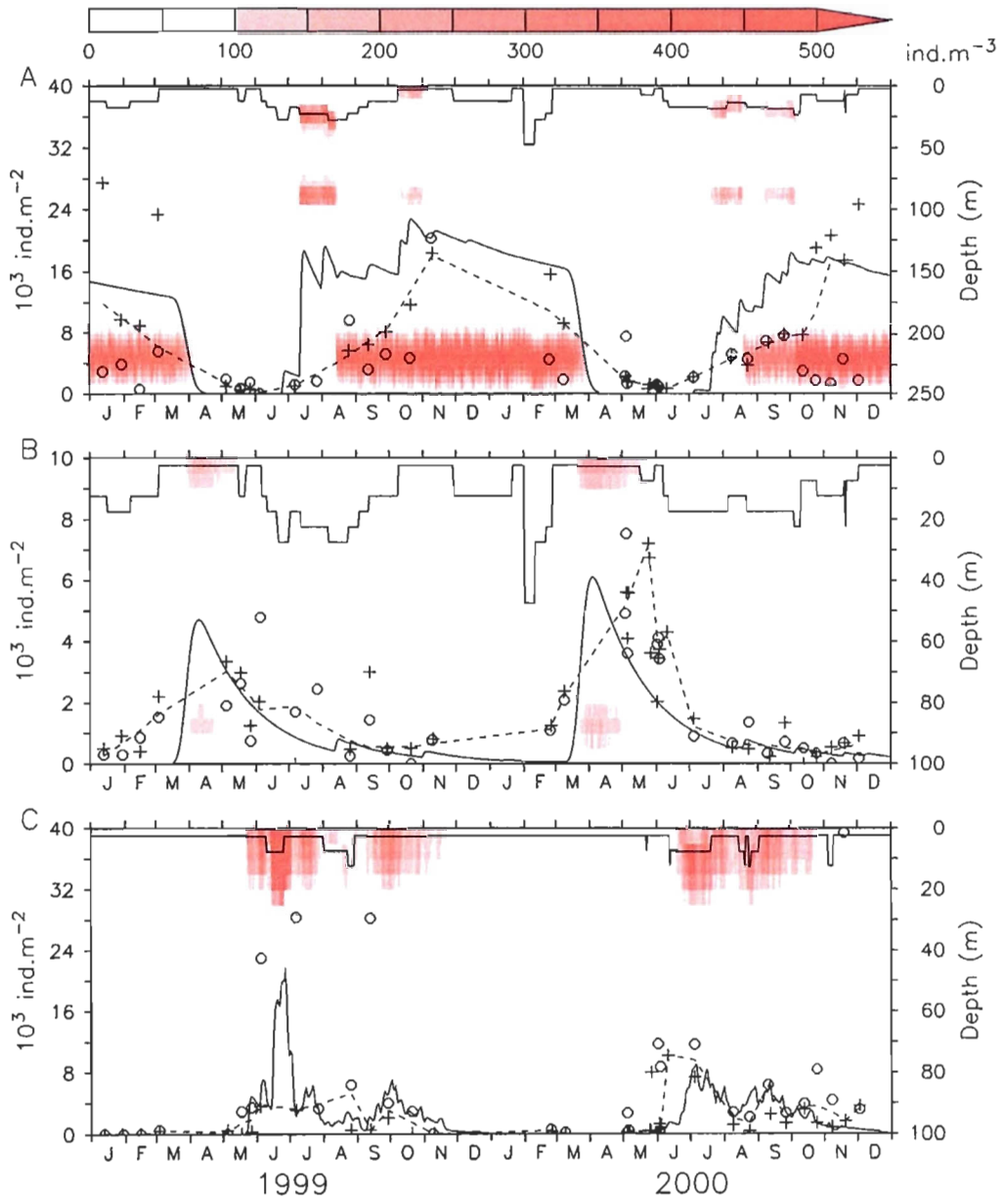


Figure III-7. 1-D simulation, DVM scenario: swimming stages seek stage-specific levels of chlorophyll *a* and C4, C5 and C6f perform DVM. (A) total C5 (active and diapausing), (B) C6f and (C) C1-3. Legend of the figure as in Fig. III-5.

*DVM scenario*. In this scenario, C4, C5 and C6f performed DVM. Optimal parameters were $p_1$ = 47% and $p_2$ = 87%. The ratio of lipid to body mass threshold allowing C5 to enter diapause ($p_1$) was similar to the one in the no-DVM, whereas the amount of growth allocated to lipid ($p_2$) was higher with DVM. The resulting abundance of *C. finmarchicus* stages were however similar (Fig. III-7), owing to the optimization procedure which actually minimized the difference between the abundances of copepodites simulated and observed. The main difference between both scenarios laid in the mean body mass of total C5 during 2000 (Fig. III-8A). Simulated body mass of total C5 were higher in summer 2000 for the DVM scenario, and they generally fell within the range of observed values. The minimum in simulated body mass of C5 were also higher and closer to the observations both years, but still almost 50 $\mu$gC less than observations. The ratio of lipid to body carbon were however similar between both scenarios (Fig. III-8B).

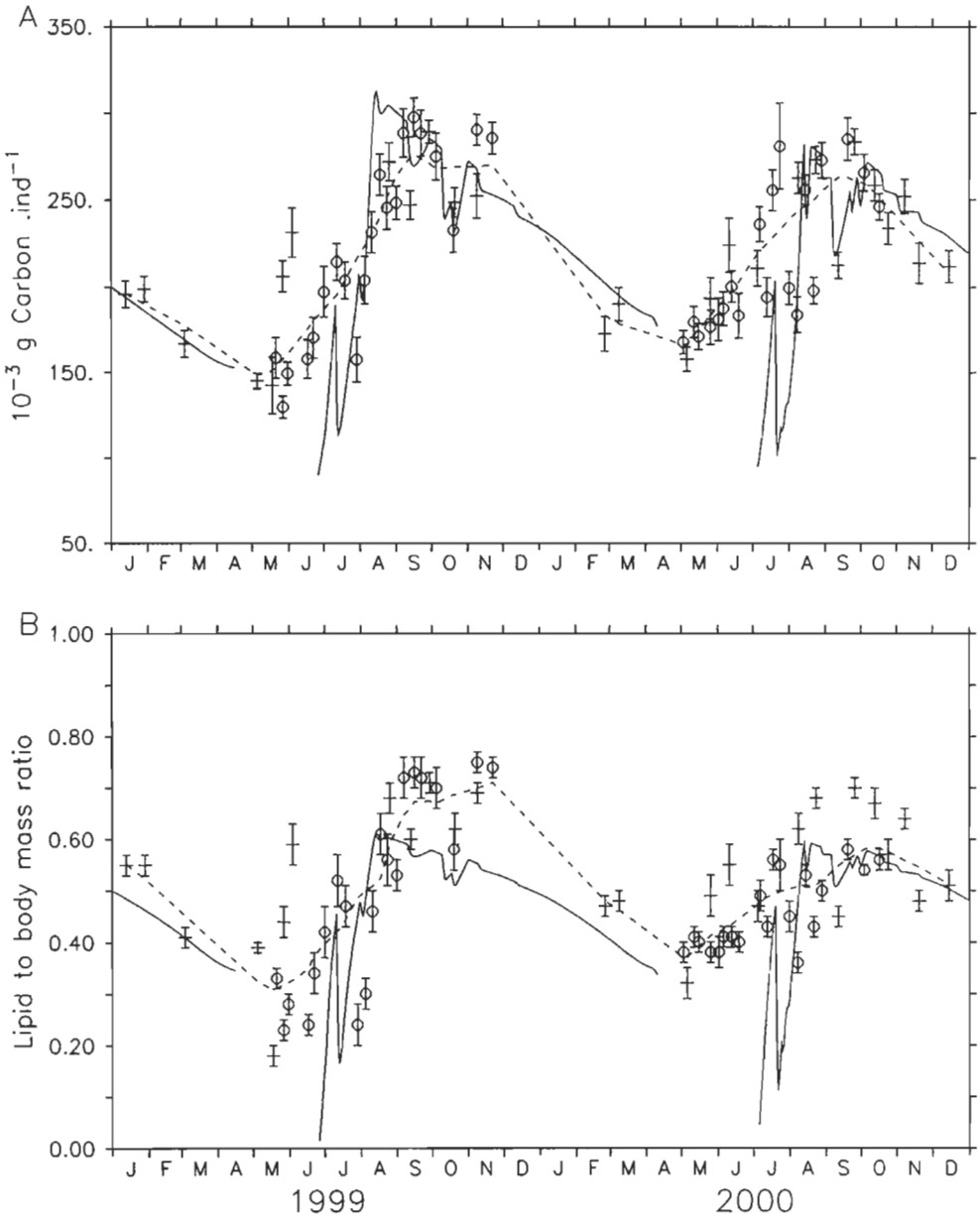


Figure III-8. 1-D simulation, DVM scenario: swimming stages seek stage-specific levels of chlorophyll *a* and C4, C5 and C6f perform DVM. (A) mean body carbon content and (B) lipid proportion of total C5 (active and diapausing). Legend of the figure as in Fig. III-6.

# 11 Discussion

An accurate determination of the stages duration in a copepod population dynamics model is essential to correctly represent the life cycle. In our model, the development of *C. finmarchicus* resulted from the interaction between the stage-specific growth rate and the critical moulting mass (CMM), both nonlinear functions of temperature and food. However, alternate formulations exist. For example, Fiksen (2000) designed a stage structured biomass model in which growth rate was a function of the temperature-dependent development rate, constant stage-specific CMM, and food. It is likely that growth and development actually interact to determine the stage-specific CMM (e.g. Aksnes et al., 2006), but data needed to validate such a conceptual model are still lacking. The strength and quality of the empirical relationships available for both stage-specific growth rates and CMM of *C. finmarchicus* (Campbell et al., 2001) allows our model to simulate realistic population dynamics and biomass of *C. finmarchicus*, with the benefit of a light computational and no numerically generated "premature maturation".

However, whenever there is strong recruitment in a growing stage, a delay of moulting to the next stage could appear. In a simplified case where mortality and transfer to the next stage are not considered, basic calculus shows that the time

evolution of the mean body mass of any stage i ($m_i$) is increased by its growth, but decreased by the recruitment of lighter individuals from the preceding stage i-1 (see Fennel, 2001). The temporal derivative of the biomass $B_i$ of the stage i, expressed in term of the product of the mean mass of the stage $m_i$ with its abundance $N_i$ gives

$$\frac{dB_i}{dt} = m_i\frac{dN_i}{dt} + N_i\frac{dm_i}{dt} \qquad \text{(D1)}$$

The rate of change of biomass is also dependent on the growth rate and the transfer rate from the preceding stage

$$\frac{dB_i}{dt} = g_i B_i + t_{i-1,i} B_{i-1} \qquad \text{(D2)}$$

while the rate of change in abundance is dependent solely from the transfer rate from the preceding stage

$$\frac{dN_i}{dt} = t_{i-1,i} N_{i-1} \qquad \text{(D3)}$$

Reorganizing equation (2) gives

$$\frac{dm_i}{dt} = \frac{1}{N_i}\left(\frac{dB_i}{dt} - m_i\frac{dN_i}{dt}\right) \qquad \text{(D4)}$$

which becomes

$$\frac{dm_i}{dt} = g_i m_i - t_{i-1,i}\frac{N_{i-1}}{N_i}\left(m_i - m_{i-1}\right) \qquad \text{(D5)}$$

when substituting equations (D2) and (D3) into equation (D4).

Any increase in the transfer rate from stage i-1, in the abundance of stage i-1, or in the difference between the mean body mass of successive stages would result in a higher penalty on the growth of the mean body mass of stage i, and thus on its stage duration. Sensitivity analysis showed that the effect of this dynamic of the model was typically below 20% of the theoretical development duration of the stage, with a maximum of 50% in a worst case scenario, i.e. high recruitment, low growth rate, and a two-fold increase of the mass needed to reach the CMM (e.g. N3). This "pooling effect" is inherent to population level models formulated in term of differential equations, aiming at describing the mean properties of a group of individuals. The production of abundance pulses also resulted from this inherent property of the model. As the mean body mass of a given stage reaches its CMM, moulting to the next stage occurs. By reducing the proportion of the heaviest individuals while lighter individuals from the preceding stage still recruits, moulting leads to a reduction of the mean body mass of the stage. Moulting will occur once again after growth increases body mass toward CMM, generating pulses in abundance with a time-scale dependent on the development duration of the stage and the eventual pooling effect described above.

The simulated population dynamics of *C. finmarchicus* in 1999 was

characterized by a strong first generation of C5 in both scenarios. The high abundance of C5 simulated in summer 1999 was similar only to the abundance observed three months later. The summer stratification of the water column lead to a sharp increase in surface temperature (Fig. III-1C), which allowed the growth rate of surface-dwelling nauplii to be more than twice as high in June than in May. The consequent faster development implied a decrease of the cumulated mortality of the larval stages, hence generating a recruitment burst in the following copepodite stages (Fig. III-5C and III-7C). The trade-off between development duration and daily mortality rate in the early development stages appeared critical for the population dynamics of *C. finmarchicus*. The model was indeed sensitive to changes in the mortality of young stages (Fig. III-9). The model was even more sensitive to the mortality of females, owing to their role in producing offspring. Mortality is actually time and space dependent (Ohman et al., 2004). According to modeling studies, the dependence of mortality to season, region and depth could dramatically alter abundance patterns (e.g. Fiksen and Carlotti, 1998; Neumann and Kremp, 2005; Speirs et al., 2006). Exploring further the complex issue of variable mortality patterns was however beyond the scope of this work, which was to develop a formulation of diapause control through lipid metabolism and test it against the strong environmental variations observed.

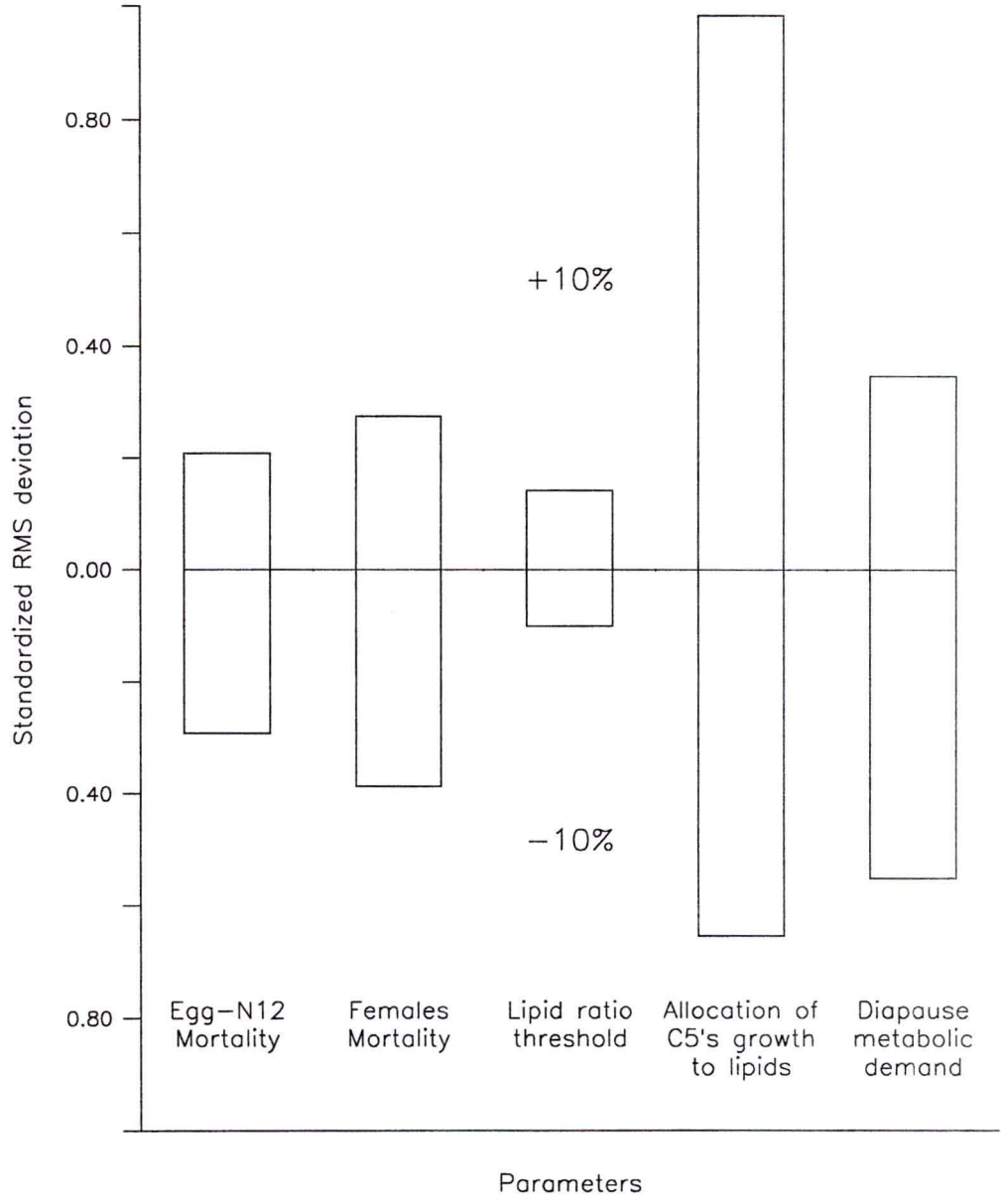


Figure III-9. Sensitivity of the 1-D model to selected parameters estimated by the RMS deviation standardized by the mean of the C5d abundance. This metrics represents the mean deviation of the results from the simulation with altered parameter (±10%) with respect to the DVM scenario as reference.

The annual minimum in body mass of C5 occurred in June in both the observations and the simulations (Fig. III-8A). Body mass data thus suggested that the appearance of the first generation of C5 occured as soon as June in the North-West GSL, in contrast with abundance data which showed no significant increase before August. The discrepancy between both observations could result from the advection. The mean residual surface circulation in the north-west GSL heads downstream toward the Atlantic, but meso-scale horizontal circulation is dominated by the interactions of a baroclinic coastal current along the Gaspé peninsula (Gaspé Current - GC) driven by the St. Lawrence river run-off, and a quasi-permanent off-shore anticyclonic gyre (Anticosti Gyre - AG). Instabilities of the GC sporadically alter the circulation by displacing the AG core and re-circulating around it water masses of estuarine origin with their load of zooplankton (Tang et al., 1980; Mertz et al., 1988; Saucier et al., 2003; Sourisseau et al., 2006). The deep-dwelling diapausing stock is not however influenced by surface circulation, but rather by the slow deep upstream residual circulation prevailing in the GSL system (Saucier et al., 2003, 2009). According to this advection pattern, the drastic fall in the abundance of C5 between the end of March and the beginning of May should provide a more reliable estimate of local timing of exit from diapause than the later increase in the abundance of female. The delay between the maximum abundance of females in May and the decrease in abundance of C5 sometime in April could result from the strong spring freshet providing the North-West GSL with females exiting diapause in

the LSLE upstream. Similarly, the sustained high spring and summer abundance of the younger C1-3 could partly result from the "Calanus pump" effect, which is the hypothesized impact of the delayed summer production in the LSLE in providing the North-West GSL with young stages through the residual surface circulation (Plourde and Runge, 1993; Plourde et al., 2001). On the contrary, flushing from the surface layer could contribute to the low abundance of C5 observed in early summer, while the increase in abundance in August could result in part from the build-up of the diapausing stock and its slow upstream advection at depth.

Individual biomass gave information complementary to abundance on the population dynamics of *C. finmarchicus*. Whereas abundance data were used to optimize the free parameters of the model, body mass observations served as independent control variables. The comparison between simulated and observed lipid content in C5 was crucial to estimate the pertinence of our mechanistic control of diapause based on lipid metabolism. The simulated body mass of C5 lied within the range of observed values only for late copepodite stages developing in a cold environment. The difference between the temperature at the depth of maximum chlorophyll *a* (no-DVM scenario) and the median temperature experienced by migrating stages (DVM scenario) during the major summer recruitment event of C5d was 4.2 °C in August 2000, compared to 1.4 °C in August 1999. The colder temperature experienced by the migrating C4 and C5 stages in summer 2000 in the

DVM scenario lead to heavier C5 within the range of observed values.

The observed minimum in body carbon (c.a. 175 $\mu$g C) and ratio of lipid to body carbon (c.a. 0.35) simulated for C5 in April at the end of the diapause period laid within the range of the observations. Moreover, these measurements are comparable to the carbon content of immature females arising from diapause in spring in the LSLE (160 to 220 $\mu$g C $fem^{-1}$, Plourde and Runge, 1993), and the associated range of relative oil sac volume (0.15 to 0.3, Plourde and Runge, 1993). The values reported by Plourde and Runge (1993) are equivalent to a range of lipid carbon remaining in immature females freshly arising from diapause of 50 to 70 $\mu$g C. This corresponds to several estimations of the minimum lipid carbon needed by diapausing C5 for the terminal molt and the maturation of the gonads, ranging from 40 $\mu$g C in Rey-Rassat et al. (2002) to 70 $\mu$g C in Ingvasdottir et al. (1999).

Later in summer, the observed minimum lipid fraction in newly recruited C5 was higher than in the simulation results because no lipid compartment was simulated in C4. This has important implications for the parameterization of the allocation of growth toward lipids in C5. The 9% higher allocation of growth toward lipids between the DVM and the no-DVM scenarios resulted from the higher CMM of migrating C4 exposed to lower temperatures during their development.

Higher CMM in C4 means higher initial structural mass for recruiting C5 (eq. 4, Table III-1), which hence need a higher proportion of their growth to be routed toward lipid in order to accumulate the amount required to enter diapause. The lipid compartment should be taken into account in stage C4 and new data are needed, especially as the control of diapause entry could involve the C4 stage (Johnson et al., 2008). However the contribution of C4 from late generations in terms of abundance to the diapausing population seemed limited in the north-west GSL. The proportion of C4 among total C4, C5 and C6f stages found below 100m at night (Fig. II-3E, 3F) were 17% in late summer and 2.5% in spring. This corresponds to the lower range of what was reported for the western Atlantic, with 10% in the Labrador Sea (Heath et al., 2004) and 12% in the Slope Waters off Nova-Scotia (Head and Pepin, 2007).

The model was very sensitive to parameters involved in the control of diapause duration and less sensitive to demographic parameters (Fig. III-9). A 10% increase or decrease in the parameter of growth allocation toward lipids in C5 ($p_2$) resulted in dramatic alteration of the abundance pattern. The basal metabolic rate of lipid consumption in C5d was the second most sensitive parameter. While the former parameter defined the amount of lipid which can be accumulated during the growth of C5 before diapause, the later defined the rate of use of lipid during diapause. Their combination determined the duration of diapause according to our

assumptions. In the case of a 10% increase (decrease) of growth allocation toward lipids, the time of exit from diapause of C5d was several months later (earlier) than expected, which lead to spurious abundances and to an increase (decrease) of the *C. finmarchicus* population at the end of the second year. The model responded inversely to a 10% increase (decrease) of the the basal metabolic rate of lipid consumption in C5d. The sensitivity of our model to the growth allocation toward lipids probably resulted from the use of a constant value. The ability to store lipids is probably linked to the size of the C5 individuals as proposed by Miller et al. (2000) and suggested by the observations of Saumweber and Durbin (2006) on diapausing C5. A better understanding of the complex process of growth in copepodites (Miller, 2008), and specifically of the process of lipid accumulation will lead to formulations more responsive to changes in environmental conditions and internal status of the individual. Contrary to the current lack of knowledge about the accumulation of lipid in copepodites, several studies of the respiration rates in diapausing individuals allowed an accurate parameterization of the basal rate of lipid consumption in C5d (e.g. Ingvarsdottir et al., 1999; Saumweber and Durbin, 2006). The sensitivity of the model to both parameters however enlightens the limit of the population level approach, which does not take into account the expression of individual variability as the variance about the mean behavior of the individuals.

Our model is to our knowledge the first prognostic model to test a lipid-

controlled diapause mechanism at the population level. Our mechanism is based on the internal lipid status of the mean individual, as an integrative response to the environment over the time scale of its development from egg to C5. Our model reproduced the observed coincidence of surface-dwelling developing C5 and deep-dwelling diapausing C5 (e.g. Hirche, 1983; Miller et al., 1998b), which incited modelers to prescribe the fraction of the C5 needed to initiate diapause at each generation (e.g. Carlotti and Wolf, 1998; Lynch et al., 1998; Miller et al., 1998a; Tittensor et al., 2003; Zakardjian et al., 2003; Speirs et al., 2006; Slagstad and Tande, 2007). Our model also allowed diapause to occur long before the environment becomes adverse, in accordance with theories regarding optimization of life histories in species undergoing a recurrent adverse period (Taylor, 1980; Norrbin, 1996). Short term induction of diapause in response to a catastrophic event (for example a low food concentration threshold) as proposed by Hind et al. (2000), proved not to be adequate over a wide range of environmental variability at the scale of the North Atlantic (Speirs et al., 2006). Strong environmental variability can occur at even smaller spatial scale. For example, within the AZMP covering the Gulf of St. Lawrence and the Newfoundland and Scotian shelves, the diapause time-window varies by several months (Johnson et al., 2008). The plastic response of our model to environmental variability, and its light computational cost, allows it to be readily embedded in an Eulerian GCM (e.g. Fennel and Neumann, 2003) in order to test its ability to produce a realistic phenology for *C. finmarchicus* populations

undergoing strong influences from the hydrodynamics in the continental shelf of the north-west Atlantic (Gentleman, 2000; Johnson et al., 2006; Miller et al., 1998a; Plourde et al., 2001; Zakardjian et al., 2003).

CHAPITRE IV

# MORTALITY AND SURVIVAL IN EARLY STAGES CONTROL RECRUITMENT IN *Calanus finmarchicus*

## 12 Résumé

Nous présentons des observations décrivant la climatologie saisonnière et les patrons spatiaux de mortalité et de recrutement des premiers stades de *Calanus finmarchicus* dans l'estuaire et le golfe du Saint-Laurent, respectivement. La mortalité subie durant le développement des œufs à N3 ou N6 montrent des variations saisonnières et spatiales importantes, le plus souvent indépendantes des patrons de production d'œufs. Les patrons de recrutement des derniers stades nauplii dictent les patrons d'abondance de nauplii N4-6 (ESL) ou copépodites C1-2 (GSL). Ils sont essentiellement liés aux patrons de survie et donc largement indépendant des patrons de production d'œufs. Un modèle de régression multiple démontre les effets opposés de la biomasse phytoplanctonique et de l'abondance des femelles dans le contrôle de la mortalité. Ceci illustre l'impact bénéfique d'une forte biomasse phytoplanctonique sur la survie, que ce soit par une relaxation du cannibalisme ou de l'inanition. Une analyse de modélisation démontre l'impact de différentes formulations des taux de mortalité sur l'amplitude et le timing du recrutement vers les derniers stades nauplii. Nos simulations suggèrent de plus que la température n'est pas déterminante pour les patrons de survie des stades, en raison de son impact général sur le métabolisme (le développement). Notre étude insiste sur l'importance de représenter de façon mécaniste la mortalité et la survie dans les modèles numériques de dynamique des population de *C. finmarchicus*.

# 13 Introduction

Accurate description of mortality patterns is one of the most important challenges in marine ecology and in modeling zooplankton population dynamics (Runge et al., 2004). Despite its well-recognized importance in the control of population dynamics in planktonic copepods (Myers and Runge, 1983; Kiørboe et al., 1988; Kiørboe and Sabatini, 1994; Hirst and Kiørboe, 2002; Twombly et al., 2007), mortality has been mainly overlooked in marine ecology because of the inherent difficulty to obtain reliable estimates on the field. This difficulty mainly arises from the openness of most marine ecosystems, i.e. that planktonic populations are subjected to losses and gains through advective processes. Because of this constraint, the few studies describing marine copepod mortality using horizontal life table analysis (HLT) (Wood, 1994) were consequently restricted to semi-enclosed systems such as fjords (Ohman and Wood, 1996), or based on high-resolution time series of relatively short duration (Ohman and Hirche, 2001; Eiane and Ohman, 2004). The need for robust approaches for applications in more open regions has recently promoted the development of the Vertical Life Table method (VLT) (Aksnes and Ohman, 1996). The VLT approach uses the instantaneous ratios between successive life stages rather than the variability of their absolute abundance over time, which implies different assumptions allowing its use with

data collected on synoptic spatial surveys or during long time series in more open marine habitats (Aksnes and Ohman, 1996; Ohman et al., 2002; Hirst et al., 2007).

In marine copepods in general, mortality decreases sharply from the egg and early naupliar stages to older development stages, and shows distinct stage-specific patterns among species, regions, and seasons (Kiorboe et al., 1988; Kiorboe and Sabatini, 1994; Eiane and Ohman, 2004; Ohman et al., 2004; Ohman et al., 2008). Only a few studies directly demonstrated that mortality in early stages could exert a strong effect on the population dynamics of marine copepods, mostly in small neritic species (Peterson and Kimmerer, 1994; Uye and Liang, 1998; Hirst et al., 2007). This phenomenon has been mainly attributed either to density-dependent processes (cannibalism) (Liang et al., 1994; Peterson and Kimmerer, 1994; Ohman and Hirche, 2001; Ohman et al., 2002; Ohman et al., 2008) or to predation from other copepod species (Liang and Uye, 1996a, b; Ohman et al., 2008). It is known that copepods could ingest con-specific eggs and early nauplii even in presence of alternate algal food, although the feeding mode remains equivocal (prey switching: Landry, 1981; independent feeding mode: Basedow and Tande, 2006). In *Calanus finmarchicus*, egg mortality rate could exceed birth rate prior to the spring bloom, and could potentially control the seasonal pattern in recruitment to copepodid stages in the Norwegian Sea (Hirche et al., 2001; Ohman and Hirche, 2001). Based on a limited set of data, Heath et al. (2008) hypothesized that spatial pattern in

naupliar mortality and survival would control regional differences in recruitment to copepodid stages in the Irminger Sea (Heath et al., 2008). However, there is still very few direct demonstration of the effect of mortality and survival on copepod recruitment and population dynamics, neither functional relationships relating mortality rate to environmental parameters. This lack of knowledge precludes the development of mechanistic functions of mortality that are needed in biological model of zooplankton population dynamics (Runge et al., 2004).

Our study aimed at testing the null hypothesis that patterns in recruitment to late naupliar stages in *C. finmarchicus* is determined solely by population egg production rate, implying relatively constant rate of mortality. Conversely, our alternate hypothesis was that variations in mortality and survival in early development stages control patterns in recruitment. We also aimed at developing an empirical relationship between mortality in early stages and key environmental parameters for its inclusion in a biological model. We applied the VLT approach to data describing seasonal and spatial environmental conditions (temperature, phytoplankton biomass) and *C. finmarchicus* population dynamics (egg production, stage abundance). Results were used to describe the seasonal climatology and spatial pattern in mortality in early stages and survival (recruitment) to late naupliar stages. Data from both sources were then used to test the hypothesis that density-dependent processes (cannibalism) in *C. finmarchicus* would be favored at

low level of alternative food by examining the relation between mortality, ambient phytoplankton biomass and abundance of adult females. Finally, we synthesized our results as a dynamic mortality formulation incorporated in a simple biological model of *C. finmarchicus* that was used to compare the effect of different deterministic and dynamic mortality formulations on population dynamics.

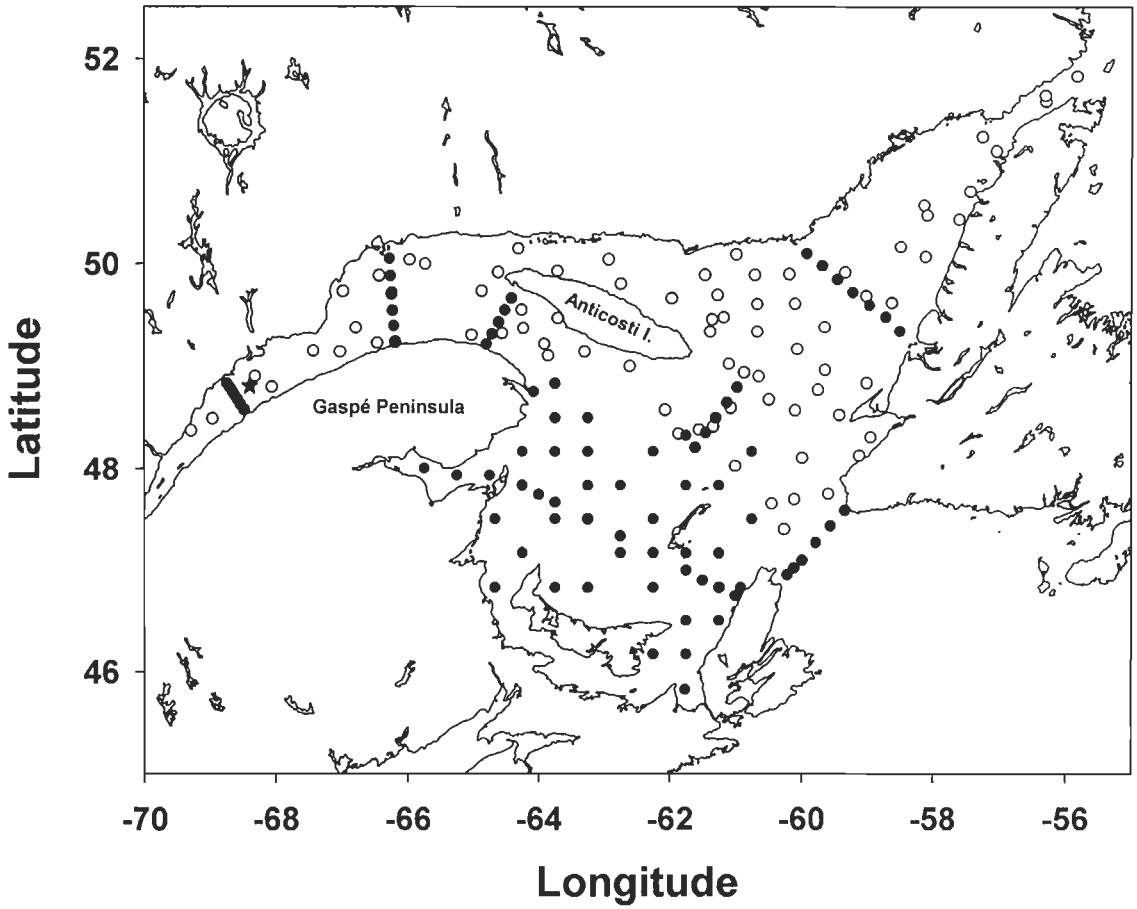


Figure IV-1. Map of the Gulf of St. Lawrence showing locations of the Rimouski station in the lower St. Lawrence estuary (Star), and stations sampled in June (Black circles) and August (Open circles) 2006.

# 14 Methods

## *14.1 Field work, environmental variations and basic population parameters*

A 340-m deep monitoring station located 12 nautical miles off Rimouski in the central lower St. Lawrence estuary (LSLE) was visited on a quasi-weekly basis from April to October-November in 1994, 1996-2000, and 2006 (Fig. IV-1). Zooplankton was collected concurrently with hydrographic data (CTD, chlorophyll *a* biomass) with a 333-$\mu$m (1994, 1996-2000) or a 200-$\mu$m (2006) plankton net vertically towed at 0.5 m $s^{-1}$ from 320-m to the surface, and with a 73-$\mu$m net from 50 m to surface (Plourde et al., 2001; Plourde et al., 2003). For the purpose of our study, abundance of naupliar stages of *C. finmarchicus* was estimated from 73-$\mu$m samples, while abundance of con-specific females was determined from depth-integrated samples collected with the 333-$\mu$m or 200-$\mu$m (only in 2006) nets as both sampling gears yield similar abundance estimates of late development stages (Plourde, unpublished data). Zooplankton samples and hydrographic data were also collected at 178 stations in the GSL in June and August 2006 (Fig. IV-1). Zooplankton was sampled with a 200-$\mu$m net vertically towed at 1 m $s^{-1}$ from 5m above the bottom to the surface. Naupliar stages of *C. finmarchicus* were distinguished from those of *C. glacialis* and *C. hyperboreus*, mostly present in April and May, based on stage-specific size frequency distributions, and from *Pseudocalanus* spp and *Metridia longa*

from both size and morphological criteria (Plourde, unpublished data; Durbin et al., 2000). Because nauplii N1 and N2 of *C. finmarchicus* could have been confounded with *Metridia longa* N1-2 during some years, we considered that N3 was the first stage for which a reliable identification was achieved.

A quantitative assessment of the mesh selection indicated that N3 and N6 of *C. finmarchicus* were quantitatively sampled with the 73-$\mu$m and 200-$\mu$m net respectively. The relationship between the width of organisms and mesh size described by Nichols and Thompson (1991) (their equation 4) showed that the 73-$\mu$m net captured 100% of *C. finmarchicus* N3 (body width of 128 $\mu$m, Durbin unpublished data). Additionally, more than 95% of nauplii stages N3-6 of *C. finmarchicus* are found in the upper 20 m of the water column in the LSLE (Plourde unpublished data; Durbin et al., 2000), indicating that our sampling strategy (0-50 m) was appropriate to reliably estimate abundance of *C. finmarchicus* N3. The same analysis applied to the 200-$\mu$m net resulted in an estimated capture efficiency of 20% and 80% for N5 and N6 (body width N5= 169 $\mu$m, N6= 203 $\mu$m, Durbin unpublished data). Considering that (1) tow speed affects the capture efficiency of the smaller organisms collected by a given mesh size (Colton et al., 1980), (2) our 200-$\mu$m net was towed at a speed typically 3 times lesser than the one used in the Nichols and Thompson (1991) study (1 vs 3 m $s^{-1}$), and (3) we only had a limited number (20-25) of direct comparisons between the 73-$\mu$m and 200-$\mu$m (2006), we

adopted a conservative approach and assumed that *C. finmarchicus* N6 were adequately sampled. Nevertheless, we assessed the potential impact of underestimating N6 abundance on our results by correcting N6 abundance based on the 80% capture efficiency estimated above and comparing daily mortality rates obtained with those estimated from non-corrected abundance data (see Results).

The population egg production rate (PopEpr) was used as the input parameter in the mortality estimate (see bellow). *In situ* Epr and hatching success were routinely measured at the fixed station (see Plourde and Joly, 2008 for technical details) with the exception of hatching success in 1994. We did not measure *In situ* Epr during the spatial surveys in 2006 but predicted it using an Ivlev (Type II) function relating specific Epr to ambient chlorophyll *a* biomass (Plourde and Joly, 2008). Chlorophyll *a* biomass during the August 2006 cruise was estimated from region-specific relationships between *in situ* fluorescence and in situ direct measurement of chlorophyll *a* biomass done during the cruise conducted in June 2006 (Starr, unpublished data). Epr was combined to abundance of adult females to estimate PopEpr assuming that all females were reproductively active during the spatial survey.

*14.2 Calculation of mortality rate, survival and daily recruitment*

We used the Vertical life table (VLT) approach to calculate instantaneous daily mortality rate (losses) in the combined egg-N3 (seasonal data) or egg-N6 (spatial surveys) stages (Ohman et al., 2002). We restricted our analysis to these stages (1) because the high mortality rates in early development stages would disproportionately impact the population dynamics relative to mortality in later stages (Ohman et al., 2008) and (2) to minimize the potential effect of advection. As most of these early stages are located in the upper 0-30 m layer in the St. Lawrence system (Runge and de Lafontaine, 1996), they would experienced the same influence of transport, a prerequisite for the application of the VLT (Aksnes and Ohman, 1996). Development times ($D$, in days) were estimated with temperature averaged in the upper 30 m of the water column (Campbell et al., 2001). We did not consider food limitation in the determination of $D$ in N3, N4 and N5 because mortality estimates appear generally little affected by variations in $D$ within a factor of 2 (Ohman et al., 2004; Hirst et al., 2007).

Mortality (m) averaged across egg-N3 ($m_{egg\text{-}N3}$) was estimated from equation (4) in Ohman et al. (2002):

$$\frac{A_{N3}}{PopEpr} = \frac{\exp^{-mD_{E-N2}}[1-\exp^{-mD_{N3}}]}{m}$$

where $A_{N3}$ is the abundance of N3 (ind.m$^{-2}$) and $D_{egg\text{-}N2}$ and $D_{N3}$ is *D* of the aggregate stage eggs-N2 and the stage N3 respectively. For the estimate of $m_{egg\text{-}N6}$, *D* from egg-N5 and in N6 were used instead.

The proportion surviving through egg-N3 ($S_{egg\text{-}N3}$) was computed based on equation (6) and (7) of Hirst et al. (2007):

$$S_{egg-N3} = \exp(-m_{egg-N3} \times D_{egg-N3})$$

where egg-N3 is replaced by egg-N6 for the estimate of $S_{egg\text{-}N6}$.

Assuming that the population is in steady state, recruitment to N3 ($R_{N3}$) (ind.m$^{-2}$.d$^{-1}$) was obtained with:

$$R_{N3} = PopEpr \times S_{egg-N3}$$

where N3 is substituted by N6 in the estimate of $R_{N6}$.

We used the abundance of nauplii N4-6 (seasonal, LSLE) and copepodite C1-2 (spatial, GSL) to examine the relative importance of the PopEpr and our indices of recruitment $R_{N3}$ and $R_{N6}$ in the control of the seasonal and spatial patterns in recruitment. We used these stages because they were not included in the estimates of mortality, survival and recruitment rate (independent variables) but close

enough in the cohort development schedule to minimize bias caused by variations in the development state of the population.

### *14.3 Condition of application of the VLT*

PopEpr shows important seasonal variations in the LSLE (Plourde et al., 2001), representing a potential bias when estimating mortality with the VLT because it assumes that the population is in steady state during a period equivalent to the development duration of the stages considered in calculations (Aksnes and Ohman, 1996). We tested this assumption following Hirst et al. (2007) by examining $\log_e$ transformed PopEpr during the 7 years of data in order to identify periods with consistent temporal trends. We then compared for each of the 17 periods identified the daily rates of change in PopEpr (slopes of linear regressions) with the mean $m_{egg\text{-}N3}$ during each period. The former metric represented daily variations in egg input while the later represented the daily variation in the standing stock of egg-N3. Daily rate of changes in PopEpr during the 17 periods identified was on average 0.054 ± 0.048 $d^{-1}$ (mean ± standard deviation), typically one order of magnitude lower than $m_{egg\text{-}N3}$ (0.628 $d^{-1}$, all data). Therefore, we concluded that temporal changes in PopEpr would not significantly bias our mortality estimates.

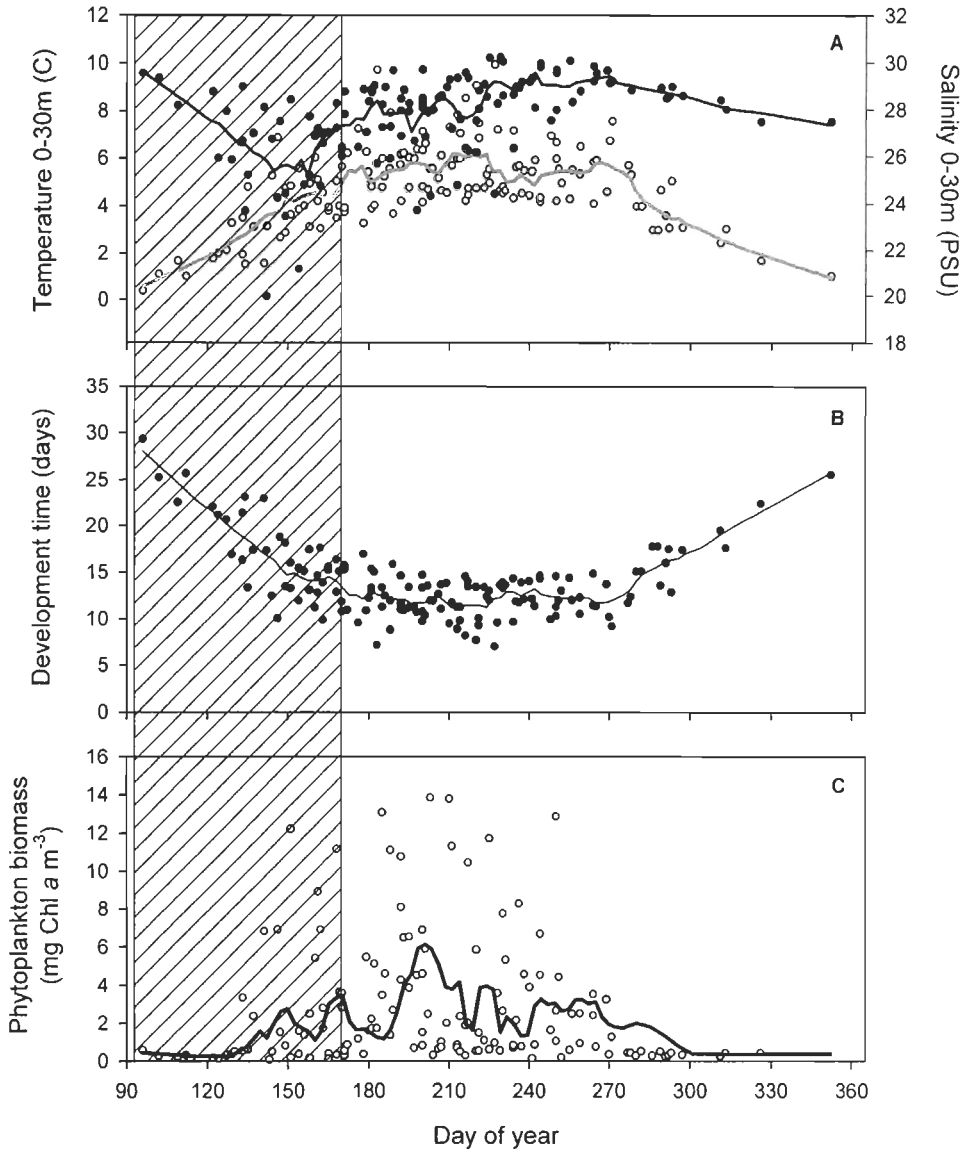


Figure IV-2. Seasonal climatology (1994-2006) in the lower St. Lawrence estuary of (A) temperature (open circles) and salinity (filled circles) in the surface layer (0-30 m), (B) temperature-dependent development time (D) of Calanus finmarchicus from egg to N3, and (C) phytoplankton biomass (mg chl *a* $m^{-3}$) averaged in the upper 50 m. Lines: LOWESS smoothing function fitted to all data. Area with diagonal lines: period excluded from statistical analysis (see text for explanations).

VLT is also appropriate to estimate mortality in stage pairs that experience the same effect of transport (Ohman et al., 2004). The short residence time of surface waters (< 12 days; El-Sabh, 1979) and *D* from egg to N3 greater than 14 days during the spring maximum in freshwater runoff (Fig. IV-2A, B) indicate that eggs produced in spring would encounter a greater probability of being transported downstream before developing to N3 than those laid during the summer-autumn period. Additionally, the Rimouski station is located at the upstream end of the Laurentian Channel, the overwintering ground of *Calanus* population in GSL, suggesting limited contribution from upstream at our sampling location (Fig. IV-1; Plourde et al., 2002). Therefore, there was a high potential for the egg/N3 abundance ratio used in the mortality calculations being biased towards the egg stage due to advection from late April to mid June. We therefore excluded data prior to day 170 (37 out of 127 sampling events) from our statistical analyses in order to limit the potential effect of advective losses and limit the interpretation to 'local' environmental conditions (Fig. IV-2).

### *14.4 Statistical analysis*

The seasonal climatology at the Rimouski station was described using LOWESS functions fitted to data from all years and spatial data were interpolated

using a cubic spline function. The main objective of our study was to relate daily mortality rates to environmental conditions or recruitment to population Epr and mortality-derived population parameters, not to contrast periods or regions. Therefore, multiple linear regression models were performed with individual data to describe the relationship between $m_{egg\text{-}N3}$ or $m_{egg\text{-}N6}$ with female abundance and ambient phytoplankton biomass. Independent variables were normalized in order to respect the conditions of application of statistical analyses. Non-linear regression model was used to relate mortality estimates to female abundance. Any significant relationships obtained with this approach would indicate that the inherent uncertainties of individual mortality estimates with the VLT included in these relationships would have been overcast by the underlying effect of independent variables (Aksnes and Ohman, 1996). Temperature was excluded in the analyses because its effect is already included in the mortality calculation using temperature-dependent *D*. However, we did present the general relationship between daily mortality rates and ambient temperature to illustrate the general imprint of temperature on mortality rate as commonly done in the literature. No negative mortality estimates were obtained and stations where abundance of N3 (Rimouski station time series) and N6 (spatial surveys in 2006) was zero were included.

## *14.5 Biological model*

We used a stage-based model of *C. finmarchicus* (Zakardjian et al., 2003) to test the effect of different mortality formulations on the population dynamics. Simulations were driven by seasonal patterns in surface temperature and chlorophyll *a* biomass typical of the climatology in the NWGSL (see Fig. IV-2A and 9B). Five thousands females appeared in the system around day 90 and gradually disappeared according to a constant mortality rate. No subsequent recruitment into reproducing females was allowed. We tested the effect of four different formulations of mortality on recruitment to nauplii N4-6: (1) mortality decreasing exponentially from egg to late copepodid stages within the range of reported values for *C. finmarchicus* at different locations, and remaining constant with time (see Fig. IV-9A; Ohman et al., 2004); (2) density-dependent $m_{egg\text{-}N2}$ on Georges Bank (Ohman et al., 2002) and (3) $m_{egg\text{-}N3}$ in the LSLE including the negative effect of algal biomass (our study). These two formulations in early stages were combined to constant mortality in older stages used in formulation (1). Finally, (4) we applied the formulation based on LSLE data weighted for variations in temperature using a $Q_{10} = 3.5$ and a base temperature of 5°C, derived from Figure 8A in Ohman et al. (2002). $Q_{10}$ was not applied on mortality in females in order to keep reproductive output in spring and early summer constant among scenarios. We used a $Q_{10}$ function as temperature could not be included in the multiple regression model

because of non-independence from the dependent variable (mortality), and to consider the obvious effect of temperature on mortality in marine copepods in general (Hirst and Kiorboe, 2002), and in *Calanus* species in particular (Ohman et al., 2002; Hirst et al., 2007).

## 15 Results

### *15.1 Seasonal climatology in the LSLE*

Temperature and salinity in the upper 30 m and phytoplankton biomass in the upper 50 m were characterized by marked seasonal variations (Fig. IV-2). Temperature increased gradually from a minimum of 0.4 °C in early April to its maximum in August (5.5 to 6°C) (Fig. IV-2A), a pattern mirrored by an opposite trend in *D* in egg-N3 (Fig. IV-2B). Freshwater always has a strong influence in the LSLE with averaged values of salinity typically lower than 29 PSU with a minimum (< 26 PSU) observed from late April to mid June (Fig. IV-2A). The climatology of chlorophyll *a* biomass averaged in the upper 50 m showed values > 1 mg $m^{-3}$ with the main bloom occurring in July. A second bloom was observed in autumn (Fig. IV-2C). Blooms of lesser amplitude and shorter durations were also observed in late May and June (Fig. IV-2C).

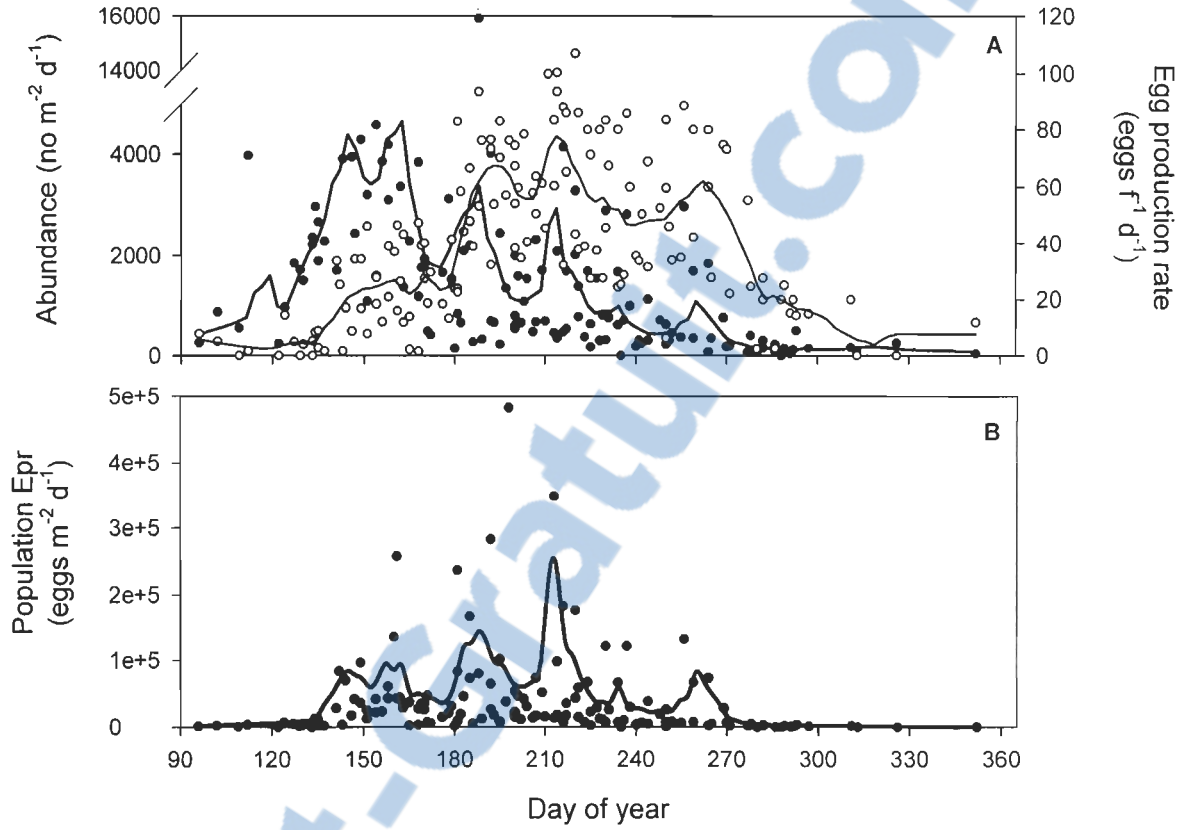


Figure IV-3. Seasonal climatology (1994-2006) in the lower St. Lawrence estuary of (A) *C. finmarchicus* female abundance (filled circles) and specific egg production rate (open circles) and (B) population egg production rate. Lines: LOWESS smoothing function fitted to all data.

Climatology of *C. finmarchicus* female abundance and reproduction showed marked seasonal variations (Fig. IV-3). Female abundance sharply increased in May and remained high until late June; this main peak in abundance was followed by two brief periods of high abundance in early July and early August and by a small peak in abundance in late September (Fig. IV-2A). Specific *in situ* Epr increased in May and reached maximal values (50-80 eggs $f^{-1}$ $d^{-1}$) in July in response to the main phytoplankton bloom; specific Epr remained high until late September (Fig. IV-3A). PopEpr was characterized by three distinct peaks (> 100 X $10^3$ eggs $m^{-2}$ $d^{-1}$) in late May- early June, July and August corresponding to periods of high abundance of females (Fig. IV-3B).

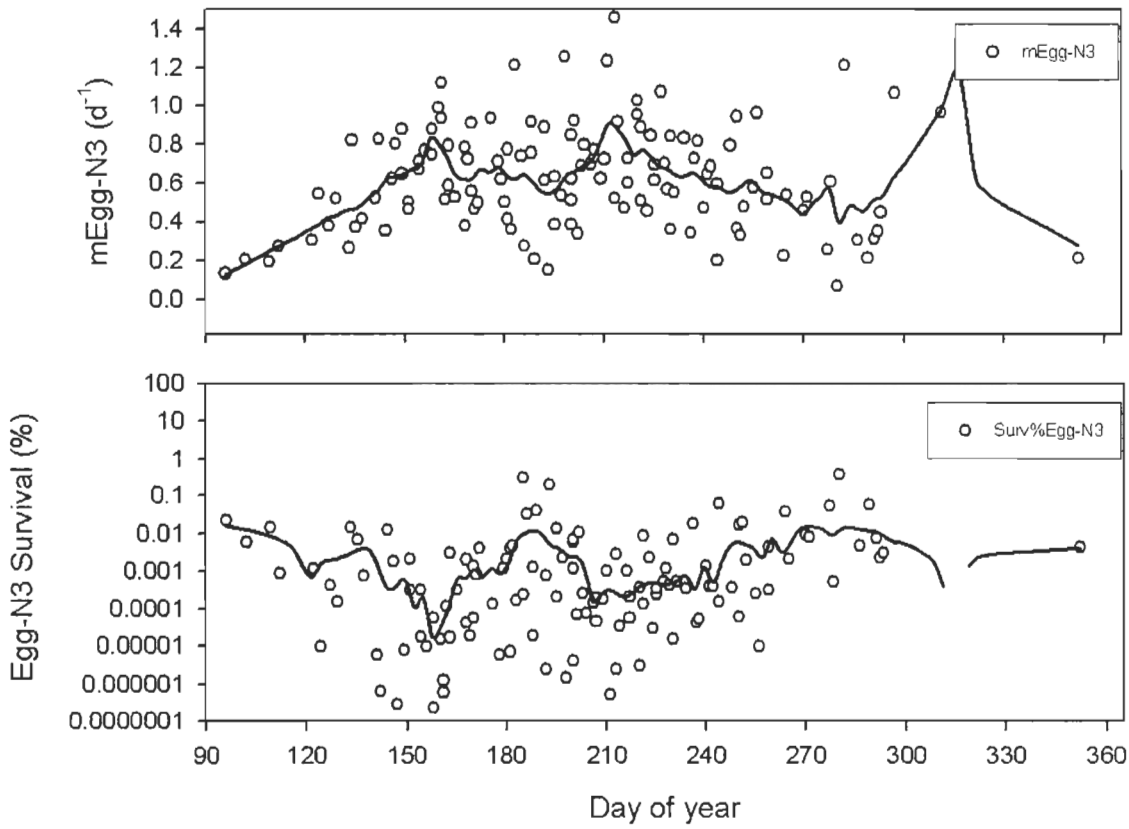


Figure IV-4. Seasonal climatology (1994-2006) in the lower St. Lawrence estuary of (A) daily mortality rate in egg-N3 ($m_{egg\text{-}N3}$) and (B) proportion surviving from egg to N3 ($S_{egg\text{-}N3}$). Lines: LOWESS smoothing function fitted to all data.

Daily mortality in egg-N3 ($m_{egg\text{-}N3}$) and proportion surviving during development to N3 ($S_{egg\text{-}N3}$) showed important variations (Fig. IV-4). Individual observations of $m_{egg\text{-}N3}$ (0.659 ± 0.317 $d^{-1}$) varied by a factor of 10 while the LOWESS fit (time-averaged values) showed values ranging between 0.2 $d^{-1}$ and 0.8 $d^{-1}$ (Fig. IV-4A). Daily $m_{egg\text{-}N3}$ peaked on two occasions during summer, once in early June (day 150-160) and the other in late July and early August (days 210-220). The peak in $m_{egg\text{-}N3}$ around day 315 (November) has to be cautiously interpreted due to the paucity of data during this period. $S_{egg\text{-}N3}$ showed minimum values corresponding to the periods of high mortality, and maximum values (0.01) in July (days 180-210) and in autumn when $m_{egg\text{-}N3}$ was lower (Fig. IV-4B).

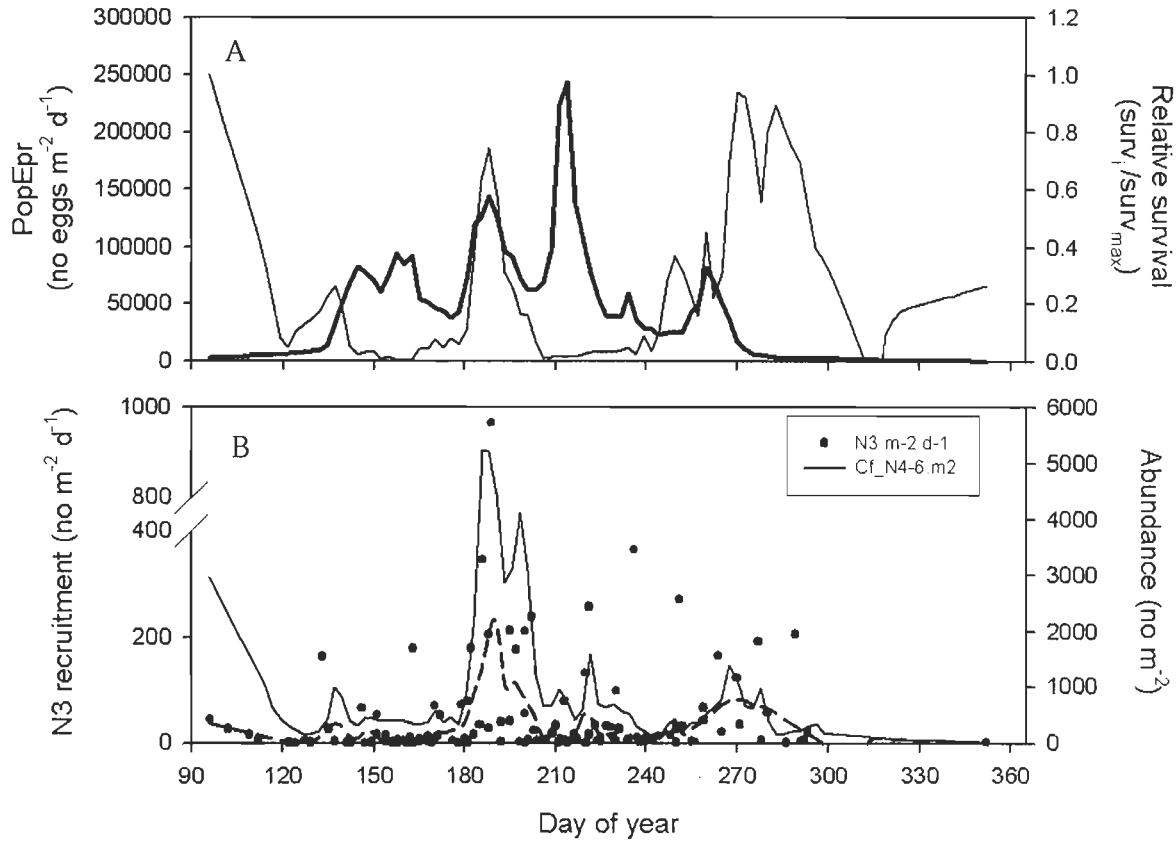


Figure IV-5. Seasonal climatology (1994-2006) in the lower St. Lawrence estuary of (A) population egg production rate (LOWESS fit only: bold line) and relative survival (%) in egg to N3 (thin line) estimated from LOWESS fit data taken from Fig. 4B ($survival_i$/ $survival_{max}$), (B) daily recruitment rate of *C. finmarchicus* N3 (filled circles, dashed line), and abundance of *C. finmarchicus* N4-6 (thin line). Lines: LOWESS smoothing function fitted to all data.

The seasonal pattern in daily recruitment to the first feeding stage N3 ($R_{N3}$) resulted from the interplay between the pattern in survival and PopEpr (Fig. IV-5A). Periods of high PopEpr in late May- early June and early August resulted in poor $R_{N3}$ due to a very low survival, while the peak in $R_{N3}$ occurred in July during the period of greater survival from egg to N3 (c.a. 0.01) and high PopEpr (Fig. IV-5A, B). This period of greater $R_{N3}$ in July corresponded to the one of high abundance of N4-6 (Fig. IV-5B). A secondary peak in $R_{N3}$ in late September and early October (centered on day 270) resulted from a short period of elevated PopEpr and survival (Fig. IV-5A, B). However, this late peak in $R_{N3}$ did not correspond to one in abundance of N4-6 (Fig. IV-5B).

### *15.2 Spatial pattern in the GSL in summer 2006*

Averaged daily mortality rates in egg-N6 ($m_{egg\text{-}N6}$) obtained with abundance data corrected for potential undersampling of N6 with the 200-$\mu$m net (0.548 ± 0.3 $d^{-1}$) and non-corrected abundance data (0.559 ± 0.3 $d^{-1}$) differed by only 2% and were not significantly different ($p<0.05$). We therefore concluded that $m_{egg\text{-}N6}$ were reliable and adequately described mortality patterns in the GSL.

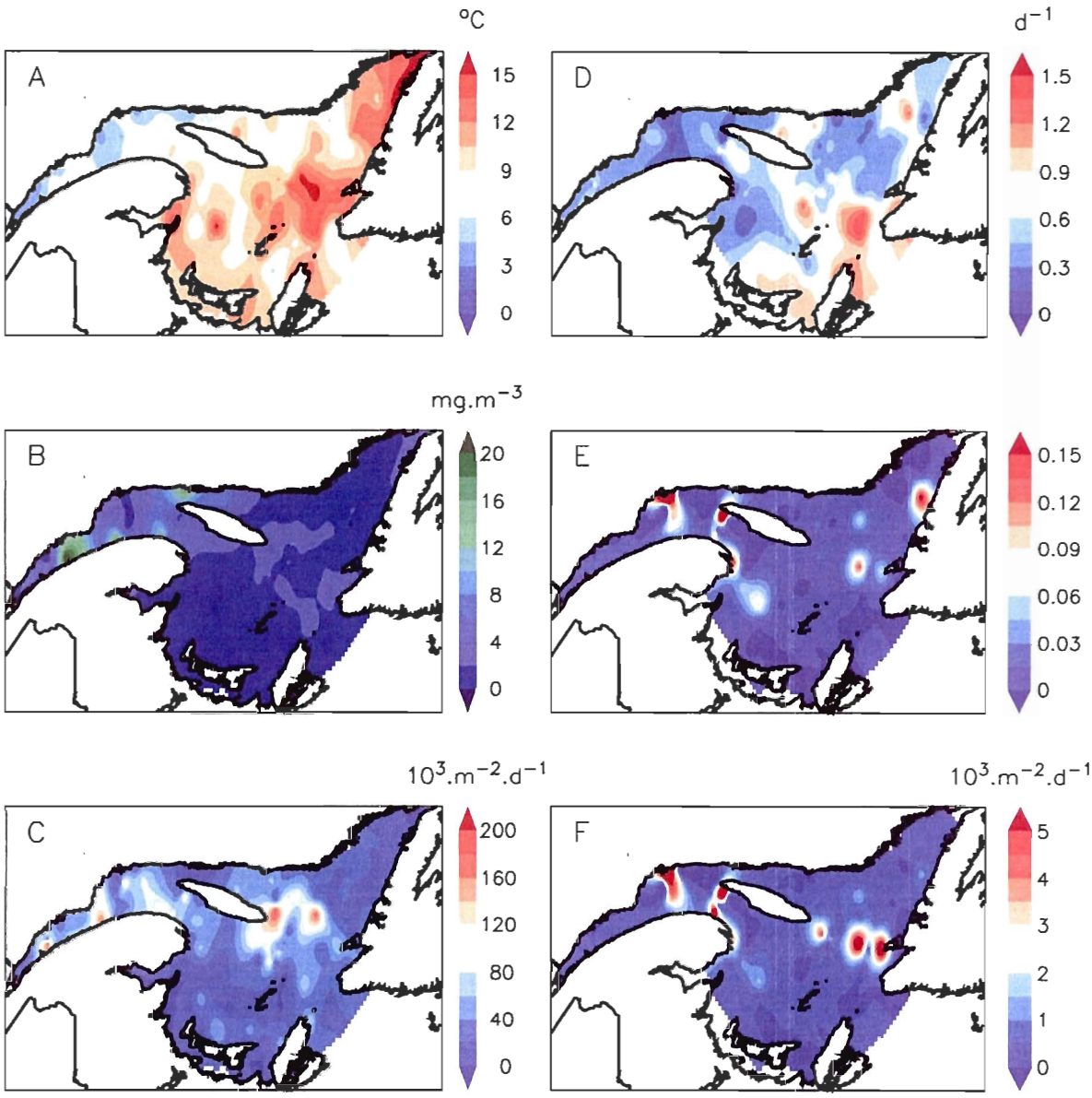


Figure IV-6. Spatial pattern in the Gulf of St. Lawrence in summer 2006 of (A) surface layer temperature (0-30 m) and (B) phytoplankton biomass (mg chl *a* $m^{-3}$) averaged in the upper 25 m, and *C. finmarchicus* (C) population egg production rate (population Epr), (D) daily mortality rate in egg-N6 ($m_{egg\text{-}N6}$), (E) proportion surviving from egg to N6 and (F) daily recruitment rate to N6. Data were interpolated using a cubic spline function.

Data from the spatial surveys are shown as an overall representation of the processes in the GSL in summer 2006 (Fig. IV-6). Temperature and chlorophyll *a* biomass in the upper layer of the water column were generally lower and greater respectively in the northwest GSL relative to the eastern regions (Fig. IV-6A, B). Using the same sub-regions, daily $m_{egg\text{-}N6}$ was significantly lower (Kruskal-Wallis, $p<0.001$) west of the Anticosti Island ($0.389 \pm 0.228\ d^{-1}$) than elsewhere in the GSL ($0.644 \pm 0.324\ d^{-1}$). PopEpr showed important spatial variations with several regions of intense production ($> 120 \times 10^3$ egg $m^{-2}\ d^{-1}$) located in the LSLE, and in regions located west and east of the Anticosti Island (Fig. IV-6C). However, daily recruitment to N6 ($R_{N6}$) showed a different spatial pattern with regions of elevated $R_{N6}$ restricted to few areas in the northwest GSL, off Gaspé Peninsula and in the eastern GSL (Fig. IV-6F). This spatial pattern closely corresponded to the one in $S_{egg\text{-}N6}$ (Fig. IV-6E) resulting from the integration of daily $m_{egg\text{-}N6}$ (Fig. IV-6D) over *D* from egg to N6 estimated from temperature (Fig. IV-6A).

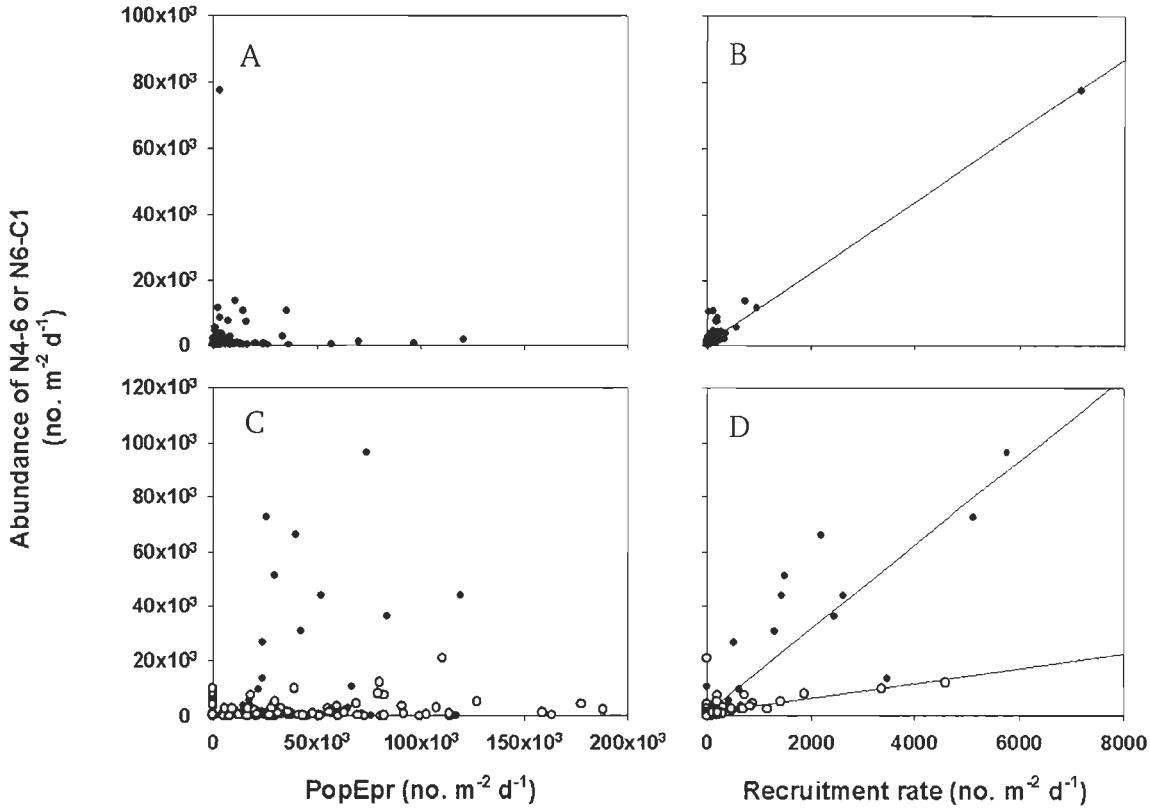


Figure IV-7. Recruitment in *C. finmarchicus*. Abundance of N4-6 (A-B) or N6-C1 (C-D) in relation to population egg production rate (PopEpr: A, C) and daily recruitment rate to N3 (B) or N5 (D). Panels A-B: seasonal data from the lower St. Lawrence estuary (1994-2006). Panels C-D: spatial data from the Gulf of St. Lawrence in June (filled circles) and August (open circles) 2006. Lines: linear regression fitted to the data in (B) $y= 10.8x + 828.3$, $r^2= 0.94$, (D) filled circles: $y= 9.4x + 2218.7$, $r^2= 0.89$; open circles: $y= 1.1x + 1023.9$, $r^2= 0.24$.

### *15.3 Relationship between PopEpr, recruitment rate and abundance of early stages*

Our results clearly support our alternate hypothesis that variations in mortality and survival in early development stages control patterns in recruitment in *C. finmarchicus*. Daily recruitment ($R_{N3}$ or $R_{N6}$) derived from mortality and survival estimates clearly controlled the seasonal and spatial patterns in abundance of N4-6 in the LSLE and C1-2 in the GSL, respectively (Fig. IV-7). While abundance of theses stages showed no significant relationship with PopEpr ($p>0.05$) (Fig. IV-7A, C), $R_{N3}$ and $R_{N6}$ explained a significant percentage of the variance in the abundance of N4-6 in the LSLE ($r^2= 0.95$, Fig. IV-7B) and in C1-2 in the GSL in 2006 ($r^2$ of 0.89 and 0.24 in June and August respectively, Fig. IV-7D). Note that the relationship between abundance of N4-6 and $R_{N3}$ in the LSLE remains highly significant without the high value ($r^2= 0.54$, $p<0.0001$, Fig. IV-7B). Lower abundance of C1-2 relative to PopEpr or to $R_{N6}$ in August than in June 2006 also suggests that 'recruitment efficiency' of *C. finmarchicus* was lower in late summer in the GSL (Fig. IV-7C, D).

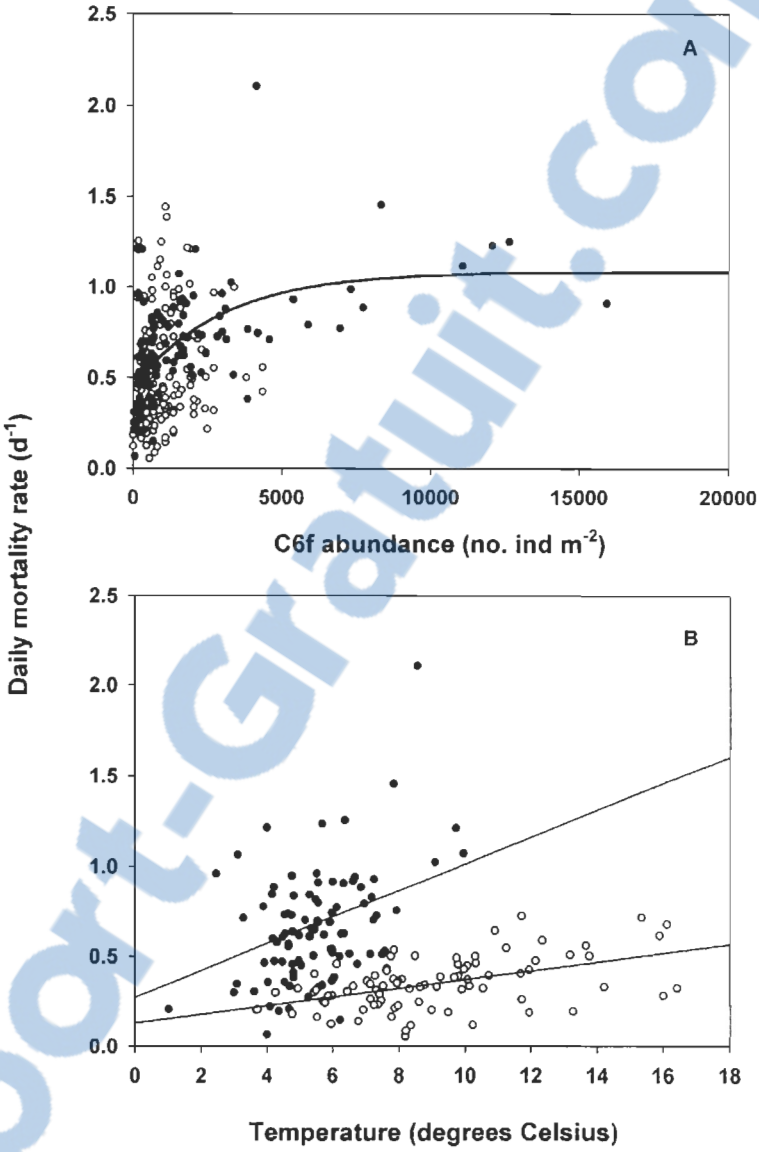


Figure IV-8. Mortality in *C. finmarchicus*. Daily mortality rate in egg-N3 ($me_{gg\text{-}N3}$, filled circles) and egg-N6 ($m_{egg\text{-}N6}$, open circles) in relation to (A) female abundance and (B) temperature (0-30 m). Regression models fitted to the data in (A) Type II fit with $m_{egg\text{-}N3}$: y= 0.45+ 0.63*(1-e-0.0003*x), $r^2$= 0.34, (B) linear fits for $m_{egg\text{-}N3}$: y= 0.074x + 0.275, $r^2$= 0.18; $m_{egg\text{-}N6}$: y= 0.024x + 0.133, $r^2$= 0.24.

### *15.4 Relation between daily mortality and the environment*

Mortality in early stages of *C. finmarchicus* was influenced by phytoplankton biomass and abundance of con-specific females (Table IV-1). A multiple linear regression model ($p<0.0001$) between $m_{egg\text{-}N3}$ and these two parameters explained 56% of the variability in mortality at the Rimouski station with opposite effects of female abundance (positive) and phytoplankton biomass (negative, Table IV-1). A similar regression model applied to $m_{egg\text{-}N6}$ from the spatial surveys in 2006 was barely not significant ($p= 0.06$). However although mortality was not influenced by female abundance ($p>0.05$), it was again negatively related to chlorophyll *a* biomass ($p<0.02$) (Table IV-1). This lack of effect of female was likely due to its low abundance during the surveys in 2006 (few observation > 2500 ind.$m^{-2}$) as compared to our seasonal data based on several years at the Rimouski station (Fig. IV-8A). The relationship between $m_{egg\text{-}N3}$ and female abundance in the LSLE was best described with a non-linear fit (Type II), explaining 34% of the variability with constant mortality rate above c.a. 8 000 female $m^{-2}$ (Fig. IV-8A). Finally, neither egg hatching success (%) or the proportion of eggs successfully developing to N2 (data not shown) significantly affected $m_{egg\text{-}N3}$.

Table IV-1. Statistics of the linear multiple regression models of mortality in early stages of *C. finmarchicus* in the lower St. Lawrence estuary (seasonal climatology of $m_{egg\text{-}N3}$) and the whole GSL in 2006 (spatial pattern in $m_{egg\text{-}N6}$) against phytoplankton biomass (mg chl *a*.$m^{-3}$) and abundance of *C. finmarchicus* females (C6f) (ind.$m^{-2}$). Partial correlation coefficients are included to indicate the sign of the effect. Bold characters denote significant contribution of independent variables.

| Independent variables | Dependent variables | | | |
|---|---|---|---|---|
| | Seasonal | | Spatial 2006 | |
| | mEgg-N3 | | mEgg-N6 | |
| | Partial corr. coeff. | *p* | Partial corr. coeff. | *p* |
| Intercept | **-0.426** | **0.0001** | 0.445 | 0.0642 |
| Phytoplankton biomass | **-0.134** | **0.036** | **-0.241** | **0.0310** |
| *C. finmarchicus* C6f abundance | **0.392** | **< 0.0001** | 0.096 | 0.166 |
| $r^2$ adjusted | 0.56 | | 0.027 | |
| p | 0.0001 | | 0.0641 | |

Temperature was not included in the multiple regression model as an independent variable because it was used to estimate the development times necessary to mortality calculations. Although these relationships should be considered with caution, we nevertheless presented $m_{egg\text{-}N3}$ and $m_{egg\text{-}N6}$ in relation to ambient temperature to illustrate the overall general effect of temperature on mortality. Daily mortality was significantly related to temperature but with a considerable variability (low $r^2$) (Fig. IV-8B).

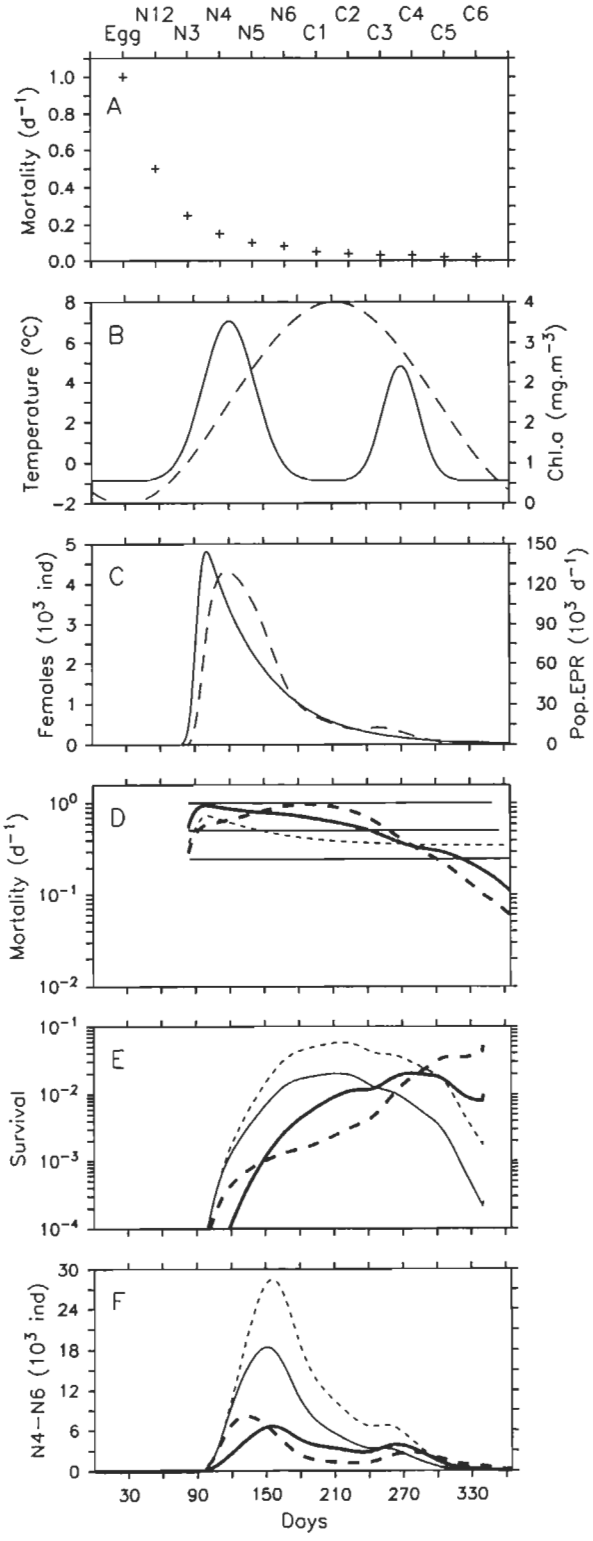


Figure IV-9. Impacts of four mortality formulations on the recruitment to nauplii N4-6 using a 0-D model of *C. finmarchicus*. (A) Stage-specific constant mortality, (B) temperature (dashed line) and phytoplankton biomass (mg chl *a* $m^{-3}$) (line) typical of the northwest GSL, (C) abundance of females (line) and population egg production rate (PopEpr) (dashed line), mortality in early stages (D), proportion surviving from egg to N3 (E) and abundance of nauplii N4-6 (F). Only daily mortality in early stages varied among scenarios: (1) stage-specific constant mortality in eggs, N1-2 and N3 (lines); (2) density dependent mortality in egg-N2 (thin dashed line) (Ohman et al., 2002); (3) mortality in egg-N3 ($m_{egg\text{-}N3}$) dependent to the abundance of female and phytoplankton biomass (bold line) (our study); (4) $m_{egg\text{-}N3}$ dependent to the abundance of female and phytoplankton biomass adjusted to variations in temperature with a $Q_{10}$ (bold dashed line, our study).

### *15.5 Impacts of mortality formulations on modeled population dynamics*

Mortality formulations in early stages profoundly affected the modeled population dynamics (Fig. IV-9). First, constant daily mortality in early stages (Fig. IV-9A, D) combined to the seasonal cycle in temperature resulted in a generally dome-shaped pattern in survival from egg to N3 (Fig. IV-9B-E). Second, the inclusion of density-dependence based on data from Georges Bank (Ohman et al., 2002) generated temporal changes in daily mortality rate more or less similar to the pattern in female abundance, but a less variable seasonal pattern in survival and recruitment because its effect mainly occurred at low temperature when survival was already really low (Fig. IV-9D-E). However, mortality pressure was generally lower than in the 'constant mortality' scenario, leading to much higher abundance of N4-6 (Fig. IV-9D-F). The density- and chlorophyll *a*- dependent mortality rates in the LSLE were generally higher than in previous scenarios with a slightly different seasonal pattern, resulting in some differences in the patterns of survival and recruitment to N4-6 (Fig. IV-9D-F). Survival and recruitment was hindered early during the high female abundance prior to the spring bloom and resulted in a delayed and much lower peak in abundance of N4-6. The addition of temperature-adjusted mortality with our $Q_{10}$ modified the seasonality in daily mortality and survival (%) relative to the LSLE set-up with a greater survival (depressed

mortality) in spring under cold conditions and greater mortality (lower survival) in summer during the maximum in temperature (Fig. IV-9B-E). This change in seasonal pattern resulted in an earlier peak in abundance of N4-6 (Fig. IV-9F). Finally, all formulations resulted in a secondary peak in abundance of N4-6 in Autumn during a period of relatively low PopEpr that was compensated by low number of females, high phytoplankton biomass, and relatively high temperature (Fig. IV-9B-F).

## 16 Discussion

Our results clearly illustrated the importance of mortality and survival in early stages in the control of *C. finmarchicus* recruitment. In the following sections, we compared our mortality estimates in early stages of *C. finmarchicus* in the St. Lawrence system to similar data from other regions in the North Atlantic. We then interpreted our results in the context of how environmental conditions control mortality and survival, and how these parameters affect recruitment and population dynamics. Finally, implications of our results and the importance of using dynamic functions describing mortality in modeling population dynamics of *C. finmarchicus* are discussed.

## *16.1 Comparison of mortality in early stages in the Gulf of St. Lawrence with other regions*

Daily mortality in early stages egg-N3 ($m_{egg\text{-}N3}$, seasonal) and egg-N6 ($m_{egg\text{-}N6}$, spatial) of *C. finmarchicus* in the LSLE and GSL appeared greater than in other regions across the North Atlantic. The most robust comparison could be done with daily $m_{egg\text{-}N3}$ observed during a multi-year program on Georges Bank (Ohman et al., 2008). In this region, the overall averaged daily $m_{egg\text{-}N3}$ was c.a. 0.4 $d^{-1}$ (based on Fig. IV-2B in Ohman et al., 2008) in comparison to an average of 0.659 ± 0.317 $d^{-1}$ in the LSLE (Fig. IV-4A). Similarly, the averaged daily $m_{Egg\text{-}N6}$ in the LSLE-GSL in summer 2006 (0.566 ± 0.320 $d^{-1}$, Fig. IV-6D) could have been somewhat greater than $m_{egg\text{-}N3}$ observed on Georges Bank because including N4-N5 would likely diminish the 'averaged' mortality. Although these comparisons are somewhat qualitative, it does suggest a potential for a greater 'mortality losses' in early stages in the LSLE-GSL. A comparison with mortality in early stages of *C. finmarchicus* observed in other areas in the North Atlantic is difficult because of different stage resolutions and approaches used to estimate mortality (VLT or HLT) (Ohman et al., 2004; Heath et al., 2008). However, it does suggest that mortality rates estimated in our study were in the same range than those observed in deep oceanic regions (Norwegian Sea, Irminger Sea) and could be greater than in the North Sea and in two Norwegian fjords (Ohman et al., 2004; Heath et al., 2008). The comparison

among regions would be reinforced by the use of similar mortality indexes estimated using the same approach.

## *16.2 Processes controlling mortality and survival*

Temperature is an important factor in the control of marine copepod metabolism, affecting egg production, development, growth and mortality (Huntley and Lopez, 1992; Hirst and Bunker, 2003; Bunker and Hirst, 2004). Temperature influences daily mortality in *C. finmarchicus* (Ohman et al., 2002), and certainly represent an underlying factor controlling the seasonal and spatial patterns in daily mortality rate in early stages. However, temperature alone should not be an important factor in the control of the seasonal and spatial patterns in proportion surviving within the 'optimal' temperature range of *C. finmarchicus*. Survival is the integration of the effect of daily mortality rate during the development from egg to N3 or N6 and represents the key variable to consider when relating processes such as EPR and daily mortality to stage abundance (recruitment). Theorical considerations indicate that temperature would scale both mortality and development rates, which should result in relatively constant survival.

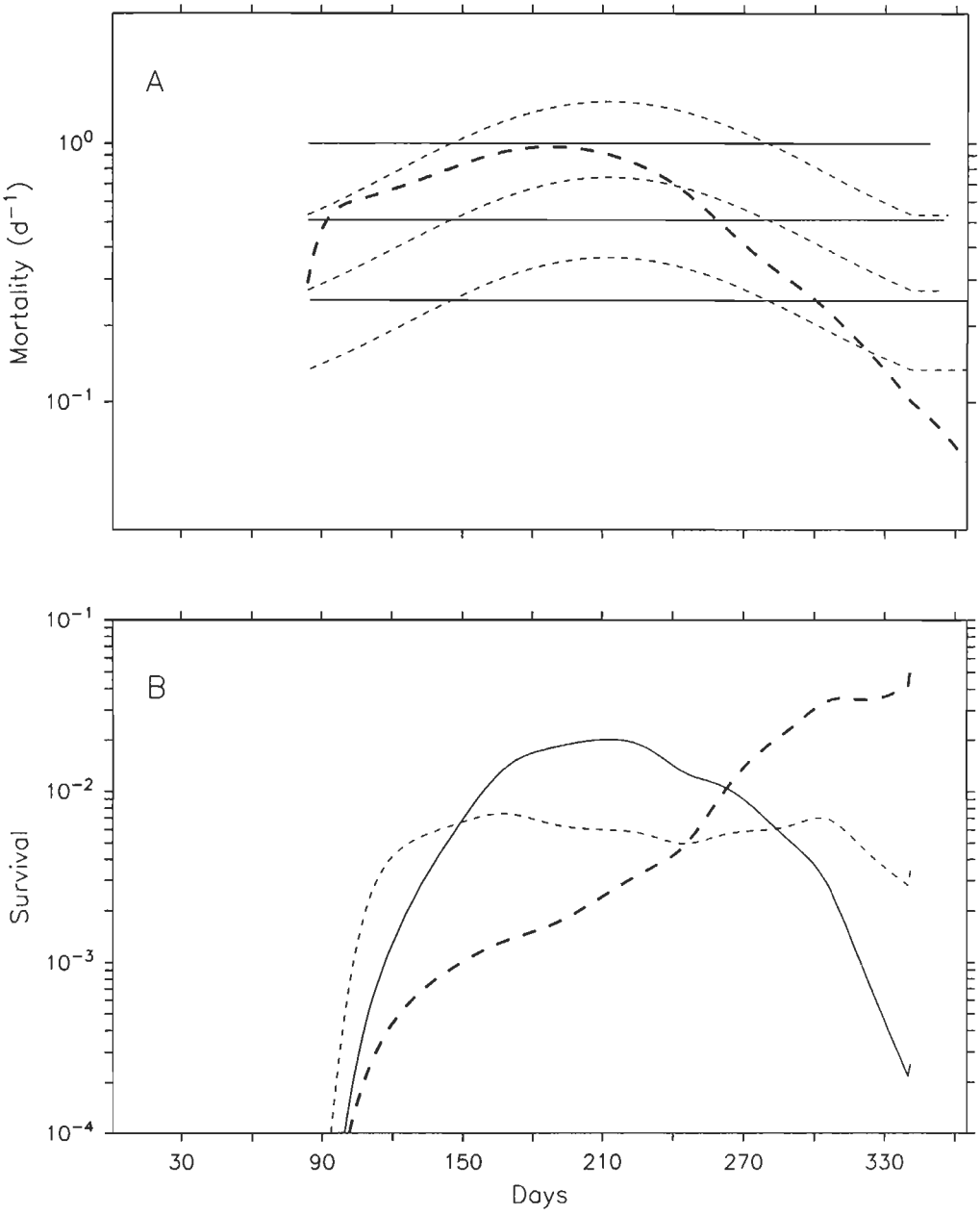


Figure IV-10. Impacts of temperature-adjusted constant mortality on survival in early stages of *C. finmarchicus*. Mortality in early stages (A) and survival (%) from egg to N3 (B). Lines: constant daily mortality rate in egg, N1-2, and N3; thin dashed lines: constant daily mortality rate in egg, N1-2, and N3 adjusted to temperature with $Q_{10}$; bold dashed line: daily mortality in egg-N3 dependent to the abundance of female and phytoplankton biomass adjusted to variations in temperature with $Q_{10}$.

Results from our model best illustrated this phenomenon: our scenario of constant daily mortality rates weighted for the seasonal change in temperature with a $Q_{10}$ function yielded a relatively constant survival in comparison to mortality formulations with constant mortality or including effects from density-dependent process and phytoplankton biomass (Fig. IV-10). Patterns in mortality and survival observed in early stages of *C. finmarchicus* in the LSLE and in *C. helgolandicus* in the English Channel considerably deviated from the seasonal cycle in temperature (Fig. IV-2, 4; Hirst et al., 2007), resulting in highly significant relationships but with a considerable variability (low $r^2$) (Fig. IV-8B, Ohman et al.; 2002, Hirst et al., 2007). Based on this body of evidences, we suggest that patterns in survival would be governed by factors other than temperature that would change the equilibrium between temperature-driven mortality and development rates such as density-dependent processes (cannibalism), phytoplankton biomass, and predation.

Our study supports previous findings suggesting density-dependent processes as important factors controlling mortality in early stages of *C. finmarchicus*, especially during periods of low phytoplankton biomass as suggested by our results (see bellow). Density-dependent mortality was only observed at relatively high abundance of adult females. Mortality was significantly related to female abundance in the LSLE but not in the GSL in summer 2006 owing to their relatively low numbers in the latest, with only a few observations above 2500 ind.$m^{-2}$ (Fig. IV-

8A). Interestingly, a similar abundance threshold of 2000 ind.$m^{-2}$ for the occurrence of density-dependent mortality in *C. finmarchicus* was evidenced by Ohman et al. (2002) and Ohman et al. (2004). The Type II relationship in the LSLE indicates that constant mortality would occur at female abundance greater than c.a. 8000 ind $m^{-2}$, which would be somewhat similar to the relationship shown for $m_{egg\text{-}N3}$ on Georges Bank (Ohman et al., 2002). Other evidences of density-dependent mortality in *C. finmarchicus* showed linear relationships with a slope on Georges Bank (7.9 X $10^{-5}$) considerably weaker than in the Norwegian Sea (2.5 X $10^{-4}$) (Ohman et al., 2004). These differences are not surprising because different stages were considered in the mortality estimates (egg-N3, egg-N2, egg) and could partly arise from the use of VLT or HLT (Ohman et al., 2004). Moreover, such relationships are only a crude proxy of the underlying mechanism hypothesized to mediate density-dependence in *C. finmarchicus* (and copepods), i.e. cannibalism by late development stages on eggs and early naupliar stages (Landry, 1981; Basedow and Tande, 2006). The good correspondence between estimated daily egg loss in *C. finmarchicus* and daily predation by potential predators (including *C. finmarchicus* C4-6) illustrates the benefit of refining our approach (Ohman et al., 2008).

Phytoplankton biomass depressed mortality in early stages of *C. finmarchicus* in presence or absence of density-dependent processes. Because $m_{egg\text{-}N3}$ in the LSLE mostly included non-feeding stages, this detrimental effect of chlorophyll *a* biomass

on mortality suggest that high level of phytoplankton biomass would diminish cannibalism pressure on early stages by late copepodid stages, supporting our initial hypothesis that density-dependent processes would be promoted at low ambient phytoplankton biomass. Although evidences are scarce, *Calanus* species showed their ability to ingest their own eggs in presence of algal food and exhibited potentially different feeding mode such as prey switching (*C. pacificus*: Landry, 1981) or an independent feeding mode (*C. finmarchicus*: Basedow and Tande, 2006). We argue that both feeding modes would result in a lower ingestion of eggs and early nauplii at high phytoplankton biomass either because females switch to algal preys when phytoplankton is disproportionally more abundant or attain satiety more quickly (feed less time) when the overall food concentration is greater. The level of phytoplankton biomass could also have affected our results because of food limitation in naupliar stages. Food limited growth and survival would likely play a bigger role in the estimate of $m_{egg\text{-}N6}$ from our spatial survey in 2006 than in the $m_{egg\text{-}N3}$ in the LSLE (more feeding stages involved in the estimate). Nauplii growth and development rates are limited bellow a chlorophyll *a* biomass of 1.75 mg $m^{-3}$ (using a chl *a* / C ratio of 40 as in Heath et al., 2008; Campbell et al., 2001), while a food concentration above 0.6 mg chl *a* $m^{-3}$ appears necessary for *Calanus* nauplii to survive (Lopez, 1996; Irigoien et al., 2003). In the Irminger Sea, mortality in the first feeding stages N3-4 was 2-4 times greater at chlorophyll *a* concentrations lower than 0.6 mg $m^{-3}$ dominated by flagellates, suggesting that starvation was a major

cause of mortality in these stage (Irigoien et al., 2003; Heath et al., 2008). This situation is no stranger to the St. Lawrence system where algal biomass limiting for nauplii growth (<1.75 mg chl *a* $m^{-3}$) and survival (<0.6 mg chl *a* $m^{-3}$) accounted for 50-55% of the observations included in our multiple regression models. Low phytoplankton biomass (< 1 mg chl *a* $m^{-3}$) dominated by flagellates are common features during post-bloom conditions in large areas of the GSL (Ohman and Runge, 1994; Runge and Plourde 1996).

Our study targeted density-dependent processes driven by *C. finmarchicus* females but predation by other filter-feeding copepods could represent another important source of mortality in early stages of *C. finmarchicus* in the LSLE and GSL. Several other copepod species had shown their ability to ingest copepod eggs and naupliar stages but very little is known about their feeding behavior and, consequently, their predation impact (Sell et al., 2001; Ohman et al., 2008). Copepodid C4-5 of *C. finmarchicus* have been included in the assessment of the density-dependent mortality in other studies (Ohman and Hirche, 2001; Heath et al., 2008; Ohman et al., 2008). We did not include them in our analysis because our sampling scheme did not allow discriminating between the 'active' and overwintering components of the population. However, the presence of high abundance of copepodid C4-5 in the surface layer in late July and August in the LSLE and northwest GSL suggests that these stages could contribute to the high

mortality, low survival and low recruitment during this period (Fig. IV-6) (Plourde et al., 2001). Additionally, late stages of *C. hyperboreus*, *C. glacialis* and *M. longa* are very abundant in the surface layer at the onset of *C. finmarchicus* reproduction in May and June, and could constitute an additional cause of the high mortality/low survival in early stages during this period (Fig. IV-4) (Plourde et al., 2002; Plourde et al., 2003). Predation on *C. finmarchicus* eggs by these copepod species has been observed (Plourde, unpublished data) and could provide them with an adaptive advantage in exploiting the early stage of the phytoplankton bloom, an ecological strategy called intraguild predation believed to be of primary importance in shaping communities (Polis et al., 1989). In future studies, we do need to distinguish between the active and overwintering components of *Calanus* species to include all potential predators. Clearly, more knowledge on the feeding behavior and ecology in filter-feeding copepods is required in order to understand the effect of cannibalism and predation on mortality and survival in eggs and early naupliar stages of *C. finmarchicus*.

Predation regime has been mentioned as the most probable factor explaining regional differences in mortality patterns on Georges Bank and in the Irminger Sea (Heath et al., 2008; Ohman et al., 2008). The copepod community differs markedly between the LSLE and Georges Bank with a much greater contribution from large-bodied copepods such as *C. finmarchicus*, *C. hyperboreus*, *C. glacialis* and *Metridia*

*longa* in the LSLE relative to a community dominated by small-bodied *Centropages* spp, *Pseudocalanus* spp and *Temora longicornis* on Georges Bank (Davis, 1984; Plourde et al., 2002). *C. hyperboreus* and *C. glacialis* differ from *C. finmarchicus* in their life cycle strategy as they occur in the surface layer early in the season during the onset of reproduction of the *C. finmarchicus* population (Conover, 1988; Plourde et al., 2003; Plourde et al., 2001), on the contrary to Georges Bank where predators are mostly abundant later in the season relative to *C. finmarchicus* dynamics (Ohman et al., 2008). Similar regional differences in the composition of the copepod community are also observed between the shallow southern GSL and deeper areas of the LSLE and northern GSL (Harvey et al., 2005). Such differences in predator composition and phenology would likely be of primary importance in defining region-specific differences in level and patterns in mortality in *C. finmarchicus* in the GSL.

### *16.3 Processes controlling recruitment*

Daily recruitment rate estimated from the PopEpr and survival was the main factor controlling *C. finmarchicus* late naupliar and early copepodid abundance. A peak in daily recruitment to N3 or N6 (and in abundance of subsequent stages) only occurred during periods or in regions of elevated survival (Fig. IV-5, 6).

Alternatively, periods or regions of high PopEpr did not necessarily result in high recruitment rate, although significant PopEpr (reproductive output) had to occur in conjunction with good survival to generate a peak in early stages (Fig. IV-7). Therefore, high survival in early stages was a prerequisite for high recruitment in *C. finmarchicus*. Our indexes of daily recruitment allowed a clear illustration of opposite forces exerted by reproduction (bottom-up process) and mortality/survival (top-down process) in the control of population dynamics in *C. finmarchicus* (Twombly et al., 2007). This interplay between bottom-up and top-down processes and its effect on population dynamics was implicitly considered only in a few studies on *Calanus* spp. and *Pseudocalanus* spp. (Ohman and Wood, 1996; Pierson et al., 2007; Hirst et al., 2007; Heath et al., 2008). More exhaustive description of the effect of these processes on population dynamics were done on small neretic copepod species (Liang et al., 1994; Peterson and Kimmerer, 1994; Liang and Uye, 1996a, b). Our study clearly identified the importance of considering multiple environmental parameters in order to get a glimpse at the complex nature of the control of recruitment and population dynamics in copepods (Twombly et al., 2007).

### *16.4 Mortality estimates: limitations and assumptions*

The use of the VLT implies theoretical assumptions and conditions of applications that are sometimes difficult to meet on the field (Aksnes and Ohman, 1996). We believe that the restriction of our study to early stages and our general approach would have minimized potential violations of the conditions of application of the method. We first explored if temporal changes in *C. finmarchicus* PopEpr would significantly affect our mortality estimates as it has been demonstrated that VLT is sensitive to trends in recruitment (Aksnes and Ohman, 1996). We found that daily change in the PopEpr represented on average 8% of the daily rate of change in $m_{egg\text{-}N3}$, meaning it would not significantly bias our results (Hirst et al., 2007). Secondly, the fact that our study was limited to the mortality from egg to N3 should minimize the potential problems caused by variations in development time or successive development stages not being at short term equilibrium (recruitment-mortality) over the time considered in our estimates (D from egg to N3; Aksnes and Ohman, 1996; Ohman et al., 2002). Thirdly, temperature is certainly a good predictor of development time as stages included in our estimates were mostly non-feeding stages egg, N1 and N2 although food limitation could delay development in N3 of *C. finmarchicus* (Campbell et al., 2001). However, the VLT is relatively robust to variations in stage development by a factor of two (Aksnes and Ohman, 1996;

Hirst et al., 2007). Finally, we excluded data that could have been affected by the combined effect of the station location in the LSLE and losses due to advection in spring (see Methods section), hence likely minimizing the bias caused by differential transport in successive stages (Aksnes and Ohman, 1996; Ohman et al., 2002).

Hirst et al. (2007) described mortality patterns in early stages of C. helgolandicus during two consecutive years and used smoothed values of mortality estimates in their relationships with environmental parameters. They were motivated by the fact that mortality estimates from the VLT are more robust when averaged over 5-7 values (Aksnes and Ohman, 1996; Hirst et al., 2007). We applied the same approach to our data using LOWESS fits and obtained very similar results in our statistical analysis (not shown). However, our time-dependent smoothed values actually represented means of data from several years (seasonal climatology based on several years), which markedly differed from Hirst et al. objectives (Hirst et al., 2007). We therefore concluded that using discrete data of both mortality estimates and environmental parameters was more appropriate in the context of our study. We argue that the significant relationships obtained with this approach indicate that the underlying effect of independent variables would dominate over the inherent uncertainties of individual mortality estimates with the VLT (Aksnes and Ohman, 1996).

## 16.5 *Mortality formulations and modeling population dynamics in Calanus finmarchicus*

Simulations with our stage-based model of *C. finmarchicus* demonstrated that differences in mortality formulations generate important variations in population dynamics (Fig. IV-9). Historically, mortality has been used in biological models of zooplankton as a closure term with imposed stage-specific mortality that could be 'manipulated' to fit modeled results to observations (Heath et al., 1997; Lynch et al., 1998; Miller et al., 1998). Contrary to bottom-up processes such as egg production, development and growth for which the use of mechanistic formulations is widespread, only in a few instance mortality was 'adjusted' from environmental parameters such as temperature or food (Bryant et al., 1997; Zakardjian et al., 2003; Runge et al., 2004; Speirs et al., 2006). The different mortality formulations used in our study depicted either a deterministic stage-specific mortality schedule representative of the overall values found in the literature (see Fig. IV-9A) or the addition of a dynamic component to this schedule by the inclusion of density-dependent mortality in early stages. This density-dependent mortality was for egg-N2 from Georges Bank (Ohman et al., 2002) or for egg-N3, weighted for phytoplankton biomass and temperature from LSLE (our study). These different formulations resulted in distinct seasonal pattern in daily mortality rate, survival, and significant alterations to the seasonal pattern and absolute level of recruitment

to late nauplii stages N4-6 (Fig. IV-9), illustrating the sensitivity of population model to mortality and the importance of using region-specific mortality patterns. Mortality is one of the greatest challenges in zooplankton modeling and the ability to 'apply' representative region-specific mortality patterns would be a significant improvement to the current situation (Runge et al., 2004).

Giving the importance of mortality in the control of population dynamics, mechanistic mortality functions constitute a prerequisite for simulating seasonal, inter-annual and spatial variations in population dynamics of zooplankton (Runge et al., 2004). To our knowledge, our 'multivariate' formulation of mortality in early stages egg-N3 based on female abundance (density-dependent process), phytoplankton biomass and temperature ($Q_{10}$ for seasonal forcing) represents the first attempt at integrating multiple effects from environmental and population-related (density-dependent) parameters on mortality and survival into a dynamic function in modeling of *C. finmarchicus*, and in zooplankton in general. Accurate formulations of processes regulating production, mortality, survival and recruitment in early development stages of copepods appear critical owing to the elevated losses experienced by early stages relative to older ones (Ohman et al., 2008; Heath et al., 2008). However, our formulation is based on empirical relationships between mortality and environmental parameters rather than representing the 'true' mechanism involved (example: feeding rate of female on their eggs and early

nauplii stages). It nevertheless provides a set-up that would introduce non-linearity in population response to variations in environmental forcing and the capability of biological models to simulate temporal and spatial patterns in population dynamics of *C. finmarchicus* (Ohman et al., 2002; Runge et al., 2004; Speirs et al., 2006).

# CHAPITRE V

# CONCLUSION GÉNÉRALE

"The choice of the biological model [...] should be determined by the question being asked, and the data available – not driven by the fact that more complicated models exist" (Franks, 2002). Au cours de ce travail de doctorat, différents modèles numériques de populations de *Calanus finmarchicus* ont été développés et validés grâce à d'abondantes données de qualité. L'emploi pertinent de la modélisation numérique a permis de mieux comprendre et quantifier le couplage entre la variabilité des processus physiques et certains aspects critiques de la dynamique des populations de *C. finmarchicus* dans le système de l'estuaire et du golfe du St Laurent (ESL-GSL).



*C. finmarchicus* domine les communautés zooplanctoniques de l'Atlantique au nord du Gulf Stream (Barnard et al., 2004). Cette espèce ubiquiste se retrouve en abondance du Mid-Atlantic Bight (Kane, 2005) à l'Océan Arctique (Hirche et Kosobokova, 2007), et du cœur des basins océaniques aux plateaux continentaux.

Cependant, la présence de *C. finmarchicus* dans les zones côtières aux marges de son aire de distribution habituelle est le plus souvent saisonnière et fortement dépendante de la circulation océanique (par ex. Speirs et al., 2006). Le second chapitre de cette thèse confirme ainsi le caractère exceptionnel du golfe du St Laurent qui héberge une population de *C. finmarchicus* résidente et auto-suffisante. Notre étude identifie pour la première fois les principaux patrons de distribution et d'abondance de la population de *C. finmarchicus* dans le système très dynamique de l'ESL-GSL, pour une année spécifique et sur une échelle spatiale s'étalant du rayon de déformation de Rossby à la région. D'après notre modèle, la présence pérenne de *C. finmarchicus* repose essentiellement sur le comportement de migration verticale des stades de développement, et en particulier sur l'adoption de migrations nycthémérales chez les derniers stades copépodites et les femelles adultes. L'intégration des migrations verticales journalières et ontogéniques à un modèle 3-D couplé Cycle de vie – Circulation a permis de révéler le rôle crucial qu'occupe la résonance entre les échelles spatio-temporelles impliquées dans ces migrations et dans les divers patrons de circulation au cœur de la stratégie de cycle de vie de *C. finmarchicus*. C'est une étape importante vers le développement d'explications robustes au « circuit *Calanus* » formé par des structures hydrodynamiques distinctes dans l'espace et le temps, mais reliées par le cycle de vie de *C. finmarchicus*.

En effet, certains courants sont transitoires et ne s'étendent que sur quelques

kilomètres, alors que d'autre structures récurrentes impliquent des mouvements de quelques dizaines à quelques centaines de kilomètres, telles la circulation estuarienne résiduelle ou encore les tourbillons et méandres à méso-échelle. Tout l'art du zooplancton est d'être parvenu à adapter à travers les temps géologiques ses comportements de nage journalier et ontogénique face aux courants qui le maintiennent perpétuellement en mouvement (voir Fiksen et al., 2007). *C. finmarchicus* se révèle particulièrement efficace dans ce contexte, grâce à son comportement de migration lors de sa phase productive en surface qui peut répondre en quelques heures à la variabilité environnementale (e.g. Basedow et al., 2008), ainsi qu'à un comportement saisonnier plus prévisible impliquant de plus grandes échelles de temps et d'espace lors de la période de diapause en profondeur. Le processus de diapause est une adaptation fondamentale à un environnement subissant une forte variabilité saisonnière, c'est à dire récurrente, périodique et semblable d'une année à l'autre (Alekseev et Starobogatov, 1996). Cependant les processus qui contrôlent l'entrée, la sortie et la durée même de la diapause demeurent encore largement méconnus, bien que le métabolisme des lipides en apparaisse depuis quelques année comme un élément central (Johnson et al., 2008; Tarrant et al., 2008). Ainsi, nous avons présenté dans le troisième chapitre de cette thèse le premier modèle de population de *C. finmarchicus* dont le mécanisme de contrôle de la diapause est basé sur la quantité de réserves lipides accumulée pendant le stade copépodite 5. Ce modèle simple permet dans le contexte

environnemental du GSL de reproduire la phénologie observée au sein de la population de *C. finmarcicus*, ainsi que la saisonnalité de la masse corporelle des copépodites 5 et de leurs réserves lipidiques sur deux années consécutives. Il autorise également la présence simultanée de copépodites 5 actifs et en diapause, du fait de l'apparition de la diapause plusieurs mois avant que les conditions environnementales ne soient défavorables à *C. finmarchicus* en termes de croissance et de mortalité. Cette dernière caractéristique représente en fait la clé du succès d'une telle stratégie de vie (Norrbin, 1996). Toutefois, des événements exceptionnels en regard de la climatologie et de la périodicité des variables environnementales peuvent nuire à l'efficacité du cycle de vie d'une espèce adapté à la saisonnalité de son milieu (Mackas et al., 2007). Dans un environnement aussi saisonnier que l'ESL-GSL, il apparaît donc fondamental de bien distinguer et comprendre les conséquences diverses des forçages physiques à haute fréquence agissant à l'échelle du développement des stades, de ceux opérants à l'échelle saisonnière pendant laquelle apparaissent les générations successives.

Le second chapitre de cette thèse illustre le fait que le cadre physique constitué par la topographie et la circulation détermine l'environnement physique (température) mais aussi biologique (production primaire) au sein duquel est distribuée la population de *C. finmarchicus*. Le troisième chapitre met quant à lui en lumière le processus de diapause, qui dans cet environnement variable permet à

l'espèce d'éviter pendant l'hiver les conditions les plus défavorable en terme de production et de mortalité. Pendant le reste de l'année cependant, les patrons de mortalité des stades qui se développent activement en surface vont déterminer le succès du recrutement d'individus en diapause, qui produiront la population active de l'année suivante. Le quatrième chapitre de cette thèse s'attache ainsi à comprendre la réponse face à la variabilité environnementale des patrons de mortalité des premiers stades de développement de *C. finmarchicus*, en raison des pertes élevées subies par ces stades comparativement aux suivants. Nos résultats démontrent que les périodes et les zones de recrutement important de *C. finmarchicus* correspondent systématiquement à de faibles taux de mortalité (forts taux de survie) des œufs et des premiers stades nauplii, et non pas seulement à de forts taux de production d'œufs, souvent observés dans le système ESL-GSL. La température, l'abondance de nourriture et l'abondance de femelles *C. finmarchicus* influent sur les taux de mortalité des jeunes stades. La mortalité augmente avec la température, mais la réduction simultanée du temps de développement conduit à des taux de survie relativement constant, en conformité avec les hypothèses concernant la pression évolutive exercée par la mortalité (Myers et Runge, 1983). Les influences opposées de l'abondance des femelles (positive) et de la nourriture (négative) indiquent un contrôle densité-dépendant des taux de mortalité par cannibalisme lorsque la densité de femelle est élevée mais la nourriture peu abondante. En venant modifier l'équilibre établi entre les taux de mortalité et de

développement dépendants de la température, le cannibalisme ou la prédation seraient les principaux contrôles des patrons de survie des premiers stades de développement. La mortalité est un important terme de fermeture dans les modèles de populations zooplanctoniques. Elle est souvent paramétrée de façon à faire correspondre au mieux les résultats avec les observations (Heath et al., 1997; Miller et al., 1998), et non formulé en tant que fonction des variables environnementales, contrairement aux autres processus démographiques tels que la production d'œufs, le développement et la croissance des individus (Bryant et al., 1997; Zakardjian et al., 2003; Speirs et al., 2006). Notre tentative d'intégrer de façon cohérente les effets divers du cannibalisme par les femelles, de l'abondance de nourriture et de la température dans une fonction de mortalité au sein d'un modèle de cycle de vie *C. finmarchicus* représente une avancée nécessaire pour une représentation réaliste de la variabilité spatiale, saisonnière et inter-annuelle de la dynamique des populations de *C. finmarchicus*.

L'ensemble des travaux entrepris au long de ce doctorat visent à améliorer la description mécaniste des processus fondamentaux du cycle de vie de *C. finmarchicus*. Depuis les travaux fondateurs de Wroblewski, qui fut le premier à aborder de façon moderne au moyen de la modélisation numérique les interactions complexes entre l'environnement physique dynamique et les populations planctoniques (O'Brien et Wroblewski, 1973; Wroblewski et O'Brien, 1981;

Wroblewski, 1982), jamais la recherche océanographique n'a été aussi proche de développer de réelles capacités de prédiction de l'évolution temporelle des écosystèmes dans un environnement en continuel changement. Saucier et al. (2009) ont par exemple démontré pour le GSL que des variations réalistes des forçages de vent ou de débit d'eau douce peuvent modifier considérablement l'hydrodynamisme du GSL, ainsi que les échanges avec les masses d'eau du Labrador et de l'Atlantique nord-ouest à travers les détroits de Cabot et de Belle-Isle. Or dans le contexte des changements climatiques appréhendés (Denman et al., 2007) les forçages atmosphériques et hydrologiques du GSL vont sans aucun doute subir d'importantes modifications, dont l'amplitude et la tendance restent toutefois encore incertaines. Ainsi, l'hydrodynamisme au sein du système complexe de l'ESL-GSL va en être affecté, et par voie de conséquence les espèces planctoniques telles que *C. finmarchicus* dont la présence pérenne repose sur des patrons de circulation, de température, de production primaire et de mortalité relativement prévisibles et récurrents. Les résultats présentés dans cette thèse permettront d'identifier les zones optimales, sub-optimales et néfastes de variation des variables environnementales pour *C. finmarchicus*. Intégrés de façon adéquate dans des modèles numériques de dynamique des populations de *C. finmarchicus*, ils peuvent aussi aider à comprendre la vitesse des changements induits (tolérés) et le caractère stochastique de ces derniers.

# RÉFÉRENCES

Aksnes, D.L. et Ohman, M.D. 1996. A vertical life table approach to zooplankton mortality estimation. Limnol. Oceanogr., 41, 1461-1469

Aksnes, D.L., Troedsson, C. et Thompson, E.M. 2006. Integrating developmental clocking and growth in a life-history model for the planktonic chordate *Oikopleura dioica*. Mar. Ecol. Prog. Ser., 318, 81-88

Alekseev, V.R. et Starobogatov, Y.I. 1996. Types of diapause in Crustacea: definitions, distribution, evolution. Hydrobiol., 320, 15-26

Alheit, J., Möllmann, C., Dutz, J., Kornilovs, G., Loewe, P., Mohrholz, V. et Wasmund, N. 2005. Synchronous ecological regime shifts in the central Baltic and the North Sea in the late 1980s. ICES J. Mar. Sci., 62, 1205-1215

Andersen, V. et Nival, P. 1991. A model of the diel vertical migration of zooplankton based on euphausiids. J. Mar. Res., 49, 153-175

Anderson, J.T. 1994. Feeding ecology and condition of larval and pelagic juvenile redfish *Sebastes* spp. Mar. Ecol. Prog. Ser., 104, 211-226

Arnkværn, G., Daase, M. et Eiane, K. 2005. Dynamics of coexisting *Calanus finmarchicus, Calanus glacialis* and *Calanus hyperboreus* populations in a high-Arctic fjord. Polar Biol., 28, 528-538

Backhaus, J., Harms, I., Krause, M. et Heath, M. 1994. An hypothesis concerning the space-time succession of *Calanus finmarchicus* in the northern North Sea. ICES J. Mar. Sci., 51, 169-180

Banks, R.E. 1966. The cold intermediate layer of the Gulf of St. Lawrence. J. Geophys. Res., 71, 1603-1610

Barnard, R., Batten, S., Beaugrand, G., Buckland, C., Conway, D., Edwards, M., Finlayson, J., Gregory, L., Halliday, N., John, A., Johns, D., Johnson, A., Jonas, T. et Lindley, J. 2004. Continuous Plankton Records: Plankton Atlas of the North Atlantic Ocean (1958-1999). 2. Biogeographical charts. Mar. Ecol. Prog. Ser. Suppl., 11-75

Basedow, S.L. et Tande, K.S. 2006. Cannibalism by female *Calanus finmarchicus* on naupliar stages. Mar. Ecol. Prog. Ser., 327, 247-255

Basedow, S.L., Edvardsen, A. et Tande, K.S. 2008. Vertical segregation of *Calanus finmarchicus* copepodites during the spring bloom. J. Mar. Sys., 70, 21-32

Batchelder, H.P., Edwards, C.A. et Powell, T.M. 2002. Individual-based models of copepod populations in coastal upwelling regions: implications of physiologically and environmentally influenced diel vertical migration on demographic success and nearshore retention. Prog. Oceanogr. 53, 307-333

Bathmann, U., Bundy, M.H., Clarke, M.E., Cowles, T.J., Daly, K., Dam, H.G., Dekshenieks, M.M., Donaghay, P.L., Gibson, D.M., Gifford, D.J., Hansen, B.W., Hartline, D.K., Head, E.J.H., Hofmann, E.E., Hopcroft, R.R., Jahnke, R.A., Jonasdottir, S.H., Kiørboe, T., Kleppel, G.S., Klinck, J.M., Kremer, P.M., Landry, M.R., Lee, R.F., Lenz, P.H., Madin, L.P., Manahan, D.T., Mazzocchi, M.G., McGillicuddy, D.J., Miller, C.B., Nelson, J.R., Osborn, T.R., Paffenhofer, G.A., Pieper, R.E., Prusova, I., Roman, M.R., Schiel, S., Seim, H.E., Smith, S.L., Torres, J.J., Verity, P.G., Wakeham, S.G. et Wishner, K.F. 2001. Future marine zooplankton research - a perspective. Mar. Ecol. Prog. Ser., 222, 297-308

Baumgartner, M.F. et Fratantoni, D.M. 2008. Diel periodicity in both sei whale vocalization rates and the vertical migration of their copepod prey observed from ocean gliders. Limnol. Oceanogr., 53, 2197-2209

Beaugrand, G., Reid, P., Ibañez, F., Lindley, J. et Edwards, M. 2002. Reorganization of North Atlantic Marine Copepod Biodiversity and Climate. Science, 296, 1692-1694

Bonnet, D., Titelman, J. et Harris, R. 2004. *Calanus* the cannibal. J. Plankton Res., 26, 937-948

Bonnet, D., Harris, R.P., Hay, S., Ingvarsdottir, A. et Simon, O. 2007. Histological changes of the digestive epithelium in *Calanus finmarchicus*: an index for diapause? Mar. Biol., 151, 313-326

Bourgault, D. et Koutitonsky, V.G. 1999. Real-Time Monitoring of the Freshwater Discharge at the Head of the St. Lawrence Estuary. Atmos.-Ocean, 37, 203-220

Broekhuizen, N., Heath, M.R., Hay, S.J. et Gurney, W.S.C. 1995. Modelling the dynamics of the North Sea's Mesozooplankton. Neth. J. Sea Res., 33, 381-406

Bryant, A.D., Heath, M., Gurney, W.S.G., Beare, D.J. et Robertson, W. 1997. The seasonal dynamics of *Calanus finmarchicus*: development of a three-dimensional structured population model and application to the northern North Sea. J. Sea Res., 38, 361-379

Bryant, A.D., Hainbucher, D. et Heath, M. 1998. Basin-scale advection and population persistence of *Calanus finmarchicus*. Fish. Oceanogr., 7, 235-244

Buckley, L.J. et Durbin, E.G. 2006. Seasonal and inter-annual trends in the zooplankton prey and growth rate of Atlantic cod (*Gadus morhua*) and

haddock (*Melanogrammus aeglefinus*) larvae on Georges Bank. Deep Sea Res. II, 53, 2758-2770

Bugden, G.L. 1991. Changes in the temperature-salinity characteristics of the deeper waters of the Gulf of St. Lawrence over the past several decades. Can. Spec. Pub. Fish. Aquat. Sci., 113, 139-147

Bunker, A.J. et Hirst, A.G. 2004. Fecundity of marine planktonic copepods: Global rates and patterns in relation to chlorophyll *a*, temperature and body weight. Mar. Ecol. Prog. Ser., 279, 161-181

Campbell, R.G., Wagner, M.M., Teegarden, G.J., Boudreau, C.A. et Durbin, E.G. 2001. Growth and development rates of the copepod *Calanus finmarchicus* reared in the laboratory. Mar. Ecol. Prog. Ser., 221, 161-183

Carlotti, F. et Sciandra, A. 1989. Population dynamics model of *Euterpina acutifrons* (Copepoda: Harpacticoida) coupling individual growth and larval development. Mar. Ecol. Prog. Ser., 56, 225-242

Carlotti, F. et Wolf, K. 1998. A Lagrangian ensemble model of *Calanus finmarchicus* coupled with a 1D ecosystem model. Fish. Oceanogr., 7, 191-204

Carr, S.D., Capet, X.J., McWilliams, J.C., Pennington, J.T. et Chavez, F.P. 2008. The influence of diel vertical migration on zooplankton transport and recruitment in an upwelling region: estimates from a coupled behavioral-physical model. Fish. Oceanogr., 17, 1-15

Castonguay, M., Plourde, S., Robert, D., Runge, J. et Fortier, L. 2008. Copepod production drives recruitment in a marine fish. Can. J. Fish. Aquat. Sci., 65, 1528-1531

Chelton, D.B., Bernal, P.A. et McGowan, J.A. 1982. Large-scale interannual physical and biological interaction in the California Current. J. Mar. Res., 40, 1095-1125

Christian, J. 2007. Advection in plankton models with variable elemental ratios. Ocean. Dyn., 57, 63-71

Colton, J.B., Green, J.R., Byron, R.R. et Frisella, J.L. 1980. Bongo net retention rates as effected by towing speed and mesh size. Can. J. Fish. Aquat. Sci., 37, 606-623

Conover, R.J. 1988. Comparative life histories in the genera *Calanus* and *Neocalanus* in high latitudes of the northern hemisphere. Hydrobiol.,167/168, 127-142

Coyle, K.O., Pinchuk, A.I., Eisner, L.B. et Napp, J.M. 2008. Zooplankton species composition, abundance and biomass on the eastern Bering Sea shelf during summer: The potential role of water-column stability and nutrients in structuring the zooplankton community. Deep Sea Res. II, 55, 1775-1791

Cushing, D. 1984. The gadoid outburst in the North Sea. ICES J. Mar. Sci., 41, 159-166

Davis, C.S. 1984. Predatory control of copepod seasonal cycles on Georges Bank. Mar. Biol., 82, 31-40

de Lafontaine, Y., Demers, S. et Runge, J. 1991. Pelagic food web interactions and productivity in the Gulf of St. Lawrence: a perspective. Can. Spec. Pub. Fish. Aquat. Sci., 113, 99-124

Denman, K.L., Brasseur, G., Chidthaisong, A., Ciais, P., Cox, P., Dickinson, R.,

Hauglustaine, D., Heinze, C., Holland, E., Jacob, D., Lohmann, U., Ramachandran, S., da Silva Dias, P., Wofsy, S. et Zhang, X. 2007. Couplings Between Changes in the Climate System and Biogeochemistry. *In:* Climate Change 2007: The Physical Science Basis. Contribution of Working Group I to the Fourth Assessment Report of the Intergovernmental Panel on Climate Change. Solomon, S., Qin, D., Manning, M., Chen, Z., Marquis, M., Averyt, K.B., Tignor, M. et Miller, H.L. (eds.), Cambridge University Press, 499-587

de Young, B., Heath, M., Werner, F., Chai, F., Megrey, B. et Monfray, P. 2004. Challenges of modeling Ocean Basin ecosystems. Science, 304, 1463-1466

Durbin, E.G., Campbell, R.G., Gilman, S.L. et Durbin, A.G. 1995. Diel feeding behavior and ingestion rate in the Copepod *Calanus finmarchicus* in the Southern Gulf of Maine during late spring. Cont. Shelf Res., 15, 539-570

Durbin, E.G., Runge, J.A., Campbell, R.G., Garrahan, P.R., Casas, M.C. et Plourde, S. 1997. Late fall-early winter recruitment of *Calanus finmarchicus* on Georges Bank. Mar. Ecol. Prog. Ser., 151, 103-114

Durbin, E.G., Garrahan, P.R. et Casas, M.C. 2000. Depth distribution of *Calanus finmarchicus* nauplii on the Georges Bank during 1995 and 1996. ICES J. Mar. Sci., 57, 1686-1693

Eckman, J.E. 1994. Modelling physical-biological coupling in the ocean: the U.S. GLOBEC program. Deep-Sea Res. II, 41, 1-5

Eiane, K., Aksnes, D.L. et Ohman, M.D. 1998. Advection and zooplankton fitness. Sarsia, 82, 87-93

Eiane, K. et Ohman, M.D. 2004. Stage-specific mortality of *Calanus finmarchicus*,

*Pseudocalanus elongatus* and *Oithona similis* on Fladen Ground, North Sea, during a spring bloom. Mar. Ecol. Prog. Ser., 268, 183-193

El-Sabh, M.I. 1979. The lower St. Lawrence Estuary as a physical oceanographic system. Nat. Can., 106, 55-73

Emsley, S.M., Tarling, G.A. et Burrows, M.T. 2005. The effect of vertical migration strategy on retention and dispersion in the Irish Sea during spring-summer. Fish. Oceanogr., 14, 161-174

Falk-Petersen, S., Leu, E., Berge, J., Kwasniewski, S., Nygård, H., Røstad, A., Keskinen, E., Thormar, J., von Quillfeldt, C., Wold, A. et Gulliksen, B. 2008. Vertical migration in high Arctic waters during autumn 2004. Deep Sea Res. II, 55, 2275-2284

Faucher, M., Caya, D., Saucier, F.J. et Laprise, R. 2004. Interaction between atmosphere and ocean-ice regional models over the Gulf of St. Lawrence area, Canada. Atmos.-Ocean, 45, 85-100

Fennel, W. 2001. Modeling of copepods with links to circulation models. J. Plankton Res., 23, 1217-1232

Fennel, W. et Neumann, T. 2003. Variability of copepods as seen in a coupled physical-biological model of the Baltic Sea. ICES Mar. Sci. Sym., 219, 208-219

Fiksen, Ø. et Carlotti, F. 1998. A model of optimal life history and diel vertical migration in *Calanus finmarchicus*. Sarsia, 83, 129-147

Fiksen, Ø. 2000. The adaptive timing of diapause - a search for evolutionarily robust strategies in *Calanus finmarchicus*. ICES J. Mar. Sci., 57, 1825-1833

Fiksen, Ø., Eliassen, S. et Titelman, J. 2005. Multiple predators in the pelagic: modelling behavioural cascades. J. Animal Ecol., 74, 423-429

Fiksen, Ø., Jørgensen, C., Kristiansen, T., Vikebø, F. et Huse, G. 2007. Linking behavioural ecology and oceanography: larval behaviour determines growth, mortality and dispersal. Mar. Ecol. Prog. Ser., 347, 195-205

Fortier, L., Levasseur, M., Drolet, R. et Therriault, J. 1992. Export production and the distribution of fish larvae and their prey in a coastal jet frontal region. Mar. Ecol. Prog. Ser., 85, 203-218

Franks, P.J.S. 1992. Sink or swim: accumulation of biomass at fronts. Mar. Ecol. Prog. Ser., 82, 1-12

Franks, P.J.S. 2002. NPZ models of plankton dynamics: their construction, coupling to physics, and application. J. Oceanogr., 58, 379-387

Fromentin, J.M. et Planque, B. 1996. *Calanus* and environment in the eastern North Atlantic. II. Influence of the North Atlantic Oscillation on *C. finmarchicus* and *C. helgolandicus*. Mar. Ecol. Prog. Ser., 134, 111-118

Frontier, S. 1991. Le transfert d'échelle. *In*: Christian, M. (eds) Transferts d'échelle en océanographie ORSTOM, Paris, 365-377

Frontier, S. 2004. Ecosystèmes : structure, fonctionnement, évolution. Dunod, Paris, 549pp

Frost, B.W. 2005. Diatom blooms and copepod responses: Paradigm or paradox? Prog. Oceanogr., 67, 283-285

Fuentes-Yaco, C., Vezina, A., Larouche, P., Gratton, Y. et Gosselin, M. 1997.

Phytoplankton pigment in the Gulf of St. Lawrence, Canada, as determined by the Coastal Zone Color Scanner. Part II: Multivariate analysis. Cont. Shelf Res., 17, 1441-1459

Galbraith, P.S. 2006. Winter water masses in the Gulf of St. Lawrence. J. Geophys. Res., 111, C06022

Gallego, A., Mardaljevic, J., Heath, M., Hainbucher, D. et Slagstad, D. 1999. A model of the spring migration into the North Sea by *Calanus finmarchicus* overwintering off the Scottish continental shelf. Fish. Oceanogr., 8, 107-125

Genin, A., Jaffe, J.S., Reef, R., Richter, C. et Franks, P.J.S. 2005. Swimming Against the Flow: A Mechanism of Zooplankton Aggregation. Science, 308, 860-862

Gentleman, W. 2000. Factors controlling the seasonal abundance and distribution of *Calanus finmarchicus* in the Gulf of Maine/Georges Bank region. Ph.D. dissertation, Dartmouth College, Canada

Gilbert, D., Sundby, B., Gobeil, C., Mucci, A. et Tremblay, G. 2005. A seventy-two-year record of diminishing deep-water oxygen in the St. Lawrence estuary: The northwest Atlantic connection. Limnol. Oceanogr., 50, 1654-1666

Gilbert, D. et Pettigrew, B. 1997. Interannual variability (1948-1994) of the CIL core temperature in the Gulf of St. Lawrence. Can. J. Fish. Aquat. Sci., 54, 57-67

Gislason, A., Eiane, K. et Reynisson, P. 2007. Vertical distribution and mortality of *Calanus finmarchicus* during overwintering in oceanic waters southwest of Iceland. Mar. Biol., 150, 1253-1263

Greene, C., Pershing, A., Conversi, A., Planque, B., Hannah, C., Sameoto, D., Head,

E., Smith, P., Reid, P., Jossi, J., Mountain, D., Benfield, M., Wiebe, P. et Durbin, E. 2003. Trans-Atlantic responses of *Calanus finmarchicus* populations to basin-scale forcing associated with the North Atlantic Oscillation. Prog. Oceanogr., 58, 301-312

Gurney, W.S.C., Speirs, D.C., Wood, S.N., Clarke, E.D. et Heath, M.R. 2001. Simulating spatially and physiologically structured populations. J. Animal Ecol., 70, 881-894

Hamilton, L.C. 2007. Climate, fishery and society interactions: Observations from the North Atlantic. Deep Sea Res. II, 54, 2958-2969

Hannah, C., Naimie, C., Loder, J. et Werner, F. 1997. Upper-ocean transport mechanisms from the Gulf of Maine to Georges Bank, with implications for *Calanus* supply. Cont. Shelf Res., 17, 1887-1911

Harms, I.H., Heath, M.R., Bryant, A.D., Backhaus, J.O. et Hainbucher, D.A. 2000. Modelling the Northeast Atlantic circulation: implications for the spring invasion of shelf regions by *Calanus finmarchicus*. ICES J. Mar. Sci., 57, 1694-1707

Harris, R.P., Irigoien, X., Head, R.N., Rey, C., Hygum, B.H., Hansen, B.W., Niehoff, B., Meyer-Harms, B. et Carlotti, F. 2000. Feeding, growth, and reproduction in the genus *Calanus*. ICES J. Mar. Sci., 57, 1708-1726

Harvey, M., St-Pierre, J., Devine, L., Gagné, A., Gagnon, Y. et Beaulieu, M. 2005. Oceanographic conditions in the Estuary and the Gulf of St. Lawrence during 2004: zooplankton. DFO, Canadian Science Advisory Secretariat. Research Document 2005/043, 22pp

Hassett, R.P. 2006. Physiological characteristics of lipid-rich "fat" and lipid-poor "thin" morphotypes of individual *Calanus finmarchicus* C5 copepodites in nearshore Gulf of Maine. Limnol. Oceanogr., 51, 997-1003

Head, E. et Pepin, P. 2007. Variations in overwintering depth distributions of *Calanus finmarchicus* in the slope waters of the NW Atlantic continental shelf and the Labrador Sea. J. Northw. Atl. Fish. Sci., 39, 49-69

Heath, M., Robertson, W., Mardaljevic, J. et Gurney, W.S.G. 1997. Modelling the population dynamics of *Calanus* in the Fair Isle Current off northern Scotland. J. Sea Res., 38, 381-412

Heath M., Backhaus J., Richardson K., McKenzie E., Slagstad D., Beare D., Dunn J., Fraser J., Gallego A., Hainbucher D., Hay S., Jonasdottir S., Madden H., Mardaljevic J. et Schacht, A. 1999. Climate fluctuations and the spring invasion of the North Sea by Calanus finmarchicus. Fish. Oceanogr., 8, 163-176

Heath, M.R., Astthorsson, O.S., Dunn, J., Ellertsen, B., Gaard, E., Gislason, A., Gurney, W., Hind, A.T., Irigoien, X., Melle, W., Niehoff, B., Olsen, K., Skreslet, S. et Tande, K.S. 2000. Comparative analysis of *Calanus finmarchicus* demography locations around the Northeast Atlantic. ICES J. Mar. Sci., 57, 1562-1580

Heath, M.R., Boyle, P.R., Gislason, A., Gurney, W.S.C., Hay, S.J., Head, E.J.H., Holmes, S., Ingvarsdottir, A., Jonasdottir, S.H., Lindeque, P., Pollard, R., Rasmussen, J., Richards, K., Richardson, K., Smerdon, G. et Speirs, D. 2004. Comparative ecology of over-wintering *Calanus finmarchicus* in the northern North Atlantic, and implications for life-cycle patterns. ICES J. Mar. Sci., 61, 698-708

Heath, M., Rasmussen, J., Ahmed, Y., Allen, J., Anderson, C., Brierley, A., Brown, L., Bunker, A., Cook, K., Davidson, R., Fielding, S., Gurney, W., Harris, R., Hay, S., Henson, S., Hirst, A., Holliday, N., Ingvarsdottir, A., Irigoien, X., Lindeque, P., Mayor, D., Montagnes, D., Moffat, C., Pollard, R., Richards, S., Saunders, R., Sidey, J., Smerdon, G., Speirs, D., Walsham, P., Waniek, J., Webster, L. et Wilson, D. 2008. Spatial demography of *Calanus finmarchicus* in the Irminger Sea. Prog. Oceanogr., 76, 39-88

Helaouët, P. et Beaugrand, G. 2007. Macroecology of *Calanus finmarchicus* and *C. helgolandicus* in the North Atlantic Ocean and adjacent seas. Mar. Ecol. Prog. Ser., 345, 147-165

Heywood, K.J. 1996. Diel vertical migration of zooplankton in the Northeast Atlantic. J. Plankton Res., 18, 163-184

Hind, A., Gurney, W.S.C., Heath, M., Bryant, A.D. 2000. Overwintering strategies in *Calanus finmarchicus*. Mar. Ecol. Prog. Ser., 193, 95-107

Hirche, H. 1983. Overwintering of *Calanus finmarchicus* and *Calanus helgolandicus*. Mar. Ecol. Prog. Ser., 11, 281-290

Hirche, H.J. 1996a. The reproductive biology of the marine copepod, *Calanus finmarchicus* - A review. Ophelia, 44, 111-128

Hirche, H.J. 1996b. Diapause in the marine copepod *Calanus finmarchicus* – a review. Ophelia, 44, 129–143

Hirche, H.J., Brey, T. et Niehoff, B. 2001. A high-frequency time series at Ocean Weather Ship Station M (Norwegian Sea), Population dynamics of *Calanus finmarchicus*. Mar. Ecol. Prog. Ser., 219, 205-219

Hirche, H. et Kosobokova, K. 2007. Distribution of *Calanus finmarchicus* in the northern North Atlantic and Arctic Ocean - Expatriation and potential colonization. Deep Sea Res. II, 54, 2729-2747

Hirst, A.G., Kiørboe T. 2002. Mortality of marine planktonic copepods: Global rates and patterns. Mar. Ecol. Prog. Ser., 230, 195-209

Hirst, A.G. et Bunker, A.J. 2003. Growth of marine planktonic copepods, Global rates and patterns in relation to chlorophyll *a*, temperature, and body weight. Limnol. Oceanogr., 48, 1988-2010

Hirst, A.G., Bonnet, D. et Harris, R.P. 2007. Seasonal dynamics and mortality rates of *Calanus helgolandicus* over two years at a station in the English Channel. Mar. Ecol. Prog. Ser., 340, 189-205

Hu, Q., Davis, C.S. et Petrik, C.M. 2008. A simplified age-stage model for copepod population dynamics. Mar. Ecol. Prog. Ser., 360, 179-187

Huntley, M.E. et Lopez, M.D.G. 1992. Temperature-dependent production of marine copepods, a global synthesis. Am. Nat., 140, 201-242

Hygum, B.H., Rey, C., Hansen, B.W. 2000a. Growth and development rates of *Calanus finmarchicus* nauplii during a diatom spring bloom. Mar. Biol., 136, 1075-1085

Hygum, B.H., Rey, C., Hansen, B.W. et Tande, K. 2000b. Importance of food quantity to structural growth rate and neutral lipid reserves accumulated in *Calanus finmarchicus*. Mar. Biol., 136, 1057-1073

Iida, T. et Saitoh, S. 2007. Temporal and spatial variability of chlorophyll concentrations in the Bering Sea using empirical orthogonal function (EOF)

analysis of remote sensing data. Deep Sea Res. II, 54, 2657-2671

Incze, L.S., Hebert, D., Wolff, N., Oakey, N. et Dye, D. 2001. Changes in copepod distributions associated with increased turbulence from wind stress. Mar. Ecol. Prog. Ser., 213, 229-240

Ingvarsdottir, A., Houlihan, D.F., Heath, M.R., Hay, S.J. 1999. Seasonal changes in respiration rates of copepodite stage V *Calanus finmarchicus* (Gunnerus). Fish. Oceanogr., 8, 73-83

Irigoien, X., Head, R., Klenke, U., Meyer-Harms, B., Harbour, D., Niehoff, B., Hirche, H. et Harris, R. 1998. A high frequency time series at weathership M, Norwegian Sea, during the 1997 spring bloom: feeding of adult female Calanus finmarchicus. Mar. Ecol. Prog. Ser., 172, 127-137

Irigoien, X., Titelman, J., Harris, R.P., Harbour, D. et Castellani, C. 2003. Feeding of *Calanus finmarchicus* nauplii in the Irminger Sea. Mar. Ecol. Prog. Ser., 262, 193-200

Irigoien, X. 2004. Some ideas about the role of lipids in the life cycle of *Calanus finmarchicus*. J. Plankton Res., 26, 259-263

Johnson, C., Pringle, J., Chen, C. 2006. Transport and retention of dormant copepods in the Gulf of Maine. Deep Sea Res. II, 53, 2520-2536

Johnson, C., Leising, A., Runge, J., Head, E., Pepin, P., Plourde, S. et Durbin, E. 2008. Characteristics of *Calanus finmarchicus* dormancy patterns in the northwest Atlantic. ICES J. Mar. Sci., 65, 339-350

Jónasdóttir, S. 1999. Lipid content of *Calanus finmarchicus* during overwintering in the Faroe-Shetland Channel. Fish. Oceanogr., 8, 61-72

Kane, J. 2005. The demography of *Calanus finmarchicus* (Copepoda: Calanoida) in the Middle Atlantic Bight, USA, 1977-2001. J. Plankton Res., 27, 401-414

Kiørboe, T., Mohlenberg, F. et Tiselius, P. 1988. Propagation of planktonic copepods, production and mortality of eggs. Hydrobiol., 167/168, 219-225

Kiørboe, T. et Sabatini, M. 1994. Reproductive and life cycle strategies in egg-carrying cyclopoid and free-spawning calanoid copepod. J. Plank. Res., 16, 1352-1366

Kiørboe, T. 2006. Sex, sex-ratios, and the dynamics of pelagic copepod populations. Oecologia, 148, 40-50

Knutsen, T., Melle, W. et Calise, L. 2001. Determining the mass density of marine copepods and their eggs with a critical focus on some of the previously used methods. J. Plankton Res., 23, 859-873

Kobari, T., Shinada, A. et Tsuda, A. 2003. Functional roles of interzonal migrating mesozooplankton in the western subarctic Pacific. Prog. Oceanogr., 57, 279-298

Koutitonsky, V.G. et Bugden, G.L. 1991. The physical oceanography of the Gulf of St. Lawrence: A review with emphasis on the synoptic variability of the motion. Can. Spec. Pub. Fish. Aquat. Sci., 113, 57-90

Kouwenberg, J.H.M., Browman, H.I., Runge, J.A., Cullen, J.J., Davis, R.F. et St-Pierre, J.F. 1999. Biological weighting of ultraviolet (280-400 nm) induced mortality in marine zooplankton and fish. II. *Calanus finmarchicus* (Copepoda) eggs. Mar. Biol., 134, 285-293

Lampert, W., McCauley, E. et Manly, B.F.J. 2003. Trade-offs in the vertical

distribution of zooplankton: ideal free distribution with costs? Proc. R. Soc. B, 270, 765-773

Landry, M.R. 1981. Switching between herbivory and carnivory by the planktonic marine copepod *Calanus pacificus*. Mar. Biol., 65, 77–82

Le Fouest, V., Zakardjian, B., Saucier, F. et Starr, M. 2005. Seasonal versus synoptic variability in planktonic production in a high-latitude marginal sea: The Gulf of St. Lawrence (Canada). J. Geophys. Res., 110, 1-21

Le Fouest, V., Zakardjian, B., Saucier, F. et Cizmeli, S. 2006. Application of SeaWIFS- and AVHRR-derived data for mesoscale and regional validation of a 3-D high-resolution physical/biological model of the Gulf of St. Lawrence (Canada). J. Mar. Syst., 60, 30-50

Lehodey, P., Alheit, J., Barange, M., Baumgartner, T., Beaugrand, G., Drinkwater, K., Fromentin, J., Hare, S., Ottersen, G., Perry, C., van der Lingen, C. et Werner, F. 2006. Climate Variability, Fish, and Fisheries. J. Clim., 19, 5009-5030

Leising, A.W. et Franks, P.J. 2000. Copepod vertical distribution within a spatially variable food source: a simple foraging-strategy model. J. Plankton Res., 22, 999-1024

Leising, A.W. et Franks, P.J. 2002. Does *Acartia clausi* (Copepoda: Calanoida) use an area-restricted search foraging strategy to find food? Hydrobiol., 480, 193-207

Leising, A.W., Pierson, J.J., Halsband-Lenk, C., Horner, R. et Postel, J. 2005. Copepod grazing during spring blooms: Can *Pseudocalanus newmani* induce

trophic cascades? Prog. Oceanogr., 67, 406-421

Lévy, M. 2008. The modulation of biological production by oceanic mesoscale turbulence. *In*: Transport and Mixing in Geophysical Flows, Springer, Berlin, 219-261

Liang, D., Uye, S. et Onbé, T. (1994) Production and loss of eggs in the calanoid copepod *Centropages abdominalis* Sato in Fukuyama Harbor, the Inland Sea of Japan. Bull. Plankton Soc. Japan, 41, 131-142

Liang, D. et Uye, S. 1996a. Population dynamics and production of the planktonic copepods in a eutrophic inlet of the Inland Sea of Japan. 2. *Acartia omorii*. Mar. Biol., 125, 109-117

Liang, D. et Uye, S. 1996b. Population dynamics and production of the planktonic copepods in a eutrophic inlet of the Inland Sea of Japan. 3. *Paracalanus parvus*. Mar. Biol., 127, 219-227

Lipscomb, W.H. et Hunke, E.C. 2004. Modeling Sea Ice Transport Using Incremental Remapping. Mon. Weather Rev., 132, 1341-1354

Liu, S., Sun, S. et Han, B. 2003. Diel vertical migration of zooplankton following optimal food intake under predation. J. Plankton Res., 25, 1069-1077

Liu, S., Sun, S. et Han, B. 2006. Viewing DVM via general behaviors of zooplankton: A way bridging the success of individual and population. J. Theor. Biol., 238, 435-448

Loeng, H. et Drinkwater, K. 2007. An overview of the ecosystems of the Barents and Norwegian Seas and their response to climate variability. Deep Sea Res. II, 54, 2478-2500

Lopez, M.D.G. 1996. Effect of starvation on development and survirvorship of naupliar *Calanus pacificus* (Brodsky). J. Exp. Mar. Biol. Ecol., 203, 133-146

Lough, R.G. et Broughton, E.A. 2007. Development of micro-scale frequency distributions of plankton for inclusion in foraging models of larval fish, results from a Video Plankton Recorder. J. Plankton Res., 29, 7-17

Ludovisi, A., Todini, C., Pandolfi, P. et Taticchi, M.I. 2008. Scale patterns of diel distribution of the copepod *Cyclops abyssorum* Sars in a regulated lake: the relative importance of physical and biological factors. J. Plankton Res., 30, 495-509

Lynch, D.R., Gentleman, W.C., McGillicuddy, D.J. et Davis, C.S. 1998. Biological/physical simulations of *Calanus finmarchicus* population dynamics in the Gulf of Maine. Mar. Ecol. Prog. Ser., 169, 189-210

Lynch, D.R., Lewis, C.V.W. et Werner, F.E. 2001. Can Georges Bank larval cod survive on a calanoid diet? Deep Sea Res. II, 48, 609-630

Mackas, D.L., Denman, K.L. et Abbott, M.R. 1985. Plankton patchiness: Biology in the physical vernacular. Bull. Mar. Sci., 37, 652-674

Mackas, D.L., Batten, S. et Trudel, M. 2007. Effects on zooplankton of a warmer ocean: Recent evidence from the Northeast Pacific. Prog. Oceanogr., 75, 223-252

Malchow, H., Petrovskii, S. et Medvinsky, A. 2001. Pattern formation in models of plankton dynamics. A synthesis. Oceanol. Acta, 24, 479-487

Mauchline, J. 1998. The biology of Calanoïd copepods. Academic Press Ed., Advances in Marine Biology, 33, 710pp

McLaren, I.A., Head, E. et Sameoto, D.D. 2001. Life cycles and seasonal distributions of *Calanus finmarchicus* on the central Scotian Shelf. Can. J. Fish. Aquat. Sci., 58, 659-670

Mertz, G., El-Sabh, M.I., Proulx, D. et Condal, A.R. 1988. Instability of a buoyancy-driven coastal jet: The Gaspé Current and its St. Lawrence precursor. J. Geophys. Res. Oceans, 93, 6885-6893

Mertz, G., Koutitonsky, V.G. et Gratton, Y. 1991. On the seasonal cycle of the Gaspé Current. Can. Spec. Pub. Fish. Aquat. Sci., 113, 149-152

Michel, C., Ingram, R. et Harris, L. 2006. Variability in oceanographic and ecological processes in the Canadian Arctic Archipelago. Prog. Oceanogr., 71, 379-401

Miller, C.B., Cowles, T.J., Wiebe, P.H., Copley, N.J. et Grigg, H. 1991. Phenology in *Calanus finmarchicus*: hypotheses about control mechanisms. Mar. Ecol. Prog. Ser., 72, 79-91

Miller, C.B., Lynch, D.R., Carlotti, F., Gentelman, W. et Lewis, C.V.W. 1998a. Coupling of an individual-based population dynamic model of *Calanus finmarchicus* to a circulation model for the Georges Bank region. Fish. Oceanogr., 7, 219-234

Miller, C.B., Morgan, C.A., Prahl, F.G. et Sparrow, M.A. 1998b. Storage lipids of the copepod *Calanus finmarchicus* from Georges Bank and the Gulf of Maine. Limnol. Oceanogr., 43, 488-497

Miller, C.B., Crain, J.A. et Morgan, C.A. 2000. Oil storage variability in *Calanus finmarchicus*. ICES J. Mar. Sci., 57, 1786-1799

Miller, C.B. 2008. Copepod growth in detail: pattern similarity to decapod larvae. ICES J. Mar. Sci., 65, 332-338

Muraleedharan, K., Jasmine, P., Achuthankutty, C., Revichandran, C., Dinesh Kumar, P., Anand, P. et Rejomon, G. 2007. Influence of basin-scale and mesoscale physical processes on biological productivity in the Bay of Bengal during the summer monsoon. Prog. Oceanogr., 72, 364-383

Myers, R.A. et Runge, J.A. 1983. Predictions of seasonal natural mortality rates in a copepod population using life-history theory. Mar. Ecol. Prog. Ser., 11, 189-194

Neumann, T. et Kremp, C. 2005. A model study with light-dependent mortality rates of copepod stages. J. Mar. Syst., 56, 416-434

Neumann, T. et Fennel, W. 2006. A method to represent seasonal vertical migration of Zooplankton in 3D-Eulerian models. Ocean Modell., 12, 188-204

Nichols, J.H. et Thompson, A.B. 1991. Mesh selection of copepodite and nauplius stages of four calanoid copepod species. J. Plankton Res., 13, 661-671

Norrbin, M.F. 1996. Timing of diapause in relation to the onset of winter in the high-latitude copepods *Pseudocalanus acuspes* and *Acartia longiremis*. Mar. Ecol. Prog. Ser., 142, 99-109

O'Brien, J.J. et Wroblewski, J.S. 1973. On advection in phytoplankton models. J. Theor. Biol., 38, 197-202

Ohman, M.D., Runge, J.A. 1994. Sustained fecundity when phytoplankton resources are in short supply: Omnivory by *Calanus finmarchicus* in the Gulf of St. Lawrence. Limnol. Oceanogr., 39, 21-36

Ohman, M.D. et Wood, S.N. 1996. Mortality estimation for planktonic copepods, *Pseudocalanus newmani* in a temperate fjord. Limnol. Oceanogr., 41, 126-135

Ohman, M.D. et Hirche, H. 2001. Density-dependent mortality in an oceanic copepod population. Nature, 412, 638-641

Ohman, M.D., Runge, J.A., Durbin, E.G., Field, D.B. et Niehoff, B. 2002. On birth and death in the sea. Hydrobiol., 480, 55-68

Ohman, M.D., Eiane, K., Durbin, E.G., Runge, J.A. et Hirche, H.J. 2004. A comparative study of *Calanus finmarchicus* mortality patterns at five localities in the North Atlantic. ICES J. Mar. Sci., 61, 687-697

Ohman, M.D., Durbin, E.G., Runge, J.A., Sullivan, B.K. et Field, D.B. 2008. Relationship of predation potential to mortality for *Calanus finmarchicus* on Georges bank, N.W. Atlantic. Limnol. Oceanogr., 53, 1643-1655

Ohman, M.D. et Hsieh, C. 2008. Spatial differences in mortality of *Calanus pacificus* within the California Current System. J. Plankton Res., 30, 359-366

Olli, K., Wassmann, P., Reigstad, M., Ratkova, T.N., Arashkevich, E., Pasternak, A., Matrai, P.A., Knulst, J., Tranvik, L., Klais, R. et Jacobsen, A. 2007. The fate of production in the central Arctic Ocean – top-down regulation by zooplankton expatriates? Prog. Oceanogr., 72, 84-113

Ouellet, M., Petrie, B. et Chasse, J. 2003. Temporal and spatial scales of sea-surface temperature variability in Canadian Atlantic waters. Can. Tech. Rep. Hydro. Ocean Sci., 228, 35pp

Overpeck, J., Hughen, K., Hardy, D., Bradley, R., Case, R., Douglas, M., Finney, B., Gajewski, K., Jacoby, G., Jennings, A., Lamoureux, S., Lasca, A., MacDonald,

G., Moore, J. et Zielinski, G. 1997. Arctic environmental change of the last four centuries. Science, 278, 1251-1266

Pellerin, G., Lefaivre, L., Houtekamer, P. et Girard, C. 2003. Increasing the horizontal resolution of ensemble forecasts at CMC. Nonlin. Processes Geophys., 10, 463-468

Pershing, A.J., Greene, C.H., Jossi, J.W., O'Brien, L., Brodziak, J.K. et Bailey, B.A. 2005. Interdecadal variability in the Gulf of Maine zooplankton community, with potential impacts on fish recruitment. ICES J. Mar. Sci. 62, 1511-1523

Peters, J. 2006. Lipids in key copepod species of the Baltic Sea and North Sea – implications for life cycles, trophodynamics and food quality. Ph.D. Thesis, Universität Bremen

Peterson, W.T. et Kimmerer, W.J. 1994. Processes controlling recruitment of the marine calanoid copepod *Temora longicornis* in Long Island Sound: Egg production, egg mortality, and cohort survival rates. Limnol. Oceanogr., 39, 1594-1605

Pierson, J.J., Leising, A.W., Halsband-Lenk, C. et Ferm, N. 2005. Vertical distribution and abundance of *Calanus pacificus* and *Pseudocalanus newmani* in relation to chlorophyll *a* concentrations in Dabob Bay, Washington. Prog. Oceanogr., 67, 349-365

Pierson, J.J., Frost, B.W. et Leising, A.W. 2007. The lost generation of *Calanus pacificus*: Is the diatom effect responsible? Limnol. Oceanogr., 52, 2089-2098

Piñeiro, G., Perelman, S., Guerschman, J.P., Paruelo, J.M. 2008. How to evaluate models: Observed vs. predicted or predicted vs. observed? Ecol. Model. 216,

316-322

Planque, B., Hays, G.C., Ibanez, F. et Gamble, J.C. 1997. Large scale spatial variations in the seasonal abundance of *Calanus finmarchicus*. Deep-Sea Res., 44, 315-326

Plourde, S. et Runge, J. 1993. Reproduction of the planktonic copepod *Calanus finmarchicus* in the lower St. Lawrence Estuary: Relation to the cycle of phytoplankton production and evidence for a *Calanus* pump. Mar. Ecol. Prog. Ser., 102, 217-227

Plourde, S., Joly, P., Runge, J.A., Zakardjian, B. et Dodson, J.J. 2001. Life cycle of *Calanus finmarchicus* in the lower St. Lawrence Estuary: the imprint of circulation and late timing of the spring phytoplankton bloom. Can. J. Fish. Aquat. Sci., 58, 647-658

Plourde, S., Dodson, J.J., Runge, J.A. et Therriault, J.C., 2002. Spatial and temporal variations in copepod community structure in the lower St. Lawrence Estuary, Canada. Mar. Ecol. Prog. Ser., 230, 211-224

Plourde, S., Joly, P., Runge, J.A., Dodson, J. et Zakardjian, B., 2003. Life cycle of *Calanus hyperboreus* in the lower St. Lawrence Estuary and its relationship to local environmental conditions. Mar. Ecol. Prog. Ser., 255, 219-233

Plourde, S. et Joly, P. 2008. Comparison of *in situ* egg production rate in *Calanus finmarchicus* and *Metridia longa*: discriminating between methodological and species-specific effects. Mar. Ecol. Prog. Ser., 363, 165-175

Plourde, S., Maps, F. et Joly, P. 2008. Mortality and survival in early stages control recruitment in *Calanus finmarchicus*. J. Plankton Res., doi:

10.1093/plankt/fbn126

Polis, G.A., Myers, C.A. et Holt, R.D. 1989. The ecology and evolution of intraguild predation: potential competitors that eat each other. Ann. Rev. Ecol. Syst., 20, 297-330

Pringle, J.M. 2007. Turbulence avoidance and the wind-driven transport of plankton in the surface Ekman layer. Cont. Shelf Res., 27, 670-678

Record, N.R. et Pershing, A.J. 2008. Modeling zooplankton development using the monotonic upstream scheme for conservation laws. Limnol. Oceanogr. Methods, 6, 364-372

Reszka, M.K. et Swaters, G.E. 1999. Numerical investigtion of baroclinic instability in the Gaspé Current using a frontal geostrophic model. J. Geophys. Res., 104, 25685-25696

Rey-Rassat, C., Irigoien, X., Harris, R. et Carlotti, F. 2002. Energetic cost of gonad development in *Calanus finmarchicus* and *C. helgolandicus*. Mar. Ecol. Prog. Ser., 238, 301-306

Ringuette, M., Castonguay, M., Runge, J.A. et Gregoire, F. 2002. Atlantic mackerel (*Scomber scombrus*) recruitment fluctuations in relation to copepod production and juvenile growth. Can. J. Fish. Aquat. Sci., 59, 646-656

Rivkin, R.B., Legendre, L., Deibel, D., Tremblay, J., Klein, B., Crocker, K., Roy, S., Silverberg, N., Lovejoy, C., Mesplé, F., Romero, N., Anderson, M.R., Matthews, P., Savenkoff, C., Vézina, A., Therriault, J., Wesson, J., Bérubé, C. et Ingram, R.G. 1996 Vertical Flux of Biogenic Carbon in the Ocean: Is There Food Web Control? Science, 272, 1163-1166

Roy, S., Silverberg, N., Romero, N., Deibel, D., Klein, B., Savenkoff, C., Vezina, A., Tremblay, J., Legendre, L. et Rivkin, R.B. 2000. Importance of mesozooplankton feeding for the downward flux of biogenic carbon in the Gulf of St Lawrence (Canada). Deep Sea Res. II, 47, 519-544

Runge, J.A. 1988. Should we expect a relationship between primary production and fisheries? The role of copepod dynamics as a filter of trophic variability. Hydrobiol., 167/168, 61-71

Runge, J. et de Lafontaine, Y. 1996. Characterization of the pelagic ecosystem in surface waters of the northern Gulf of St. Lawrence in early summer: The larval redfish-Calanus-microplankton interaction. Fish. Oceanogr., 5, 21-37

Runge, J.A. et Plourde, S. 1996. Fecundity characteristics of *Calanus finmarchicus* in coastal waters of eastern Canada. Ophelia, 44, 171-187

Runge, J.A., Castonguay, M., de Lafontaine, Y.D., Ringuette, M. et Beaulieu, J.L. 1999. Covariation in climate, zooplankton biomass and mackerel recruitment in the southern Gulf of St Lawrence. Fish. Oceanogr., 8, 139-149

Runge, J.A., Franks, P.J., Gentleman, W.C., Megrey, B.A., Rose, K.A., Werner, F.E., Zakardjian, B. 2005. Diagnosis and prediction of variability in secondary production and fish recruitment processes: developments in physical-biological modelling. *In:* The Sea, Vol.13, Robinson, A.R. et Brink, K. (eds), 413-473

Sameoto, D., Neilson, J. et Waldron, D. 1994. Zooplankton prey selection by juvenile fish in Nova Scotian shelf basins. J. Plankton Res., 16, 1003-1019

Saucier, F.J., Roy, F., Gilbert, D., Pellerin, P. et Ritchie, H. 2003. Modeling the formation and circulation processes of water masses and sea ice in the Gulf of

St. Lawrence, Canada. J. Geophys. Res. C, 108, 2501-2520

Saucier, F., Senneville, S., Prinsenberg, S., Roy, F., Smith, G. et Gachon, P. 2004. Modelling the sea ice - ocean seasonal cycle in Hudson Bay, Foxe Basin and Hudson Strait, Canada. Clim. Dyn., 23, 303-326

Saucier, F.J., Roy, F., Senneville, S., Smith, G., Lefaivre, D., Zakardjian, B. et Dumais, J.-F. 2009. Modelling of the circulation in the estuary and the Gulf of St. Lawrence in response to variations in fresh water runoff and winds. J. Water Sci., 22(Special), sous presse

Saumweber, W.J. et Durbin, E.G. 2006. Estimating potential diapause duration in *Calanus finmarchicus*. Deep Sea Res. II, 53, 2597-2617

Sell, A.F., van Keuren, D. et Madin, L.P. 2001. Predation by omnivorous copepods on early developmental stages of *Calanus finmarchicus* and *Pseudocalanus* spp. Limnol. Oceanogr., 46, 953-959

Seuront, L. et Lagadeuc, Y. 2001. Multiscale patchiness of the calanoid copepod *Temora longicornis* in a turbulent coastal sea. J. Plankton Res., 23, 1137-1145

Sevigny, J., Sinclair, M., El-Sabh, M., Poulet, S. et Coote, A., 1979. Summer plankton distributions associated with the physical and nutrient properties of the northwestern Gulf of St. Lawrence. J. Fish. Res. Board Can., 36, 187-203

Sheng, J.Y. 2001. Dynamics of a buoyancy-driven coastal jet: The Gaspé Current. J. Phys. Oceanogr., 31, 3146-3162

Simard, Y., Lacroix, G. et Legendre, L. 1985. In situ twilight grazing rhythm during diel vertical migrations of a scattering layer of *Calanus finmarchicus*. Limnol. Oceanogr., 30, 598-606

Skreslet, S. 1997. A conceptual model of the trophodynamical response to river discharge in a large marine ecosystem. J. Mar. Sys., 12, 187-198

Skreslet, S., Borja, A., Bugliaro, L., Hansen, G., Meerkotter, R., Olsen, K. et Verdebout, J. 2005. Some effects of ultraviolet radiation and climate on the reproduction of *Calanus finmarchicus* (Copepoda) and year class formation in Arcto-Norwegian cod (Gadus morhua). ICES J. Mar. Sci., 62, 1293-1300

Slagstad, D., Tande, K.S. 2007. Structure and resilience of overwintering habitats of *Calanus finmarchicus* in the Eastern Norwegian Sea. Deep-Sea Res. II, 54, 2702-2715

Smith, S.L. 1995. The Arabian Sea: Mesozooplankton response to seasonal climate in a tropical ocean: II. Regional interactions of physics and population dynamics. ICES J. Mar. Sci., 52, 427-438

Smith, G.C., Saucier, F.J. et Straub, D. 2006a. Response of the Lower St. Lawrence Estuary to External Forcing in Winter. J. Phys. Oceanogr., 36, 1485-1501

Smith, G.C., Saucier, F.J. et Straub, D. 2006b. Formation and circulation of the cold intermediate layer in the Gulf of Saint Lawrence. J. Geophys. Res. 111, C06011

Sourisseau, M., Simard, Y. et Saucier, F.J. 2006. Krill aggregation in the St. Lawrence system, and supply of krill to the whale feeding grounds in the estuary from the gulf. Mar. Ecol. Prog. Ser., 314, 257-270

Speirs, D.C., Gurney, W.S.C., Heath, M.R. et Wood, S.N. 2005. Modelling the basin-scale demography of *Calanus finmarchicus* in the north-east Atlantic. Fish. Oceanogr., 14, 333-358

Speirs, D.C., Gurney, W.S.C., Heath, M.R., Horbelt, W., Wood, S.N. et de Cuevas, B.A. 2006. Ocean-scale modelling of the distribution, abundance, and seasonal dynamics of the copepod *Calanus finmarchicus*. Mar. Ecol. Prog. Ser., 313, 173-192

Stegert, C., Kreus, M., Carlotti, F. et Moll, A. 2007. Parameterisation of a zooplankton population model for *Pseudocalanus elongatus* using stage durations from laboratory experiments. Ecol. Model., 206, 213-230

Stempniewicz, L., Blachowiak-Samolyk, K. et Weslawski, J.M. 2007. Impact of climate change on zooplankton communities, seabird populations and arctic terrestrial ecosystem - A scenario. Deep Sea Res. II, 54, 2934-2945

Sundby, S. 2000. Recruitment of Atlantic cod stocks in relation to temperature and advection of copepod populations. Sarsia, 85, 277-298

Svetlichnyj, L. 1993. Locomotory function of copepods' oral appendages: Kinematic analysis. Ehkol. Morya, 44, 84-91

Tang, C.L. 1980a. Mixing and circulation in the northwestern Gulf of St. Lawrence: a study of a buoyancy-driven current system. J. Geophys. Res., 85, 2787-2796

Tang, C.L. 1980b. Observation of wavelike motion of the Gaspé Current. J. Phys. Oceanogr., 10, 853-860

Tarrant, A.M., Baumgartner, M.F., Verslycke, T. et Johnson, C.L. 2008. Differential gene expression in diapausing and active *Calanus finmarchicus* (Copepoda). Mar. Ecol. Prog. Ser., 355, 193-207

Taylor, F. 1980. Optimal switching to diapause in relation to the onset of winter. Theor. Popul. Biol., 18, 125-133

Wroblewski, J.S. et O'Brien, J.J. 1981. On modeling the turbulent transport of passive biological variables in aquatic ecosystems. Ecol. Model., 12, 29-44

Wroblewski, J.S. 1982 Interaction of currents and vertical migration in maintaining *Calanus marshallae* in the Oregon upwelling zone--a simulation. Deep Sea Res. A, 29, 665-686

Zakardjian, B.A., Runge, J., Plourde, S. et Gratton, Y. 1999. A biophysical model of the interaction between vertical migration of crustacean zooplankton and circulation in the Lower St Lawrence Estuary. Can. J. Fish. Aquat. Sci., 56, 2420-2432

Zakardjian, B.A., Gratton, Y. et Vezina, A.F. 2000. Late spring phytoplankton bloom in the Lower St. Lawrence Estuary: the flushing hypothesis revisited. Mar. Ecol. Prog. Ser., 192, 31-48

Zakardjian, B.A., Sheng, J., Runge, J.A., McLaren, I., Plourde, S., Thompson, K.R. et Gratton, Y. 2003. Effects of temperature and circulation on the population dynamics of *Calanus finmarchicus* in the Gulf of St. Lawrence and Scotian Shelf: Study with a coupled, three-dimensional hydrodynamic, stage-based life history model. J. Geophys. Res. C, 108, 1701-1722